The role of IL-4Rα in *Nippostrongylus brasiliensis*–induced chronic lung pathology

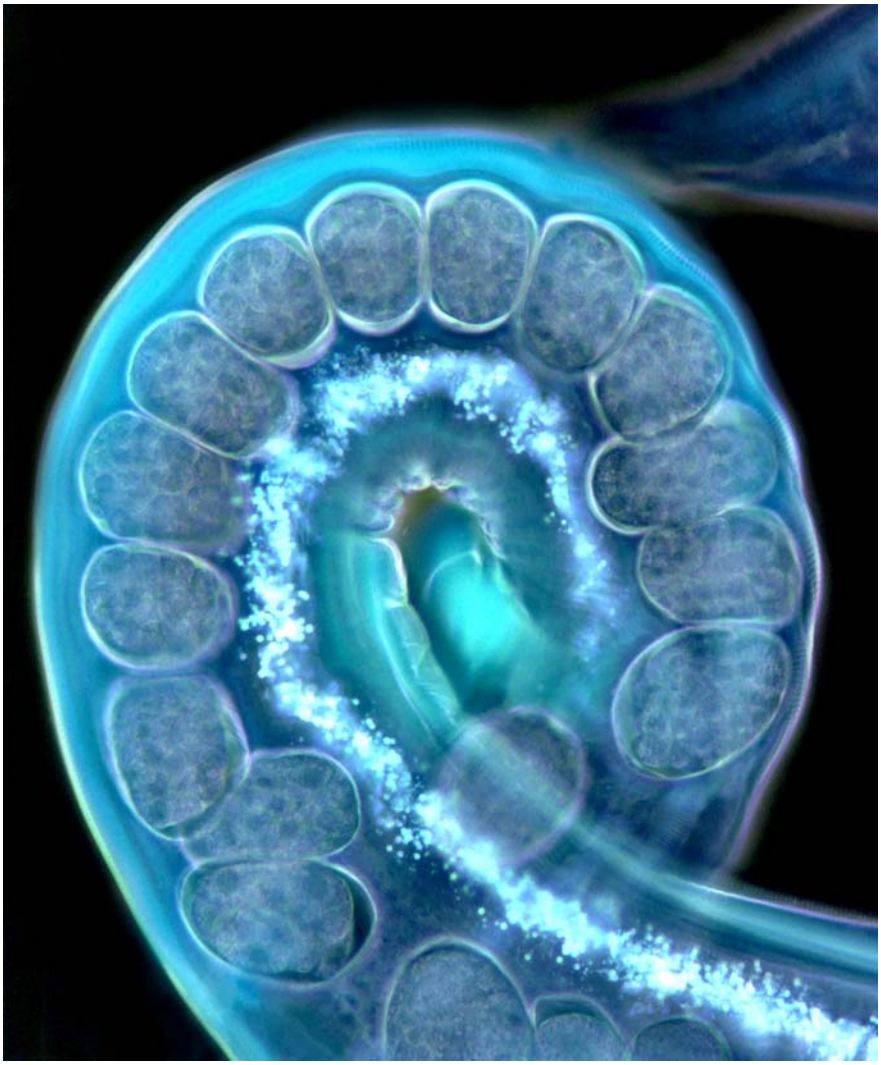

Dinko Basich (BSCDIN001)

SUBMITTED TO THE UNIVERSITY OF CAPE TOWN

In fulfilment of the requirements for the degree

MSc in Medicine

Department of Clinical Laboratory Sciences and Immunology

Faculty of Health Sciences, University of Cape Town

2010

Declaration

I, Dinko Basich, hereby declare that the work on which this thesis is based, is my original work (except where acknowledgements indicate otherwise) and that neither the whole work nor any part thereof is being, has been, or is to be submitted for another degree in this or any other university.

I empower the University of Cape Town to reproduce for the purpose of research the whole or any portion of the contents in any manner whatsoever.

……..

Dinko Basich

June 2010

Illustration on cover page: Section of female *Nippostrongylus brasiliensis* worm filled with eggs. Photograph by J.Claire Hoving (given with permission); ICGEB, UCT.

Acknowledgements

My dearest gratitude goes to my supervisor, Prof. Frank Brombacher for granting me the opportunity to work in his laboratory and for his advice, guidance and generous funding for this project and life's uncertainties. I am just as grateful to my knowledgeable co-supervisor Dr. William Horsnell for his endless hours and patience with me during these tough years. His knowledge, speed and intense critical thinking is highly inspirational. Special thanks goes to Prof. Dhiren Govender, for his crucial pathology discussions and whose long hours in front of the microscope and excellent, thorough teaching has helped me to develop my "pathologist skills". I would also like to thank Dr. Anita Schwegmann for her expert advice on all RNA work, especially with assisting in data-mining of functional annotations for genes and never ceases to offer knowledge, advice or support, especially during the critical time of writing this thesis. I am also grateful for Dr Frank Kirstein for his eager help with the AHR and to Dr Natalie Nieuwenhuizen for their knowledge on lung. Thank you to Dr. Claire Hoving for all her lab expertise and advice. I would like to thank all the above for their critical reading and scientific advice which has been invaluable in this Masters.

I would like to thank our collaborator, Dr. Alun Kirby (York, UK) for his microarray amplification and analysis data (and answering my endless emails). I would like to thank: Rosa Chang for her assistance to the "Nippo Team"; Wendy Green and Ryana Fredericks, Fadwah Booley for genotyping all the mice; Berenice Arendse and Babele Emedi for their assistance in the lab; Hiram and his team in the animal unit; Gloria and Dhuraiyah for their organisational assistance. A big thank you to all those that have helped me in one way or another. This includes nearly the entire Immunology division from support staff, to the post-doctoral and student-support-team which have been an outstanding source of friendly support from the Brombacher, Brown and Jacobs laboratories.

Finally, yet most importantly, I would like to thank the supporting "pillars" in my life for their constant support and care: my lovely wife Rosa Sfeir who is my unconditional love and support, for all the loving support and sacrifices that she willingly made for me and waited for me and also to my unborn son (sorry for

keeping your mommy awake late at night and working everyday to support us). Additional thanks to my family who never questioned my unusual arrival or working hours; and my friends who tolerated my scarceness.

Lastly, I acknowledge all 514 mice that were used to make my project a reality.

Table of Contents

List of Figures

Abbreviations

-/-	Knockout
<	Less than
>	More than
^{0}C	Degrees Celsius
γc	Common gamma chain
AAM (or M2)	Alternatively activated macrophage
Ab	Antibody
Ag	Antigen
AHR	Airway hyperresponsiveness
AlvM	Alveolar macrophage
AP	Alkaline phosphatase
APCs	Antigen presenting cells
APC-	Allophycocyanin-conjugated protein
BAL	Bronchoalveolar lavage (BAL)
BSA	Bovine serum albumin
caM	Classically activated macrophage
CB	Chronic bronchitis
CD	Cytoplasmic domain
COPD	Chronic obstructive pulmonary disorder
Cre	Cre recombinase
DAVID	Database for Annotation Visualization and Integrated Discovery
DC	Dendritic cell
ddH_2O	Double-distilled water
DMEM	Dulbecco's modified Eagle's medium
EDTA	Ethylenediamine tetraacetic acid
ELISA	Enzyme linked immuno-sorbent assay
EPO	Eosinophil peroxidase
FACS	Fluorescence-Activated Cell Sorting
FC	Fold change
FCS	Foetal calf serum
FITC	Fluorescein isothiocyanate
GM-CSF	Granulocyte-macrophage colony-stimulating factor
GO	Gene Ontology
H&E	Haematoxylin & Eosin
H_2O_2	Hydrogen peroxide
HRP	Horse radish peroxidise
HTAB	Hexadecyl trimethyl ammonium bromide
IFN-γ	Interferon-gamma
Ig	Immunoglobulin

IL	Interleukin
IL-1β	Interleukin-1-beta
IL-4Rα	Interleukin-4 receptor alpha
IL-4Rα$^{-/-}$	IL-4Rα deficient
IL-4Rα$^{-/lox}$	Hemizygous for IL-4Rα (considered wild type controls)
IL-13Rα	Interleukin-13 receptor alpha
ISPF	Isonitrosopropiophenone
JAK	Janus Kinase
KO	Knock out (or abbrev. for IL-4Rα$^{-/-}$)
L_3	Third stage larvae (of *N. brasiliensis*)
LN	Lymph node
LVRS	Lung volume reduction surgery
LysM	Lysozyme M (or abbrev. for LysM^{Cre}IL-4Rα$^{-/lox}$ mice)
LysM^{Cre}IL-4Rα$^{-/lox}$	Macrophage/neutrophil specific disrupted IL-4Rα
MCh	B-metacholine
MHCI / II	Major histocompatibility complex Class I / II
MIAME	Minimum Information about Microarray Experiments
MMP	Matrix metalloproteinase
MPO	Myeloperoxidase
MR	Mannose receptor
mRNA	Messenger RNA
N. brasiliensis	*Nippostrongylus brasiliensis*
NO	Nitric oxide
NOS2 (or iNOS)	Nitric oxide synthase 2 (or inducible NOS)
OD	Optical density
OPD	O-phenylenediamine
p.i.	Post infection
PAMP	Pathogen-associated molecular patterns
PBS	Phosphate-buffered saline
PCR	Polymerase chain reaction
PenStrep (or P/S)	Medium containing penicillin and streptomycin
PEP	Peak expiratory pressure
PI3K	Phosphoinositide 3-kinase
PIP	Peak inspiratory pressure
PNP	P-Nitrophenyl phosphate
PRR	Pattern recognition receptors
qRT-PCR	Quantitative real-time PCR
RNA	Ribonucleic acid
rpm	Revolutions per minute
SpA	Streptavidin
SEM	Standard error of the mean
SeV	Sendai virus
SOCS	Suppressor cytokine signalling

STAT	Signal transducer and activator of transcription
Te	Expiratory time
TGF-β	Tumour growth factor beta
TH	T-helper ($CD4^+$) cell
TIMPs	Tissue inhibitors of metalloproteases
TLR	Toll-like receptors
TNF	Tumour necrosis factor
Tr	Relaxation time
Treg	Regulatory T-cells
UCT	University of Cape Town
UK	United Kingdom
WT	Wild-type ($IL\text{-}4R\alpha^{-/lox}$ for the purposes of this study)
X	Times / multiplied by

Abstract

Infection by the parasitic nematode *Nippostrongylus brasiliensis* involves migration through the lungs, causing significant damage and generating chronic lung pathology. The resolution of *N. brasiliensis* infection and also the induction of pulmonary pathology, including goblet cell hyperplasia and acute airway inflammation, depend on IL-4Rα signalling. A key feature of IL-4Rα signalling is the induction of a strong TH2 response which induces the development of alternatively activated macrophages (AAMs). AAMs are associated with tissue remodelling and the control of exacerbated inflammation. In order to investigate potential roles for IL-4Rα in *N. brasiliensis*–induced lung pathology, we infected mice deficient for IL-4Rα on macrophages and neutrophils ($LysM^{Cre}IL\text{-}4R\alpha^{-/lox}$), $IL\text{-}4R\alpha^{-/-}$ and control mice ($IL\text{-}4R\alpha^{-/lox}$) with *N. brasiliensis* and examined lung pathology at days 5, 42 and 180 post infection (p.i.). All three mice strains showed similar emphysemic-like pathology (alveolar dilatation) and airway hyperresponsiveness (AHR) which was well developed by day 42 p.i. and remained chronic. However, $LysM^{Cre}IL\text{-}4R\alpha^{-/lox}$ mice consistently demonstrated earlier and increased pulmonary inflammation when compared to $IL\text{-}4R\alpha^{-/lox}$ control mice and $IL\text{-}4R\alpha^{-/-}$ mice. Immunological studies at day 5 p.i. revealed that there were increased $CD4^+$ and $CD8^+$ T-cell numbers and increased $CD4^+$ IL-4 and IL-13 production in the lungs of $LysM^{Cre}IL\text{-}4R\alpha^{-/lox}$ mice when compared to control and $IL\text{-}4R\alpha^{-/-}$ mice. $LysM^{Cre}IL\text{-}4R\alpha^{-/lox}$ mice also showed decreased pulmonary arginase activity, indicative of a reduction of AAMs. RNA transcript analysis of isolated alveolar macrophages showed a strong association with promoting inflammation in $LysM^{Cre}IL\text{-}4R\alpha^{-/lox}$ mice. Together these data demonstrate that IL-4Rα-responsive macrophages control pulmonary inflammation and play an important protective role in the lung following *N. brasiliensis* infection.

1. INTRODUCTION

1.1 Project rationale

In this study, we used the parasitic worm *N. brasiliensis* as a model of chronic lung disease in order to uncover the immunological events that drive related medical conditions. *N. brasiliensis* has a brief obligatory phase in the host lung during its life cycle, which results in chronic lung disease that continues to develop even after the actual infection has been resolved [1, 2]. This pathology has similarities with asthma in the acute phase [3, 4] and emphysema in the chronic phase [1]. At the molecular level, it is apparent that cytokine signalling via receptors containing the alpha subunit of the interleukin-4 receptor (IL-4Rα) plays an important role in the development of this pathology [4-6]. These diseases has been associated with IL-4Rα-dependent development of alternative activation of macrophages in the lung [1, 7]. In this study we investigated in detail how macrophage expression of IL-4Rα modulates the development of both acute and chronic immuno-pathology in the lung following *N. brasiliensis* infection.

1.2 The Immune System

The immune system consists of an array of organs, cells and soluble mediators, which co-ordinate together to recognise and protect the host from potentially harmful non-self factors [8]. Upon specific recognition of a pathogen or its antigens, an immune response is generated. Immune responses can be general to the challenge (innate). or highly specific following a secondary exposure to the challenge (adaptive), or consist of both innate and adaptive elements [8].

Innate immune responses are typically associated with the first line of defence against an invading pathogen. Innate immune components include neutrophils, macrophages, dendritic cells (DCs), Natural Killer (NK) cells, eosinophils, basophils, mast cells, platelets and the complement system [8]. Innate immune responses are frequently initiated through host cellular recognition of common structural moieties from pathogens or pathogen-associated molecular patterns (PAMPs), which rapidly activate the mediators of an innate response [9-11]. Recognition of PAMPs is mediated through a range of host receptors, including pattern recognition receptors (PRR) such as toll-like receptors (TLR), mannose receptors and C-type lectins [9-11]. Expression of these receptors are found on immune cells, such as phagocytic neutrophils and macrophages, B cells, DCs and certain types of T cells, and on non-immune cells lining the organs exposed to the environment such as epithelial, endothelial and smooth muscle cells in the skin, respiratory and gastrointestinal tracts [10, 12]. The receptors enable a degree of specific recognition of a PAMP that can be associated with certain types of immune challenge, e.g. TLR3 recognising double-stranded (viral) RNA [9, 13]. Typically, though not exclusively, this interaction results in the binding and phagocytosis of these microbes. In addition to phagocytic responses, cells can control immunological challenges through other innate mechanisms. For example, neutrophils and eosinophils can secrete microbiocidal or cytotoxic molecules such as myeloperoxidase (MPO) from neutrophils, or eosinophil peroxidise (EPO), which attack pathogens that are too large for phagocytosis (e.g. parasitic worms) [14].

An adaptive immune response takes longer to launch, however it is usually highly specific against its target antigen or pathogen. It is responsible for the development of an immunological "memory response" for immediate recognition and responses to

future re-infections [8]. The adaptive immune response is co-ordinated by antigen recognition by randomly generated antigen receptors on T- and B- cells, which enables these lymphocytes to recognise nearly all antigens and pathogens [8]. The antigens are presented to T- and B-cells by antigen presenting cells (APCs) such as macrophages and dendritic cells, which form the interface between innate and adaptive immunity [11]. APCs process and typically present antigens on MHC-II molecules to B- or T-cells inducing lymphocytic maturation, activation or differentiation [8]. T-cells differentiate into T-helper cells, which mainly function to produce cytokines. B-cells can develop into memory B-cells or plasma cells and depending on the cytokine and co-stimulatory signals, produce several different types of antigen-specific antibodies such as IgM, IgG, IgE, IgA or IgD [8]. Furthermore, B-cells can function as APCs as they can process and present antigens on MHC-II molecules to $CD4^+$ T-cells and possess APC co-stimulatory molecules, which induce the same lymphocytic functions as above [15]. Memory B-cells, together with memory T-cells provide an immunological memory that is able to launch a rapid response upon secondary exposure to the antigen [8].

1.2.1 Cytokines

Cytokines are essential in the communication and regulation of the cells of both innate and adaptive immune responses [8]. Cytokines are small protein ligands produced by a variety of cells. They bind to specific cell surface receptors and alter gene expression in the recipient cell via a signal transduction cascade. Cytokine-mediated responses can be autocrine, where the cytokine binds to the receptor on the same cell secreting it, or paracrine, where the cytokine binds to receptors of other cells in close proximity [16]. Cytokines include interleukins (IL) and interferons (IFN) and can be pleiotropic,

whereby a particular cytokine can have multiple effects on various different cells. Cytokine production is transient and its effects include cell differentiation, proliferation, activation, release of effector molecules or cell recruitment [16, 17]. The magnitude and variety of cytokines produced determines whether the host's immune response is protective, ineffective or detrimental and therefore cytokine levels are used as indicators of disease progression in patients [16]. Furthermore, cytokines can indicate the type of adaptive immune response involved based on the type of cytokines secreted by $CD4^+$ T-helper cells [16].

1.2.2. Differentiation of T-helper (TH) subsets

Differentiation of naïve $CD4^+$ T-cells into distinct T-helper subsets is dependent on the nature of the antigen presented by the APC and the cytokine environment [8]. These cytokines play a key role in the differentiation, proliferation and, in certain cases, the suppression of TH subset development [17]. Undifferentiated $CD4^+$ T-helper cells can differentiate into one of the following mutually exclusive cell lineages: the classical T-helper 1 (TH1) or TH2 lineages, and the more recently identified, TH17 and regulatory T-cell (Treg) lineages. Additional effector T-cell subsets may include IL-5-producing TH5 and IL-9-producing "reprogrammed" TH9 subsets [18, 19]. Each lineage is identified by its profile of intracellular transcription factors, extracellular markers (receptors), and their cytokine spectrum produced and are each involved in different processes (**Figure 1**) [17].

1.2.3. TH1 vs. TH2

The TH1 and TH2 subsets were first described by the different cytokine profiles they expressed after *in vitro* antigenic stimulation of $CD4^+$ T-cells [20]. Typically, IL-12

triggers undifferentiated $CD4^+$ T-cells, which induces TH1 differentiation via the STAT-4 pathway to activate the T-box expressed in T-cells (T-bet) transcription factor. These TH1 cells are primarily classified by the production of the TH1 hallmark cytokine, IFN-gamma (IFN-γ) [21, 22]. TH1 immunity is associated with the control of protozoan, bacterial and other single-cell pathogens. Conversely, the cytokine IL-4 triggers undifferentiated $CD4^+$ T-cells to activate the transcription factor GATA3 through the signal transduction and activator of transcription (STAT)-6 pathway to drive TH2 differentiation. GATA-3 activation then promotes IL-4, IL-13 and IL-5 production, amongst other TH2 cytokines [23]. Although it is generally accepted that IL-4 drives TH2 differentiation [24-26], evidence does exist that IL-4 is not essential for initiating TH2 responses [27, 28]. TH2 immunity is associated with the control of multicellular or metazoan parasitic infections and with the onset of allergic diseases. The development of TH1 and TH2 subsets can also be negatively regulated by the cytokines IFN-γ and IL-4, which suppress differentiation of TH2 and TH1 subsets, respectively. The differences between TH1 and TH2 cells and their properties are listed in **Table 1** below.

Table 1: Major differences between TH1 and TH2 immune responses.

	TH1	TH2
Response to:	Microbial and intracellular pathogens	Extracellular parasites and allergic reactions
Initiating Cytokines:	IL-12, IL-18	IL-4
Antibodies (secreted by plasma cells):	IgG2a IgG2b	IgE IgG1
Transcription factors:	T-bet , STAT-4	GATA3, STAT-6
Cytokines produced:	IFN-γ (IL-2)	IL-4 (IL-2), IL-13, IL-5.
Inhibited by cytokines:	IL-4, IL-10, TGF-B	IFN-γ, TGF-B

1.2.4. TH17 and Treg pathways:

The novel pathways involved in the differentiation of TH17 and Treg cells are not yet clearly defined. Although their development is mutually exclusive, Transforming growth factor (TGF)-β1 is required for the development of both TH17 and Treg cells [29]. IL-6 also appears to play an important role in either inhibiting Treg or inducing TH17 development while IL-23 promotes TH17 development [30]. The crucial transcription factors for TH17 and Treg cells are orphan nuclear receptor (RORγt) [31] and forkhead box P3 (Foxp3) [23, 32] respectively, and their key cytokines are IL-17 and TGF-β1 respectively (**Figure 1**). TH17 cells are associated with certain asthmatic symptoms [33], autoimmunity [34] and with clearing extracellular microbes [35], while Tregs are essential for controlling self tolerance and inflammatory immune responses [36].

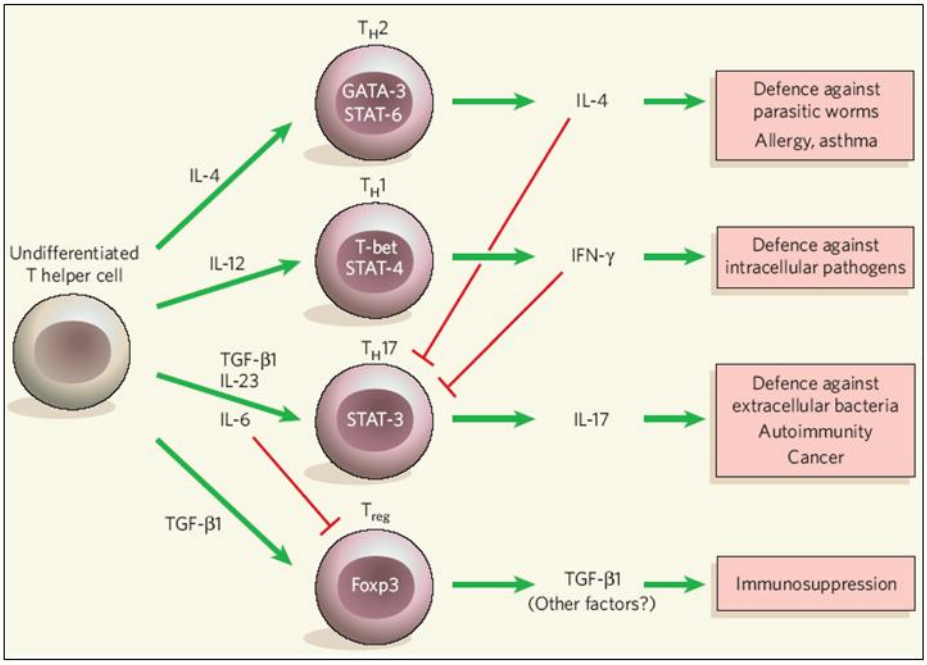

Figure 1: T-helper subset differentiation. Upon activation by antigens and cytokines, naïve $CD4^+$ T-cells can differentiate into T-helper 2 (TH2), TH1, TH17 or regulatory T-cells (Tregs). Their determining cytokines (*left-most green arrows*) induce key transcription factors (*centre of cells*), which induce post-maturation cytokine production (*on right*), resulting in their different cell lineages, which are involved in the processes on the right (*boxed*). Diagram taken from Tato & O'Shea (2006) [17].

1.3. IL-4 Receptor alpha (IL-4Rα)

1.3.1. Type I and Type II IL-4 Receptors

IL-4 and IL-13 are the fundamental cytokines in the TH2 immune response [16] and share certain functions, which is partly due to a shared common receptor transmembrane subunit, interleukin-4-receptor alpha (IL-4Rα) [37], in their receptor complexes. The IL-4Rα subunit is widely expressed on haematopoietic, epithelial, muscle, fibroblast, endothelial and hepatocyte cells and brain tissues [38]. IL-4Rα containing heterodimeric receptors can either associate with the γc subunit, forming a type I receptor, or recruit the IL-13 Receptor alpha1 (IL-13Rα1) subunit, forming a type II receptor [39, 40]. Type I receptors, found in most cells of the haematopoietic lineage [41], bind only to IL-4 [42, 43], while Type 2 receptors expressed by non-haematopoietic and myeloid-derived haematopoietic cells bind to both IL-4 and IL-13 [42, 44], accounting for the overlap in biological effects of IL-4 and IL-13 [45]. However, IL-4 and IL-13 have different affinities for the Type II receptor, which results in differences in downstream events in the signal transduction cascades, which could also explain their differences in effects [43]. Recent studies on IL-13Rα1 revealed some differences between the Type I and Type II receptor components in TH2 responses to helminth (parasite) infections and allergy [46].

Both Type I and Type II receptors signal through the Janus kinase family (Jak) and phosphoinositide 3-kinase (PI3K) pathways to activate the TH2 associated transcription factors STAT6 (signal transducer and activator of transcription 6) and GATA3, to further activate or sustain TH2 gene targets [23, 47]. Recently, it was discovered that IL-4Rα could also signal through Syk kinase to enhance phagocytosis and cell adhesion [48] (**Figure 2**)

Additionally, IL-13 can bind solely to IL-13Rα2 [16], which was previously thought to be a decoy receptor as it did not induce typical IL-13-mediated activation [49]. However, IL-13Rα2 has been discovered to play a different role in fibrosis, via AP-1 and TGF-B signalling [16, 50], and has also recently been suggested to modulate IL-4 signalling [51] and to play a role in IL-13 regulation during *N. brasiliensis* infection [52].

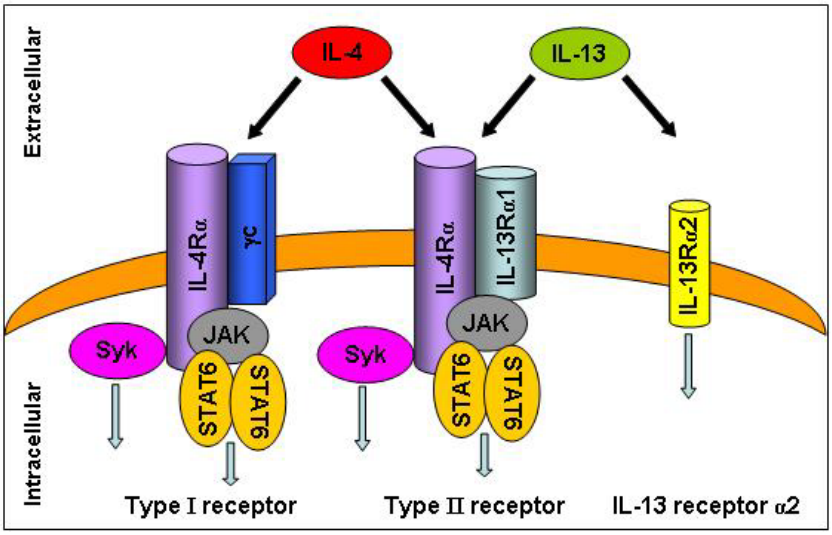

Figure 2: IL-4 and IL-13 cytokines, their receptor complexes and general signalling pathways. The IL-4 (*red*) cytokine can bind to (*black arrows*) a type I (*left*) or Type II (*middle*) receptor, while IL-13 (*olive*) can bind to the Type II (*middle*) heterodimeric receptor or IL-13Rα2 (*right*). The IL-4Rα subunit (*purple*) is shared in both receptor types and associates with either JAK which activates STAT6 upon binding, or with Syk to induce intracellular signalling (*blue arrows*).

1.3.2. Significance of IL-4Rα–dependent responses

IL-4Rα is a critical component of the TH2 immune response responsible for TH2 cell differentiation and IgE class switching via STAT-6 activation [53]. These cellular events result in physiological changes such as airway mucus hypersecretion, airway hyperresponsiveness and airway inflammation [54-56]. Additionally, IL-4Rα plays a central role in TH2 responses to a variety of helminth infection models [37, 57-59]. Germ line IL-4Rα-deficient mice have been instrumental in elucidating several functions of this receptor *in vivo* [4, 5, 37, 59-63]. For example, IL-4Rα-deficient (IL-4Rα$^{-/-}$) mice

showed an impaired IL-4 and IL-13 response *in vitro* [62] and these mice were more resistant during the acute stages of *L. major* infection[62]. Conversely, during *N. brasiliensis* infection, IL-4Rα was crucial for parasite expulsion [5, 60, 61]. Other helminth infections, such as *S. mansoni*-infected IL-4Rα$^{-/-}$ mice are susceptible to infection [59], while *Trichinella spiralis*-infected IL-4Rα$^{-/-}$ mice showed a reduced intestinal pathology and worm expulsion [58]. Furthermore, a recent study has investigated the conservative region of IL-4Rα in human susceptibility to allergic asthma [64], highlighting the importance of IL-4Rα studies in allergic asthma.

1.3.3. Cell type-specific studies

The development of the Cre recombinase-loxP (Cre-loxP) system has allowed for the *in vivo* study of gene function in a single cell type [65, 66]. The transgenic mouse contains the Cre-recombinase gene under the control of the promoter of the type of cell or tissue of interest and loxP sites flanking the specified gene [67]. The promoter induces Cre-recombinase expression, which targets loxP sites and induces homologous recombination, thus excising the gene or exons of interest within those cell lineages [67]. This technique has been used to generate cell-specific exon deletions (exon 7-9) of IL-4Rα exclusively on either CD4^{+} T-cells [4, 68, 69], lung (Clara) cells [70], smooth muscle cells [5] or macrophages and neutrophils (LysM^{Cre}IL-4Rα$^{-/lox}$) [59, 68]; while all other cells maintained functional IL-4Rα expression and signalling. These cell-specific IL-4Rα-deficient mice have been used to study intracellular parasite [69] and helminth infections [4, 5, 59], asthma [70] and anaphylaxis [68], to further uncover the importance of TH2 and hence IL-4Rα-dependent mechanisms in these cell lineages. Genes under the macrophage- and neutrophil-specific lysozyme M (LysM) promoter [71] have been used to investigate Arginase1 (Arg1$^{-/flox}$;LysM^{Cre}) [72] or IL-

4Rα (LysM^{Cre}IL-4Rα$^{-/lox}$) function in macrophage/neutrophil lineages in helminth infections [4, 5, 59], as well as in anaphylaxis [68], arthritis [73] and colon carcinoma tumour studies [74]. The LysM^{Cre}IL-4Rα$^{-/lox}$ mouse was used in this study to investigate effects of *N. brasiliensis*-induced pulmonary pathology. The details of the generation and characterization of LysM^{Cre}IL-4Rα$^{-/lox}$ mice were carried out by Herbert and colleagues (2004) [59] and are summarised in **Figure 3** below.

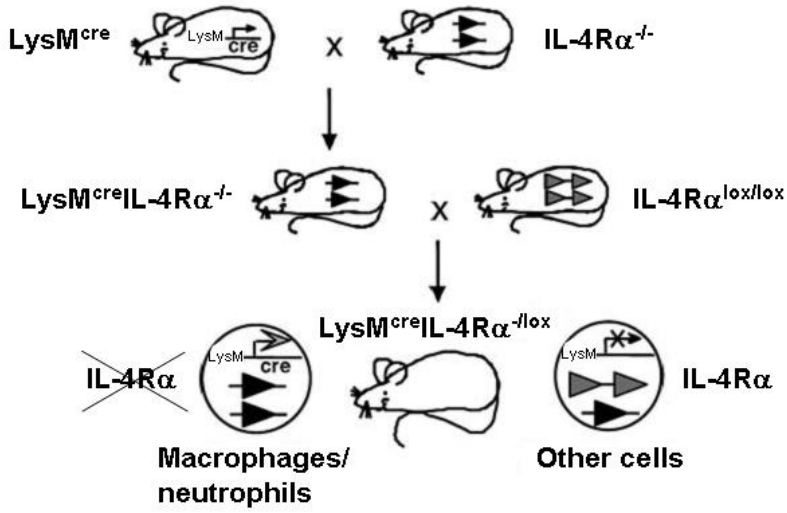

Figure 3: Generation of LysM^{Cre}IL-4Rα$^{-/lox}$ mice. IL-4Rα$^{-/-}$ mice [62] were mated with transgenic mice possessing a Lysozyme M promoter driving Cre recombinase, resulting in LysM^{Cre}IL-4Rα$^{-/-}$ offspring. These offspring were mated with mice containing IL-4Rα flanked by loxP sites (IL-4Rα$^{lox/lox}$) to produce mice with LysM driven cre-mediated deletion of IL-4Rα (LysM^{Cre}IL-4Rα$^{-/lox}$) [59]. *Grey arrows*: loxP flanked IL-4Rα allele; *black arrows*: deleted allele. Figure adapted from Radwanska *et al.* (2007) [69].

1.4 Parasitic Helminths, Nematodes and *N. brasiliensis*

1.4.1. Helminths

The term helminth refers to worm and worm-like parasites and refers to most members of the Phyla Nematoda (roundworms), Cestoda (tapeworms) and Trematoda (flukes) [75]. In this study the murine parasitic nematode *N. brasiliensis* (discussed in

detail later) was used, which is analogous to the human parasite hookworms such as *Necator americanus* and *Ancylostoma duodenale* [76, 77]. Hookworm, along with roundworm (*Ascaris lumbricoides*) and whipworm (*Trichuris trichuria*) infections, are the most prevalent of human parasites and account for approximately 570 million, 800 million and 600 million human infections, respectively, mostly affecting the developing regions of Asia, Africa and Latin America [77].

1.4.2. Significance of parasitic nematode infections

Parasitic nematode infections cause serious morbidity including chronic inflammatory pathology, anaemia, malnutrition and cognitive disorders and can be fatal in extreme cases [76, 77]. In addition to causing serious morbidity, nematodes can also alter the host's immune response to challenges by other pathogens, environmental antigens and vaccines [2, 78, 79]. For example, chronic nematode infections appear to negatively affect the host's response to Tuberculosis (TB) vaccines [80].

However the effects of nematode infections on the host are not always negative. Central to this school of thought is the "hygiene hypothesis", which proposes that reduced exposure to infections during childhood due to increased human hygiene, results in insufficient stimulation of TH1 cells, which cannot counterbalance TH2 expansion and therefore could give a predisposition to allergy [81]. In support of this, a number of studies have shown that nematode infections can also decrease allergic symptoms [2, 81-84]. Additionally, the regulatory cytokines produced in response to nematode infections offer a potential treatment method for TH1 auto-immune diseases and TH2-driven immune dysfunction such as Crohn's disease and allergic asthma, respectively [2, 81, 85, 86]. Together, the high infection rates, debilitating pathology and

immuno-modulatory effects of these parasites illustrate the relevance of studying and understanding the immunological mechanisms that are induced by nematode infections.

1.4.3. Immune responses to parasitic nematodes

Nematode parasites have been well established as models for studying the development of TH2 immune responses and parasite-host interactions [6, 59, 87-96]. Nematode infections induce a robust TH2 immune response in the host, characterised by the secretion of the cytokines IL-4, IL-5, IL-9 and IL-13, as well as the production of type 2 antibodies (e.g. IgE) and recruitment of eosinophils, basophils and mast cells [97, 98]. Control of nematode infection is associated with smooth muscle cell, epithelial cell, B-cell, T-cell, macrophage, eosinophil, mast and goblet cell responses [5, 91, 97-100]. Human [101] and mouse [61, 89] studies have shown that the production of IL-4 and/or IL-13 cytokines generally correlates with protective immunity; namely reduced worm burdens and effective worm expulsion. However, this strong TH2 response is also associated with immuno-pathology in organs unrelated to the definitive stages of the parasitic infection, such as the liver, lung airways, and peritoneal cavity [6, 59, 98, 102-107].

1.4.4 N. brasiliensis life cycle and pathology

The murine nematode *N. brasiliensis* was used in this study in an infectious disease model to examine the effects of this parasite on pulmonary pathology. *N. brasiliensis* is a medically relevant model to use as the lung pathology arising from larval migration bears important similarities to that of analogous hookworm parasites [76, 88, 108]. The murine parasitic nematode *N. brasiliensis* infects the host through the skin, migrating via the blood system to the lungs [60, 108]. Here the worms move from the

blood vessels to pulmonary airways resulting in considerable lung damage and antigen deposition [104]. The latter induces a strong TH2 response, causing pulmonary inflammation, disruption of alveolar air spaces, haemorrhaging, eosinophilia and the development of airway hyperresponsiveness (AHR) [1-3, 88, 109, 110]. This results in both acute and chronic lung pathology [3, 4]. The acute pathology is strikingly similar to allergic airway disease [109], considered to be induced by the products from the worm (*N. brasiliensis* excretory and secretory products; NES). The chronic pathology can be likened to emphysemic symptoms, due the alveolar damage caused by migration of the worm through the lung [1]. *N. brasiliensis* is not retained in the lung, but exits the lung via the bronchii, where it is coughed up and swallowed resulting in the establishment of a definitive stage in the intestinal tract 3-4 days after initial infection [110]. *N. brasiliensis* (L_4 larvae) mature into adults (L_5) and produce eggs by 6 days post infection (p.i.) and are usually expelled in immunocompetent BALB/c mice by 9-11 days p.i. [60, 61, 110] (**Figure 4**). In contrast, the human analogues *Necator americanus* and *Ancylostoma duodenale* may reside in the human intestine for up to 5 years [76].

1.4.5. Immune response to N. brasiliensis.

An infection with *N. brasiliensis* induces an IL-4/IL-13-dependent [24], polarised TH2 cytokine and cellular response in the host lung and intestine, including type 2 antibody (e.g. IgE) and TH2 cytokine production (IL-4, IL-5, IL-9 and IL-13), as well as the recruitment of eosinophils, basophils and mast cells [4, 5, 91, 92, 97, 98, 111]. This results in an IL-4Rα-mediated TH2-dependent parasite expulsion as well as immuno-pathology in the lung and intestines [4, 5, 60, 92, 112]. Specifically, expulsion of *N. brasiliensis*, is dependent on IL-13 [113] and the TH2 responses driven by IL-4Rα-responsive non-haematopoietic cells such as epithelial, intestinal smooth muscle and

goblet cells, but is independent of IL-4Rα expression on haematopoietic cells [4-6, 61, 91, 114]. This TH2 response also creates a TH2 polarised inflammatory response in the lung, characterised by IL-4Rα-responsive pulmonary $CD4^+$ T-cells [4], which persists after expulsion of *N. brasiliensis* from the mouse [2].

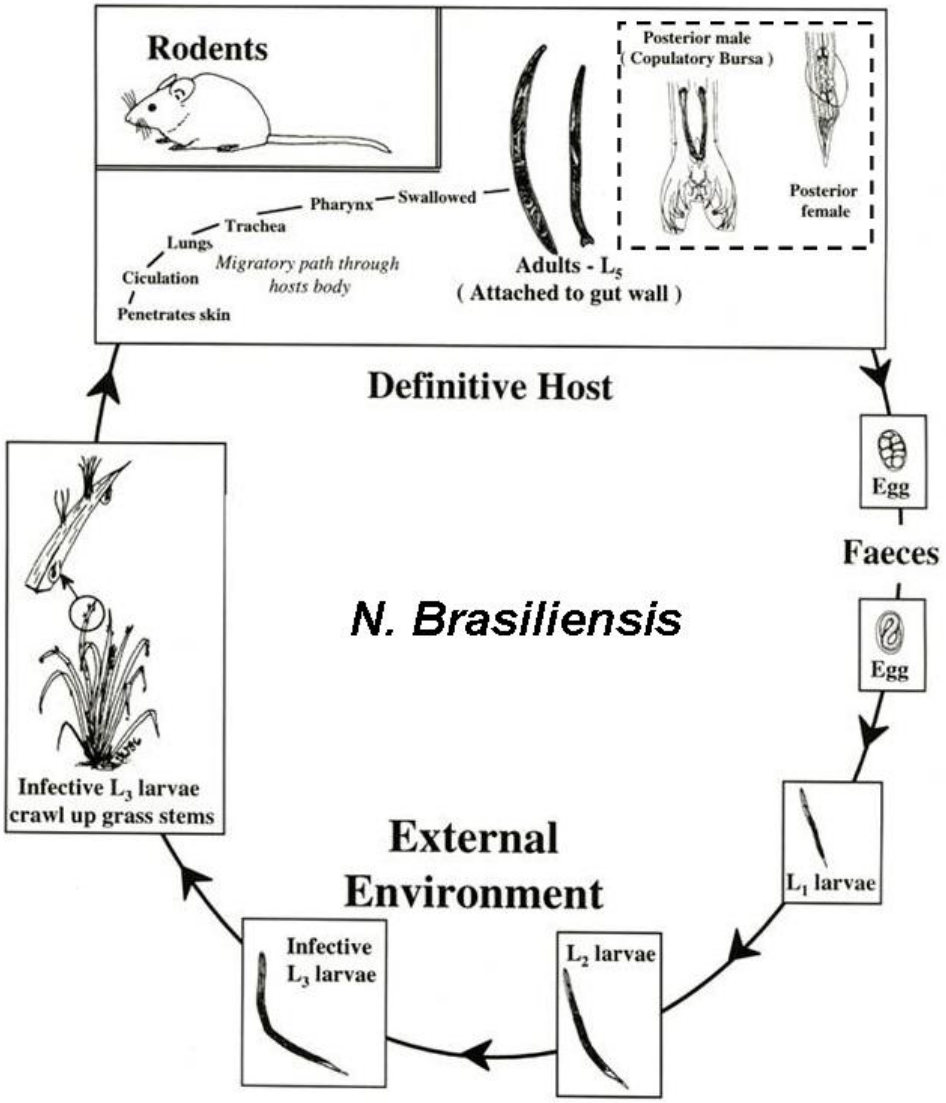

Figure 4: Life cycle of *N. brasiliensis.* Illustration adapted from the University of Cambridge [115].

1.4.6 N. brasiliensis-induced pulmonary immuno-pathology

During its development, the obligatory migratory phase of *N. brasiliensis* through the lungs of mice causes considerable pulmonary tissue damage (or lesions) and

associated cellular infiltration, airway goblet cell hyperplasia and mucus production [2, 4, 88, 116]. *N. brasiliensis*-induced pulmonary tissue damage consists of three distinct histological pathology: (i) rupturing of blood vessels, or haemorrhaging; (ii) the destruction of the alveolar architecture of the lung, known as alveolar dilatation and (iii) inflammatory lesions caused by cellular infiltration around blood vessels and bronchioles due to the migration of the parasite [88]. This is pathological evidence of the worm's migratory pathway, which involves rupturing through the pulmonary blood vessels, active migration through the lungs, disrupting alveolar architecture and migrating via the bronchioles to be coughed up and swallowed for its definitive stages in the intestine.

Although it was initially thought that these inflammatory lesions were only associated with the vascular system [117], later studies found granulomas around the parasite in secondary infections and inflammatory lesions around the bronchioles [2, 88], thus confirming the pathological evidence of worm migration. However, in chronic studies the pulmonary lesions continued to develop 36 days after the worm had been expelled from the mouse [2], suggesting that the lesions were due to a persistent immunological response rather than a direct response to the migrating parasite [2, 104, 118]. Recent studies have shown that this inflammatory response is predominantly due to IL-4Rα-responsive $CD4^+$ T-cells [4] and is driven by TH2 cytokines [92, 104]. Although the precise mechanism of this pulmonary immuno-pathology is unknown, it has been shown that *N. brasiliensis* excretory/secretory (NES) antigens can act as TH2-enhancing adjuvants and cause TH2 inflammation and asthmatic symptoms in the lung [3]. This could be a cause of the gross pathology seen in the lungs of the host.

A recent study by Marsland and colleagues (2008) [1] showed that in the chronic stages of infection, *N. brasiliensis* could cause symptoms of emphysema, even though the parasite was cleared from the host long before disease development. This was an important find as *N. brasiliensis* infections are not usually considered as a murine model of emphysema. Indeed, models of emphysema are usually induced by an imbalance of lung remodelling proteins such as matrix metalloproteinases (MMPs), cathepsins and other elastases [119-121]. These mechanisms and the immunology of chronic lung pathology will be covered in the following section.

1.5. Chronic Lung Diseases

N. brasiliensis migration through the lung causes substantial and chronic lung pathology, even after the worms have been expelled [2]. The lung pathology is similar to the pulmonary inflammation in allergic asthma [3] and the disruption of alveolar architecture seen in emphysema [1]. The following section highlights the importance of chronic lung diseases such as chronic obstructive pulmonary disease (COPD) and emphysema. *N. brasiliensis* infection of mice can be used as a model to study aspects of these chronic lung diseases [1, 2].

1.5.1. Chronic obstructive pulmonary disease (COPD)

There are a broad range of chronic lung diseases, some of which are grouped under the Chronic obstructive pulmonary disease (COPD) classification [122, 123]. COPD is a general term and classification of a group of diseases, defined by the irreversible and progressive pathological limitation or obstruction of airflow in the airways and the deterioration in lung function. COPD includes the diseases chronic bronchitis (CB) and emphysema under its classification. Chronic bronchitis refers to pathology or

inflammation in the upper respiratory tract, while emphysema is defined as the permanent enlargement, rupture or dilatation of the airways distal to the terminal bronchioles, which includes the respiratory bronchioles, alveolar ducts and alveolar sacs [122, 124, 125]. Therefore, emphysema and CB usually co-exist in the same individual, especially in severe cases [123]. Since COPD is an encompassing term, it is therefore used interchangeably with the terms emphysema and chronic bronchitis [125] .

1.5.2. Significance of COPD

COPD (and therefore emphysema and chronic bronchitis) is the fourth leading cause of death in the world, affecting 16 million people in the United States alone [121, 126]. It is predicted to be the third most common cause of death and fifth most debilitating disease in the world by 2030 [127]. COPD is such a major worldwide health problem primarily due to a poor understanding of its underlying cellular and molecular mechanisms and difficulty in early diagnosis, compounded with limited therapeutic treatment [124, 128, 129].

1.5.3. Symptoms and pathology

Being a relatively diverse group of diseases, the clinical syndrome of COPD includes a range of pulmonary manifestations [125, 130]. Patients with COPD have symptoms of a chronic cough and increased sputum production with dyspnoea (breathlessness) in the severe stages [125]. These are the pulmonary manifestations caused by the definitive airflow obstruction due to airway inflammation and lung parenchyma or alveolar destruction [131]. The diagnostic differences between emphysema and chronic bronchitis are almost indistinguishable, which is why they are grouped under COPD. However, their differences in lung pathology are clear. The pathological hallmarks of COPD are

alveolar dilatation or the destruction of the lung parenchyma seen in emphysema patients (**Figure 5**), and chronic inflammation of peripheral and central airways, characteristic of chronic bronchitis (CB) [122, 125]. The treatment for chronic bronchitis (COPD syndrome) involves daily administration of inhalant bronchodilators, with steroids and oxygen supplementation in the severe stages. However, there is unfortunately no specific treatment yet available for emphysema [132].

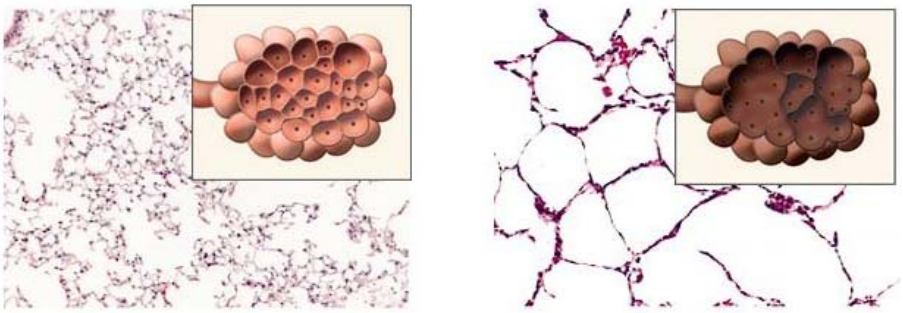

Figure 5: Lung pathology in emphysema patients. Healthy adult lungs (*left*) compared with lungs from a patient with emphysema (*right*). Magnification: 25X. Figure adapted from Taraseviciene-Stewart & Voelkel (2008) [125].

1.5.4. Causes of COPD/Emphysema

Causes of COPD/emphysema include the inhalation of noxious particles or gases. Genetic predisposition, such as alpha1-antitrypsin deficiency, which is an anti-protease that protects the lung against protease degradation, can also underlie the onset of COPD [119, 125, 133, 134]. Major causes of COPD are associated with long-term tobacco smoke exposure or smoking cigarettes and this constitutes 90% of COPD patients in developed countries [122, 126]. However, this may be a biased view as most studies are performed using smokers and non-smokers as control groups or on lung parenchyma obtained from lung volume reduction surgery (LVRS) [122, 124, 135]. Additionally, COPD can still progress in COPD patients who are non-smokers or who have stopped smoking for a number of years [122, 136]. Recent studies also indicate an immune or autoimmune component, [122-124, 136, 137] which could explain the continuous

exacerbations of both the structural (emphysema) [138] and inflammatory pathology (chronic bronchitis) of COPD in patients [129, 135, 139]. In addition to these causes of COPD, there is a well established "proteolytic hypothesis", which describes the molecular pathogenesis of protease-induced emphysema [119, 140].

1.5.5. Proteases and Emphysema

Since the discovery in 1964 that patients with severe alpha1-antitrypsin deficiency exhibited early emphysema, and that the administration of papain to rats also caused emphysema, a "proteolytic hypothesis" of the mechanisms in emphysema was formulated [119, 140]. This hypothesis describes how emphysema can be induced by an imbalance of the proteases, such as collagenases and elastases, and their anti-protease counterparts in the lung [119, 134, 141]. According to this hypothesis, this imbalance is provoked by external stimuli such as tobacco smoke that causes an infiltration of inflammatory cells (such as macrophages and neutrophils) which release their proteases, thus causing the protease-antiprotease imbalance. These factors lead to the proteolysis of lung connective tissue or elastin, and eventually emphysema [142]. Alternatively, the major pulmonary antiprotease, alpha1-antitrypsin, could be inactivated by oxidation induced by the free radicals in tobacco smoke, thereby decreasing its protective anti-proteolytic activity and thus causing the imbalance [119].

Since the birth of this hypothesis, there have been several mouse and human studies to further elucidate the molecular mechanisms of emphysema [119, 121, 122, 124, 125, 135, 136, 138-140]. Neutrophils and their protease, neutrophil elastase, can play a key role in the induction of emphysema, since neutrophil and macrophage numbers increase in the lungs of smokers and COPD patients. Therefore this potential release of neutrophil

elastase and MMP12 (or macrophage elastase) is also increased, as demonstrated by numerous MMP12 and neutrophil elastase murine and human studies [119, 125, 140, 143, 144]. It is hypothesized that the endogenous protease inhibitors are not induced enough to counteract the increased protease levels induced by smoking [119, 125, 140]. These endogenous protease inhibitors include cystatin C, which inhibits macrophage cathepsins, while the tissue inhibitors of metalloproteases (TIMPs) inhibit MMPs [140].

Interestingly, murine models of over-expression of TH1- and TH2-associated cytokines IFN-γ, TNF-α and IL-13, show an induction of chronic inflammatory conditions and alveolar dilatation associated with COPD [121, 138, 143]. The only infectious murine models of COPD used involved mice infected with either the murine-specific parainfluenza respiratory virus, the Sendai virus (SeV), or with the nematode *N. brasiliensis* [1, 145]. Since these studies, numerous different theories and classifications of COPD have been proposed from murine and human studies [119, 121, 122, 124, 125, 135, 136, 138-140].

1.5.6. Immunology of chronic pulmonary inflammation: COPD vs. asthma

Asthma and COPD, both characterized by airway obstruction, are common disorders with similar prevalence and global distribution, predominantly affecting the developed countries [123]. The strikingly similar characteristics of these disorders and their physiological overlap have resulted in the formation of two different schools of thought – both with convincing evidence. The Dutch hypothesis states that asthma and COPD are different forms of the same disease [146], while its counter argument, the British hypothesis states that these disorders are separate entities [147]. The similarities and differences in asthma and COPD immunology are outlined below.

The pulmonary pathology induced by *N. brasiliensis* and its antigens has similarities with asthma [3, 148] and COPD [1]. Asthma and COPD are both chronic inflammatory disorders of the airways [123] with several similarities and differences (**Figure 6**). Inflammation is mediated in both asthma and COPD by T lymphocytes, granulocytes and macrophages [137, 149]. Although B lymphocytes can play an important role in COPD, their function and mechanistic involvement are not fully understood [123]. In asthma, the disease-associated T lymphocytes are predominantly $CD4^+$ and the associated granulocyte populations are predominantly eosinophilic [150]. Asthmatic pathology is mediated via $CD4^+$ T lymphocytes and their TH2-associated cytokines (e.g. IL-4, IL-5, IL-13). These mediators induce asthmatic pathophysiology such as airway hyperresponsiveness, airway inflammation and excessive airway mucus production, leading to reversible airway obstruction [151]. Unlike asthma, the airway obstruction in COPD is irreversible, and the T lymphocyte populations appear to be predominantly $CD8^+$ [152] and are associated with a TH1 or TH17 response[119, 139], while neutrophils constitute the majority of the granulocyte populations [153]. The precise mechanism by which these TH responses exert their influences and physiological responses in asthma and COPD remains to be fully elucidated [123].

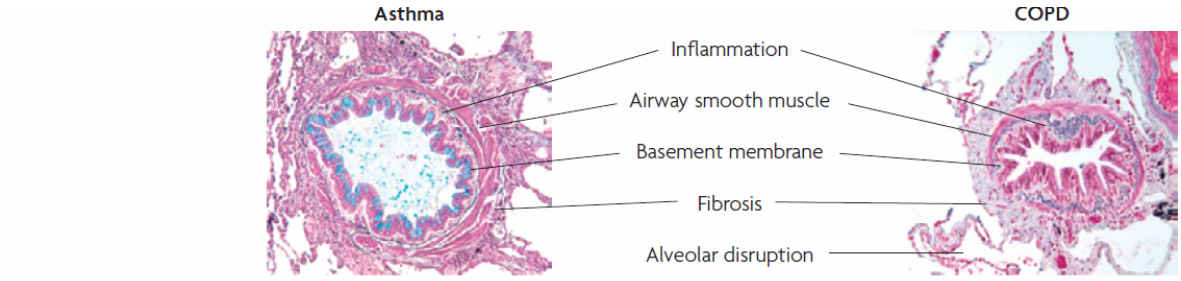

Inflammation	+++	+++
Airway smooth muscle	+++	+
Basement membrane	++	–
Fibrosis	+ (subepithelial)	+++ (peribronchiolar)
Alveolar disruption	–	+++
Airway vessels	++	No change
Mast cells	++ (and activated)	Normal
Dendritic cells	++	ND
Eosinophils	++	Normal
Neutrophils	Normal	++
Lymphocytes	T_H2 type	T_H1 and T_C1 type
Epithelium	Often shed	Pseudostratified
Goblet cells	++	++

Figure 6: Similarities and differences between Asthma and COPD. Figure taken from Barnes, P.J. (2008) [123].

1.5.7. Autoimmune component of COPD

Besides the classic paradigm that the pulmonary matrix protease-antiprotease imbalance causes alveoli destruction and inflammation in COPD, there is a recent perception that there could be an autoimmune component of COPD that could be an underlying cause of the chronic disease [129, 139].

The lungs of COPD patients show an increase in macrophages, neutrophils, DCs and T and B lymphocytes due to cellular recruitment in response to tobacco smoke [123]. The increase in macrophage and neutrophil numbers present in the lungs of COPD patients has been directly implicated in alveolar pathogenesis through secretions of proteases such as MMP12 [154] and neutrophil elastase, respectively [155, 156]. Indeed,

alveolar macrophages are central to the inflammatory response as there has been a strong correlation between increases in alveolar macrophages and COPD inflammatory progression, particularly at the sites of tissue damage, since they are known to express pro-inflammatory mediators [156, 157]. These mediators are increased in the sputum of COPD patients and include chemokines such as IL-8 to attract more neutrophils, thus further amplifying the elastin destruction by increased pulmonary matrix proteases and TH1-specific chemokines including CXCL9, CXCL10 and CXCL11 [139, 158]. This destructive process is further amplified by the increased expression of CXCR3 on the surfaces of alveolar macrophages that respond to CXCL9, CXCL10 and CXCL11 and result in the further increased production of MMP12 [159].

Additional strong evidence of autoimmunity include T-cells reactive to elastin and increased IFN-γ and elastin-specific antibody levels in the blood from COPD patients [138]. Further evidence includes increased levels of IL-17 in airways of mice exposed to long-term tobacco smoke [160], and increased numbers of effector cytotoxic $CD8^+$ T-cells and apoptosis-related tissue damage in the emphysematous lung [161].

1.6. Alternatively activated Macrophages (AAMs)

Of particular interest in this study is the role played by macrophages, specifically alternatively activated macrophage (AAM) populations, in the lung. *N. brasiliensis* elicits a TH2 response in the lung associated with the TH2 cytokines IL-4 and IL-13 and infiltration of Type 2 cells [4], which together induce macrophages to become alternatively activated [1, 7]. Therefore, it is IL-4Rα-responsive macrophages which are able to develop into the alternatively activated phenotype which has been associated with being protective against a range of pathology [59, 72, 162, 163]. Alternatively activated macrophages, or M2 macrophages, have been associated with the control of inflammation [59, 72], down-regulation of TH2 responses, enhanced wound healing [162], and tissue damage [1] in the lung. Additionally, AAMs have been shown to control viral-induced lung damage in a IL-4Rα-dependent way [164]. As such this population of macrophages may be capable of protecting the lung from COPD.

Since their identification [165], AAMs have been defined [166] as macrophages induced by the TH2 cytokines IL-4/IL-13, resulting in up-regulation of mannose receptor (MR) [165]. In contrast to their TH1 associated pro-inflammatory classically activated macrophage (caM) counterparts, AAMs elicit immunity against multicellular pathogens, anti-inflammatory, wound healing and pro-fibrotic effects [166, 167].

AAMs have been characterised by IL-4Rα-driven increased *arginase-1* expression [72, 166-170], induction of chitinase and FIZZ family members (ChaFFs) [171] and chitinase-like molecules [171-173], along with other biomarkers such as peroxisome proliferator-activated receptor γ (PPARγ) and mannose receptor (MR). Arginase-1 is associated with repression of NO production, suppression of TH2 cytokine activity [72] and

production of proline [169, 174]. Together these effects of arginase-1 activity constitute an array of anti-inflammatory, tissue repair and pro-fibrotic-associated responses [175]. MR is a C-type lectin involved in endocytosis [170], while PPARγ is a component of transcriptional regulation, mainly involved in regulating glucose and lipid metabolism, but has recently been suggested to be involved in inflammation and atherosclerosis [176].

Helminth infections have been central to AAM-associated studies due to their strong induction of TH2 responses. The up-regulation of AAMs has been associated with a range of helminth infections (**Table 2**). AAMs have been associated with the expulsion of helminths such as *N. brasiliensis* [177] and *H. Polygyrus* [93]. Using $LysM^{Cre}IL\text{-}4R\alpha^{-/lox}$ mice, which do not have IL-4Rα-responsive macrophages, mice infected with *S. mansoni* died from enhanced liver and intestinal pathology and septic shock [59]. Interestingly, the increased mortality rate of mice deficient for macrophage-specific Arginase1 was not due to septic shock but from exacerbated inflammation, which was associated with uncontrolled $CD4^+$ T-cell proliferation, and liver fibrosis [72]. Additionally, *S. mansoni*–induced AAMs controlled $CD4^+$ proliferation by depletion of the arginine source, since addition of arginine restored $CD4^+$ T-cell proliferation in co-culture studies [72]. Other helminth infection studies, such as that of *Brugia malayi*, have shown that isolated AAMs from *B. malayi*–infected mice suppress $CD4^+$ T-cell proliferation *in vitro* [178]. Additional *B. malayi* studies have shown that IL-4-dependent alternative activation of macrophages can occur without adaptive immunity and that these macrophages are involved in wound healing [162]. Despite the fact that the macrophages portray the same AAM biomarkers (**Table 2**),

these diverse studies on an even more diverse variety of parasites begs the question of whether or not the macrophages are identical in form.

Table 2 Common helminth-associated AAM biomarker molecules. Adapted from Reyes & Terrazas (2007) [179].

Parasite	AAM biomarker	Suppressive activity	Role in disease	Ref
Nematodes				
Brugia Malayi	Fizz1, Ym1, Arg1	Yes (contact dependent/TGF-β-partially dependent)	Unknown	178, 180-182
Litomosoides sigmodontis	Fizz1, Ym1, Arg1	Yes (contact dependent/TGF-β-partially dependent)	Unknown	183
Nippostrongylus brasiliensis	Fizz1, Fizz2, Yml, Arg-1, MMR AMCase IL-21R	Unknown	Lung homeostasis after acute injury	171, 172, 184
Heligmosomoides polygyrus	Fizz1, Ym1,MR AMCase, IL-4R	Unknown	Host protection, arginase-mediated parasite clearance	93
Trematodes				
Schistosoma mansoni	Fizz1, Ym1, Arg1 AMCase, MR, IL-21R	Yes (PD1-PDL pathway dependent)	Divergent role: Host protection down-modulate TH1-mediated immuno-pathology and progressive lung pathology and liver granuloma formation	59, 185
Fasciola hepatica	Fizz1, Ym1, Arg1	Unknown	Unknown	186, 187
Cestodes				
Taenia crassiceps	Fizz1, Ym1, Arg1, MR, mMGL, CD23, CCR5, TREM2	Yes (PD1-PDL pathway dependent and ROS partially dependent)	May favour parasite installation	188-191

Fizz 1, found in inflammatory zone 1; AMCase, acidic mammalian chitinase; LOX, lipoxygenase; MR, macrophage mannose receptor; Arg-1, arginase-1; PD, programmed death receptor; PDL, programmed death ligand; CCR5, CC chemokine receptor 5; mMGL, mouse macrophage galactose-type-C-type lectin; TREM, triggering receptor expressed on myeloid cells, ND, not determined.

It has been suggested that since macrophages are both innate and adaptive immune cells, they are the first to respond to pathogens and thus initiate the type of response by differentiating into classically or alternatively activated macrophages [192]. Therefore, the macrophages could produce distinct chemokine and chemokine receptor spectrums to initiate and to stabilise classical and alternative activation [193]. Mantovani and colleagues [192] have classified these chemokines and associated them

with macrophage activation or TH subset differentiation. For example, the chemokines CCL24, CCL22 and CCL17 are induced by the cytokines IL-4 and IL-13 and have been implicated as AAM biomarkers [166]. However, instead of one classification of AAMs, three classifications of AAMs have been proposed: M2a, M2b and M2c [167, 193]. M2a macrophages are considered to be IL-4/IL-13-induced macrophages, M2b are macrophages exposed to agonists of TLRs and immune cells and the M2c classification refers to IL-10 and glucocorticoid hormone induction of macrophages[167, 193]. For the sake of simplicity, macrophage activation will be classified as either classically or alternatively activated, unless stated otherwise.

From the above evidence, AAMs show a down-modulated inflammatory response associated with a healing phenotype. Although a good body of knowledge has been gained from helminth infection models to further elucidate the functions of AAMs, much needs to be elucidated with respect to *N. brasiliensis*-induced pulmonary infections.

1.7. Aims, Hypothesis and Objectives

The aim of the present study was to investigate the development of pulmonary pathology following acute (5 days p.i.) and chronic (42 and 180 days p.i.) *N. brasiliensis* infection, with focus on IL-4Rα-responsiveness by macrophages.

It has been recently established by Mearns (MSc. Dissertation, 2007) [57], that mice, which lack IL-4Rα specifically on macrophages and neutrophils ($LysM^{Cre}IL\text{-}4R\alpha^{-/lox}$) show exacerbated inflammatory lesions at 42 days p.i. (unpublished results) when compared to control littermate mice ($IL\text{-}4R\alpha^{-/lox}$) and IL-4Rα-deficient ($IL\text{-}4R\alpha^{-/-}$) mice. As it is known that AAMs down-modulate inflammation during a TH2-polarized nematode infection [59, 72] and that $LysM^{Cre}IL\text{-}4R\alpha^{-/lox}$ mice lack functional AAMs [59], we hypothesized that IL-4Rα-responsive macrophages are alternatively activated in the lung and that they may control inflammation.

To test this hypothesis we performed comparative *N. brasiliensis* infectious studies in global or macrophage/neutrophil-specific IL-4Rα-deficient mice and their littermate controls and investigated pathological, histological, immunological and molecular parameters. Thus the results section of this thesis is divided into three main chapters: 1) Lung Pathology; 2) Immune responses; and 3) Alveolar macrophage characterization.

2. MATERIALS AND METHODS

2.1 Mice

Male mice (6 to 10 weeks old and 4-5 per group) were housed in individually ventilated cages in specific-pathogen-free conditions in the Animal Unit at the University of Cape Town (UCT). IL-4Rα-deficient (IL-4Rα$^{-/-}$) mice [62] and macrophage/neutrophil cell-specific IL-4Rα-deficient (LysM^{Cre}IL-4Rα$^{-/lox}$) mice [59] were previously described, generated and characterized. Littermate control mice hemizygous for IL-4Rα (IL-4Rα$^{-/lox}$) were considered as wild type (WT) mice and used as controls in all experiments. All mice were backcrossed on a BALB/c background to at least the F9 generation and were genotyped prior to experiments to confirm their genotype using gene-specific primers (carried out by laboratory staff). Mice were euthanized at days 5, 42 and 180 p.i. by CO_2 asphyxiation. All animal procedures were carried out in an Animal Biosafety Level 2 Laboratory (Animal Unit, UCT) and all experiments were conducted in accordance with and approved by the Research Animal Ethics Committee of UCT.

2.2. Maintenance of N. brasiliensis life cycle

N. brasiliensis worms were passaged routinely in Wirstar rats. Live third-stage (L_3) larvae were prepared in 0.65% NaCl at 10 000 worms/ml. Six to eight rats were injected subcutaneously in the flank of the leg with 500 µl of the worm solution using 20G needles (Braun, Melsungen, Germany). At 5 days p.i., rats were transferred to gridded cages for faecal collection, the bottom of which were lined with damp paper to keep faecal pellets moist. Faecal pellets from infected rats were collected daily from day 6 to day 8 p.i. and soaked each day in ddH_2O water containing Fungizone (Gibco Life Technologies). Pellets were mixed into a paste-like consistency and

spread onto prepared culture dishes consisting of a large petri dish containing a filter paper and a piece of square gauze, both moistened in Fungizone (Gibco Life Technologies), to act as reservoir. The dishes were incubated in humidified containers at 25ºC for at least 5 days to allow L_3 larvae to migrate to the edge of the damp filter paper. The outer layers of filter paper containing the worms were removed and transferred to fresh culture dishes for further incubation and to keep the worms moist until they were used for infection.

2.2.1 Preparation of N. brasiliensis worms and infection

Pieces of filter paper containing fresh L_3 larvae were placed in 0.65% NaCl and counted in a petri dish on a dissecting microscope to prepare a solution of 3750 worms/ml in 0.65% NaCl. The infection of mice was carried out in an Animal Biosafety Level 2 Laboratory (Animal Unit, UCT). Mice were injected subcutaneously with 750 worms in a total volume of 200 u1 0.65% NaC1 using a 21G needle (Braun). Naïve control mice were WT (IL-4Rα$^{-/lox}$) and were injected with 200 µl of 0.65% NaCl (without *N. brasiliensis* L_3 larvae).

2.3. Measurement of airway hyperresponsiveness (AHR)

Similar to Marsland *et al.* (2008) [1], airway hyperresponsiveness (AHR) was measured using 1X PBS (control) and increasing concentrations of β-metacholine (MCh) (Sigma-Aldrich, Munich, Germany) (5, 10, 20 mg/ml) in whole-body plethysmographs (Emka Technologies, Paris, France) and analysed using Iox2 Software (Emka Technologies, Paris, France). Briefly, individual, unrestrained, conscious mice were placed in a whole-body plethysmograph (Emka Technologies) and baseline measurements were taken for 5 minutes. Mice were then subjected to

aerosolised 1X PBS (control), and exposed to increasing MCh (Sigma-Aldrich) concentrations of 5, 10, 20 mg/ml for 1 minute. Mice were then monitored and measurements were taken for 15 minutes, using Iox2 Software. Enhanced Pause (PenH), a dimensionless parameter, was calculated using the following equation from Hamelman *et al.*, (1997) [194]: PenH = (Te/Tr - 1) x (PEP/PIP) (Te: expiratory time; Tr: relaxation time; PEP: peak expiratory pressure, PIP: peak inspiratory pressure).

Averages of PenH for the first 5 minutes were subtracted by the individual average baseline readings to give a final PenH value for each individual mouse. Maximum PenH values were observed at 10mg/ml MCh and these results were used throughout the study.

2.4. Histology and Scoring of pathology

At each time point, mice were killed by CO_2 asphyxiation and the lungs were carefully removed and fixed in 4% formalin (in 1X PBS) for a minimum of 24 hours. All histology sections were prepared by the Department of Histology, Groote Schuur Hospital. The lungs were mounted in paraffin blocks for sectioning and the tissue sections were then fixed and stained with haematoxylin and eosin (H&E) by laboratory staff (Groote Schuur Hospital). All pathological scoring and analysis was carried out by viewing multiple sections of whole lungs on a light microscope by the researcher and an independent observer (clinical pathologist). In order to distinguish any differences between the groups, each section of tissue was evaluated using a scoring system for intra- and inter-group statistical analysis. Pulmonary pathological scoring was based on severity and quantity (for inflammation and alveolar dilatation), using a relative scale (0-3; 0: none, 1: mild, 2: moderate, 3: severe or more than 50% of lung area). This was carried out objectively in accordance with accepted clinical

and pathologist guidelines and adapted from Radosevic *et al* (2007) [195]. Inflammation severity scores were defined as any focal cell infiltrate and based on the density and relative size of the area occupied of the most affected lung or lobe. Similarly, alveolar dilatation scores were based on the most or worst amount of alveolar damage, and scored using the same relative scale.

2.5. Preparation of lung single-cell suspensions

Single-cell suspensions from processed lung digests were used for re-stimulation assays, flow cytometry analysis or cell sorting of alveolar macrophages. Briefly, lung lobes were perfused (1mM EDTA in 1X PBS) and individually removed, minced into fine pieces and digested in Digestion Buffer (Appendix A) for 90 minutes at 37º C. Digested lung tissue were then pushed through 70 µm nylon cell strainers (Becton-Dickson, New Jersey) and subjected to red cell lysis for 2 minutes in Red Cell Lysis Buffer (Appendix A). Remaining cells were collected by centrifugation (1200rpm, 4ºC, 5 minutes) and re-suspended in 1ml DMEM. Aliquots of the suspension (10 µl) were diluted in trypan blue (1 in 10 dilution) to determine cell viability and the cell concentrations was determined using a Neubauer haemocytometer. Cell volumes were adjusted to attain cell concentrations of $4x10^6$ cells/ml. The media was changed to either IMDM (supplemented with 10% FCS, 100U/ml penicillin G, 100µg/ml streptomycin) for lung re-stimulations, or to FACS buffer (1X PBS supplemented with 0.1% BSA and 0.05% NaN_3) for flow cytometry analysis or FACS cell sorting.

2.5.1. Lung Re-stimulations

The above single-cell suspensions of individual lung digests in IMDM (supplemented with 10% FCS, 100 U/ml penicillin G, 100 µg/ml streptomycin) were separately

seeded in triplicate into a flat-bottomed 96-well plate (Nunc Maxisorp; Thermo Fisher Scientifica, Roskilde, Denmark) at $4x10^5$ cells per well. The cells for each individual mouse lung were re-stimulated either with anti-CD3 (20 μg/well), somatic antigen (10 μg/well) or media (controls) in total volume of 200 μl in each well and incubated for 48 hours at 37ºC and 5% CO_2.

2.5.2. Flow cytometry analysis on lung cell populations

For analysis of the cellular compositions of lung inflammatory infiltrates, aliquots of $1x10^6$ single-cell lung suspensions from individual mouse lungs were transferred into FACS tubes and stained with a cocktail of antibodies (refer to Appendix B and C for antibody details and gating strategies, respectively). To identify the different cell types we used the following antibody panels: anti-CD3, anti-CD4 and anti-CD8 for T cell staining, anti-CD11c and anti-MHCII for alveolar macrophages, anti-GR-1 and anti-CCR3 for eosinophils and neutrophils and anti-B220 for B-cells. All cell staining was performed in FACS buffer (PBS supplemented with 0.1% BSA and 0.05% NaN_3) containing 1% heat-inactivated rat serum and 1% anti-FcγRII/III. Total viable cell counts (determined by trypan blue exclusion) and flow-cytometric data was used to determine absolute numbers of cell populations. A total of 50 000 cells were acquired per sample on a FACS Calibur (BD Biosciences, San Jose, CA, USA) and the acquisition data analysed using CellQuest Pro (BD Biosciences, San Jose, CA, USA) and FlowJo v7.2 (Tree Star, Inc., Ashland, Oregon, USA).

2.6. Alveolar Macrophage cell sorting by FACS

Alveolar macrophages were defined according to Kirby *et al*. (2009) [196], as autofluorescent $CD11c^{Hi}$ $MHC\text{-}II^{Int/Lo}$. Single-cell suspensions of pooled lungs (as

described above) were stained with CD11c-PE and MHC-II-Biotinylated/APC, isolated using a magnet cell sorting (MACS) bead system (Miltenyi Biotec, Germany) and sorted above 98% purity on a FACSVantage (Becton-Dickinson, South Africa) for subsequent RNA extraction and analysis under sterile conditions. (Refer to Appendix B for FACS antibody details and to **Figure 14**, Chapter 3.3 for the gating strategy.) Essentially, lung digest cells were stained with anti-CD11c-PE (1:160 dilution in FACS buffer containing 1% heat-inactivated rat serum and 1% FCyR blocker (anti-FcyRII/III)) and were enriched by positive selection for $CD11c^+$ cells on MACS columns (Miltenyi Biotec, Auburn CA, USA), as per manufacturer's instructions. Enriched $CD11c^+$ cells were stained with biotinylated anti-MHC-II antibody (with 1% anti-FcyRII/III), followed by Allophycocyanin (APC) conjugated to streptavidin (SpA-APC; 1:400 dilution) in MACS Buffer (0.5% BSA, 2mM EDTA in 1X PBS at pH 7.2). Sterile FACS buffer (PBS supplemented with 0.1% BSA and 0.05% NaN_3) was used for the final wash and cells were re-suspended to a concentration of $5x10^6$ cells/ml. Cells were sorted, for CD11c-PE^{Hi} MHC-II-Biot-$APC^{Lo/int}$ using a FACSVantage cell sorter and a 100µm nozzle. Dead cells were excluded by 7-AAD staining (Sigma).

2.6.1. RNA extraction

Purified alveolar macrophages ($CD11c^{Hi}$, MHC-II^{Lo}) [196] of >98% purity, were lysed in RLT Buffer (Qiagen, Valencia, CA, USA) and stored at -80ºC until ready for use. RNA was extracted using the RNeasy Plus Micro Kit (Qiagen, Valencia, CA, USA), as per manufacturer's instructions. Deviations from the manual included: β-mercaptoethanol was added to RLT Buffer before use and cells were lysed in 350-700 µl RLT buffer by repetitive pipetting; and the elution step was repeated and both 14µl

RNA elutes pooled. The RNA was stored at -80^{o}C until used. The quality, integrity and quantity of the RNA (2 µl aliquots) were assessed on a BioAnalyzer 2100 (Agilent, Santa Clara, California, USA) at the Centre for Proteomics and Genomics Research (University of Cape Town).

2.6.2. Microarray Design and Analysis

To examine gene expression profiles of murine CD11c^{Hi}, MHCII^{Lo} alveolar macrophages[196] (AlvM) during *N. brasiliensis* infection, microarrays were run in collaboration with Dr. Alun Kirby (University of York), according to a two-colour experimental reference design. An outline of the design is shown in **Figure 7**. The author isolated the AlvMs and extracted the RNA from naïve and infected mice lungs and performed the final data analysis and statistical tests, while microarrays were custom-designed, printed, assayed and the raw data processed by the laboratory of Dr Kirby. Each microarray contained cDNA probes for 460 gene targets that were annotated by Dr. Kirby with Gene Ontology (GO) terms including: apoptosis, cytokines, chemokines, surface receptors, signalling, pathogen recognition and immunoregulation (gene symbols, full names and aliases, functional clustering and accession numbers are listed in Appendix E). Targets were selected based on preliminary whole-genome analysis of murine alveolar macrophages (AlvM) (A. Kirby; unpublished data), and on published reports of molecules potentially involved in AlvM (and dentritic cell) function, to facilitate the definition of macrophage-specific gene expression profiles (researched by A. Kirby).

Comparison of each test sample to an identical, pooled reference RNA in this experimental design permits both intra- and inter-group comparisons to be made. The

reference ("Ref.") RNA samples were extracted by Dr. Kirby from unelicited peritoneal macrophages which were isolated from naïve mice. "Naïve" and "infected" refer to RNA samples extracted by the author, using the RNeasy Plus Micro Kit (Qiagen), from AlvMs of naïve mice or mice that were infected with *N. brasiliensis*, respectively as described above (Sections 2.6.1 and 2.6.2). Each biological infection experiment was performed independently of each other by the author and none of the RNA samples from the biological repeat experiments were pooled.

The genomic DNA-free total RNA was then sent to the laboratory of Dr Kirby, where the RNA samples were processed for microarray analysis using their standardized protocols. These custom "macrophage microarray" slides were manufactured in-house at the Genomics Division of the Technology Facility (University of York, UK) where a Genetix QArrayMini compact arrayer was used to print 70-mer oligonucleotides from Operon (Eurofins MWG Operon, Ebersberg, Germany) onto Nexterion slide E glass slides (Schott North America, Inc., Elmsford, NY, USA).

Briefly, RNA from test samples or reference RNA were linearly amplified (single round) using the Amino Allyl (aa) MessageAmp™ II CyDye aRNA Amplification Kit (Applied Biosystems Inc., Foster City, CA, USA) as per the manufacturer's instructions. Amplified aaRNA was then labeled with either Cy3 (for reference RNA) or Cy5 dye (for test sample RNA) using the same kit, and equal amounts of labeled reference and test RNA (min 500ng, max 5000ng) were combined and hybridized overnight in a humidified chamber to custom macrophage microarray slides at 42^{o}C according to the Nexterion Slide E protocol [197]. After hybridization, the microarray slides were washed and dried using Nexterion protocols. The microarray slides were

scanned immediately using an Axon GenePix 4000A (Axon Instruments/Molecular Devices Corporation, Sunnyvale, CA, U.S.A) scanner and GenePix Pro 5.1 software running on a Windows XP operating system using standardized parameters of the Technology Facility (University of York, UK). All RNA amplification, hybridization and subsequent image analysis, data normalization and background correction was done by Dr Kirby. Image data was normalized using GenePix Pro 5.1 software so that arithmetic mean of the expression ratios of the housekeeping genes was equal to 1. The background fluorescence was calculated by applying the internal background algorithm of GenePix Pro 5.1. Median backgrounds were subtracted from mean fluorescence values to obtain specific fluorescence levels for each spot on the chip. Dr Kirby provided normalized, background-corrected data to the author for in-depth analysis and biological interpretation.

2.6.2.1. Microarray Data Analysis

The normalized, background-corrected microarray data was analysed in Microsoft Excel 2003 and TM4 Multi-experiment Viewer (MeV) Software Package [198]. Due to artifacts of the hybridization process, some negative Cy5/Cy3 expression ratios (Naive vs. Reference; or Infected vs. Reference) were obtained after background subtraction, and were subsequently discarded. Gene expression values that were >10 were considered "saturated" and given a maximum default value of 10. The gene expression ratios were then $\log_2$ transformed (now called M-values) to optimally measure and visualize the degree to which different genes alter their transcription levels.

Significantly differentially expressed genes were identified by a two-tailed, paired T-test comparing the M-values of both experimental repeats of one mouse group with the another mouse group. Genes were considered to be significantly differentially expressed only if $p < 0.05$. The fold change (FC) in gene expression between IL-4Rα$^{-/lox}_{(Naïve)}$, IL-4Rα$^{-/lox}_{(infected)}$, LysM^{Cre}IL-4Rα$^{-/lox}_{(infected)}$ and IL-4Rα$^{-/-}_{(infected)}$ groups at different times post-infection, was calculated by subtracting the M-values of one group from another using the equation below:

$$FC_{(Group1\ vs.\ Group2)} = M\text{-}value_{(Group1)} - M\text{-}value_{(Group2)}$$

The FC-values were exported into the TM4 Multi-experiment Viewer (MeV) Software Package [198] and heat-maps generated to visualize global and significant changes in gene expression between experimental groups. In accordance with Minimum Information about Microarray Experiments (MIAME) compliance [199], the microarray design, methodology and data will be deposited in a MIAME compliant public database (by Dr Kirby) at a later date. Preliminary literature database mining was carried out using MILANO, created by Rubinstein *et al* (2005)[200]. The Milano Literature mining tool [200] (http://milano.md.huji.ac.il) was used to search the PubMed [201] database to see if any of the differentially expressed genes has been shown to play a role in *N. brasiliensis* infection, inflammation, lung remodelling, and/or macrophage activation (MILANO search keywords: "macrophage activation", "alternatively activated macrophage", "activation", "lung remodelling", "lung", "inflammation", "emphysema", "alternative activation", "M2"). Manual literature searches were done for a smaller set of candidate genes using PubMed [201], AceView [202], OMIM [203] and Entrez Gene [204] databases.

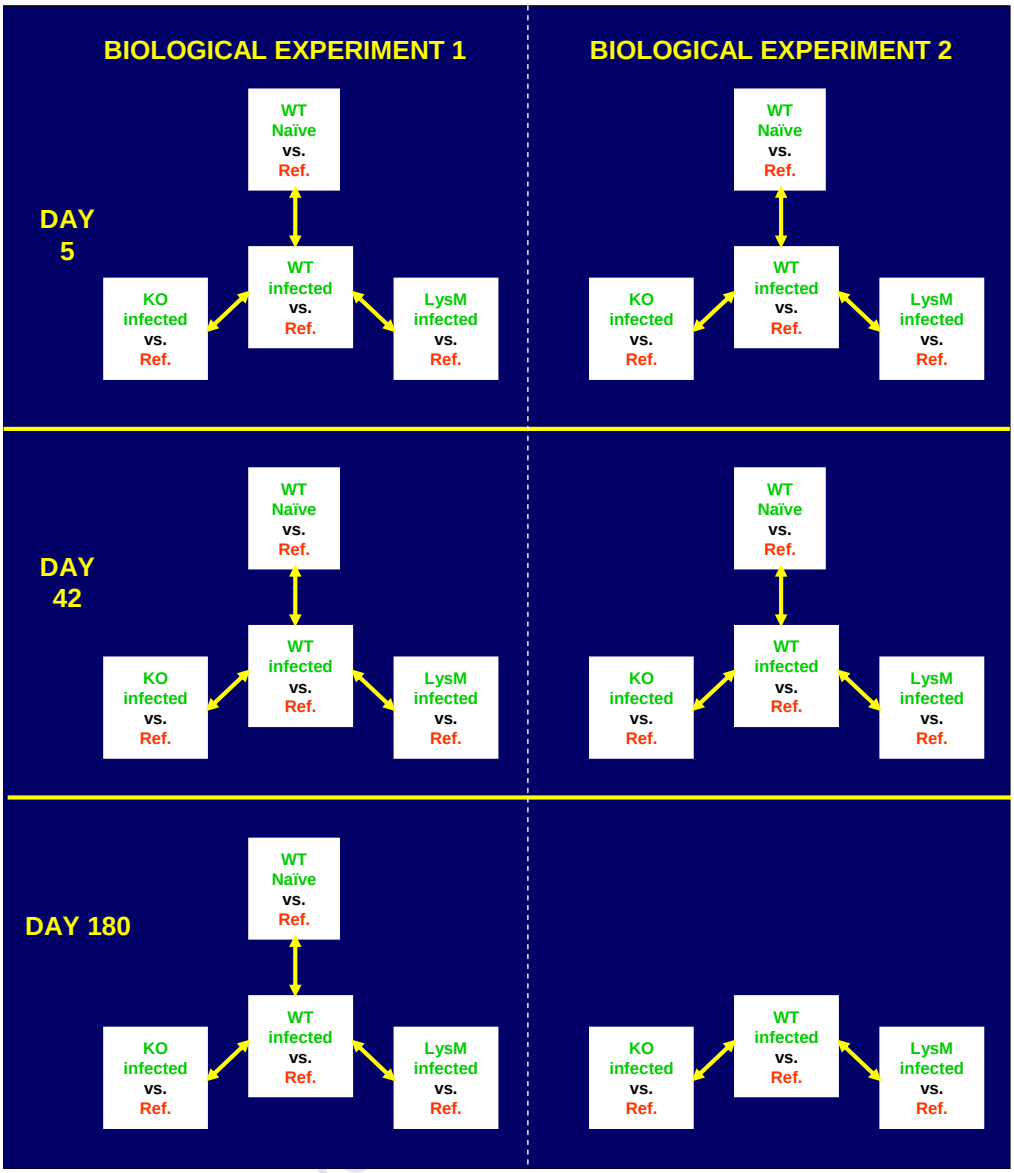

Figure 7: Experimental design for the microarray analysis of AlvM genes. The gene expression patterns of Naive vs. Reference or Infected vs. Reference within each experimental mouse group were compared. Each white rectangle represents a two channel microarray interrogating 460 genes known to be expressed in macrophages. The Reference sample (naive unelicited peritoneal macrophages) was labelled with Cy3 dye (*labelled "Ref" in red text*) and the experimental samples (from naïve IL-4Rα$^{-/lox}$ (WT) mice, or *N. brasiliensis* infected WT, IL-4Rα$^{-/-}$ (KO) and LysM^{Cre}IL-4Rα$^{-/lox}$ (LysM) mice at 5, 42 or 180 days p.i.) were labelled with Cy5 (*green text*). Comparison of the M-values (Log_2-transformed Cy5/Cy3 expression ratios) between each mouse group generated fold change (FC) values (depicted by *yellow arrows*). Significance ($p < 0.05$) of differentially expressed genes were identified by a two-tailed, paired T-test, which compared M-values of duplicate experiments between mouse groups . Two independent biological repeat experiments were analysed over 23 individual arrays (there was only one naïve IL-4Rα$^{-/lox}$ (WT) sample for day180). Key: WT: IL-4Rα$^{-/lox}$, KO: IL-4Rα$^{-/-}$, LysM: LysM^{Cre}IL-4Rα$^{-/lox}$.

2.7. Ex vivo T-cell re-stimulation

$CD4^+$ T-cells were enriched (> 80% purity) from pooled mediastinal lymph nodes (MST LN) at 5 days p.i. using the BioMag bead system (Qiagen). Briefly, MST LN were removed aseptically and kept in DMEM on ice. Single-cell suspensions were prepared by forcing the tissue through 70 μm nylon cell strainers (BD Biosciences), and subjected to red cell lysis. Remaining cells were collected by centrifugation (1200rpm, 4ºC, 5 minutes) and stained with anti-CD8 (53.6.72), CD11b (M1/70), GR-1 (RB68C5), B220 (RA36B2) and the FcγII and III receptors were blocked with anti-FcγRII/III (2.4G2) antibody (antibody dilutions and details in Appendix B). Stained cells were depleted using goat anti-rat-IgG coated BioMag beads (Qiagen). The remaining $CD4^+$ T-cells in the supernatant were collected and counted on a Neubauer haemocytometer. Sorted $CD4^+$ T-cells were plated at $2x10^5$ cells/well in a 96-well plate (Nunc Maxisorb) and re-stimulated with anti-CD3 (20 μg/well) in IMDM (containing 10% FCS, 100 U/ml penicillin G, 100 μg/ml streptomycin) and cultured for 48 hours at 37ºC in a humidified 5% CO_2 incubator. To determine the purity of $CD4^+$ cell populations, remaining cells were stained with anti-CD4 Phycoerythrin (PE)-conjugated antibodies (Appendix B; procedure similar to above) and analysed on a FACS Calibur using CellQuest Pro software.

2.8. Cytokine ELISAs

Sandwich ELISAs were performed on cell culture supernatants from *ex-vivo* T-cell and lung digest re-stimulations to measure IL-4, IL-13, IFN-γ and IL-10 levels in the mediastinal lymph nodes (MST LN) and lungs, respectively. For all solutions and ELISA antibody details, refer to Appendix A and D. Briefly, 96-well plates (Nunc Maxisorb) were coated with 50 μl capturing antibody (diluted in 1X PBS) and

incubated overnight at 4°C. The coated plates were washed four times (between each step) in Wash Buffer and subsequently blocked with 200 µl Blocking Buffer overnight at 4ºC. Three-fold dilutions of the samples were prepared in Dilution Buffer ranging from a 1/3 dilution to a 1/27 dilution, while recombinant standards were diluted two-fold from either 100ng/ml or 250ng/ml. After blocking, 50 µl of the diluted standards, samples and blanks were added and incubated overnight at 4ºC. For each cytokine, 50µl of the corresponding biotinylated anti-mouse detection antibody was added and the plates incubated at 37 ºC for 3 hours. 50 µl of streptavidin conjugated to horse radish peroxidise (HRP) (1/5000 dilution) was added to the wells and incubated at 37 ºC for 1 hour. 50µl of ELISA Substrate Buffer was added and the developing reaction was stopped by adding 25µl of 1M H_3PO_4. The absorbance of the samples were measured at 450nm (against its reference measurement at 540nm) on a VersaMax microplate reader (Molecular Devices Corporation, Sunnyvale, CA, U.S.A).

2.9. Myeloperoxidase (MPO) Assay

The MPO activity assay, adapted from Remaux *et al.* (2003) [205] was used as a measure of activated neutrophil infiltration within tissues. MPO activity was quantified, by measuring its hydrogen peroxide (H_2O_2) hydrolysis in a colorimetric reaction, on individual *N. brasiliensis*-infected and naïve lung tissue. Perfused (1X PBS, 1mM EDTA) individual lungs (upper left lobes) were weighed and placed in 300 µl MPO Buffer (0.5% hexadecyl trimethyl ammonium bromide (HTAB); 1mM EDTA in 1X PBS). The lung tissue was homogenized for 30 seconds, sonicated (20 pulses, 9 watts, 900 Hz) for 40 seconds using a Sonicator3000 (Misonix Inc., Farmingdale, NY, USA) and the resulting homogenate was centrifuged for 10 minutes

at 10 000 rpm. The supernatants were collected and stored at -80ºC until analysis. Frozen samples in MPO Buffer were thawed to release MPO stored in the azurophilic granules of neutrophils, and diluted in MPO Buffer in four three-fold dilutions (starting from undiluted sample to 1/27 dilutions). Twelve two-fold serial dilutions of horseradish peroxidise (HRP) standards (Sigma-Aldrich, Munich, Germany) in MPO Buffer, starting at 0.25 U/ml, were prepared. Sample dilutions and standards were added at 50 µl per well in a 96-well plate (Nunc Maxisorb). 50 µl per well of O-dianisidine (1.25 mg/ml) was added to all wells and the plate was incubated at 35ºC for 10 minutes. Immediately thereafter the plate was read at 460 nm to obtain a background reading, using a VersaMax microplate reader. 50 µl of freshly made 0.005% H_2O_2 was then added to all wells. The plate was monitored for a colorimetric reaction (5 minutes), and the reaction was stopped by adding 1% NaN_3 at 50 µl/well. The final plate reading was then read at 460 nm and subtracted from the background OD values. Final MPO activity was calculated from the standard curve (U/ml) and divided by the mass of lung tissue in 50 µl to give a final MPO activity expressed as units of activity per gram tissue (U/g).

2.10. Eosinophil peroxidase (EPO) Assay

EPO is an effector molecule secreted by mature eosinophils [14]. The colorimetric EPO Assay was used to assess activated eosinophil recruitment [206] within the lungs of *N. brasiliensis*-infected mice. Individual lungs (lower left lobes) were perfused (1X PBS, 1mM EDTA), excised, weighed and placed in 300 µl EPO Buffer (Tris 100mM, 0.1% Triton-X100 in 1x PBS). As described in the MPO Assay, the individual lungs were homogenized, sonicated, centrifuged (10 minutes at 10 000 rpm) and the supernatants collected and stored at -80ºC. The thawed samples were diluted, three-fold, in EPO

Buffer and 50 µl added per well to a 96-well plate (Nunc Maxisorb). Similarly, 12 HRP standards (Sigma-Aldrich, Munich, Germany) were diluted, starting at 0.5 U/ml in two-fold serial dilutions, and added 50 µl/well. The plate was incubated at 37ºC and a background reading was measured at 490 nm. 50 µl of the substrate solution consisting of 16 mM o-phenylenediamine (OPD) (Sigma-Aldrich, Munich, Germany) in EPO Buffer containing fresh 0.01 % HRP was added per well to samples and standards. The reaction was stopped after 1 minute with the addition of 50 µl 2M H_2SO_4 and absorption was measured at 490nm using a VersaMax microplate reader. Final EPO activity readings were calculated, as described in the MPO assay, to give Units/gram (U/g) EPO activity.

2.11. Arginase Assay

Lung cell digests were prepared as stated above (Section 2.5.). Cells were plated out at $4x10^5$ cells per well in IMDM (containing 10% FCS, 100 U/ml penicillin G, 100 µg/ml streptomycin). Culture plates were then incubated at 37 ºC for 72 hours. Using a protocol adapted from Pesce *et al.* (2006) [207] and Corraliza *et al.* (1994) [208] and following stimulation, cells were washed repeatedly with 1X PBS and lysed with 0.1% TritonX-100. Lysates were incubated with 50 µl of 10 mM $MnCl_2$ and 50 mM Tris HCl (pH 7.5) to activate the enzyme for 10 minutes at 55°C. 25 µl of the lysate solution was then transferred to 1.5 ml eppendorf tubes with 25 µl 500mM L-Arginine (pH 9.7) and incubated for 1 hour at 37ºC. The reaction was then stopped using 400 µl of acid mixture (H_2SO_4**:**H_3PO_4**:**H_2O at a ratio of 1:3:7). Thereafter, the colorimetric reaction was initialised by adding 25ul of 9% α-Isonitrosopropiophenone (ISPF) and incubated at 100ºC for 45 minutes, followed by 10 minutes in the dark (at room temperature). 200 µl aliquots were added and serially diluted, three-fold, in ddH_2O on

a 96-well plate (Nunc Maxisorb) and read at 540 nm on a VersaMax microplate reader. Controls had ddH_2O instead of L-Arginine and blanks had ddH_2O added instead of cell lysates. Standards consisting of doubling dilutions of 1000 µg/ml urea were treated under identical assay conditions. Arginase activity was calculated from the standard curve using urea concentrations (µg/ml).

2.12. Nitric oxide (NO) measurements

Cell culture supernatants from re-stimulated lungs were analysed for the production of gaseous NO using the Griess reaction assay, which measures the concentration of nitrite, a stable liquid product from the reaction of NO with O_2 [209]. Supernatant samples of re-stimulated lung cells were collected after 72 hours of incubation at 37ºC and stored at –20ºC until analysis. Supernatant samples were serially diluted three-fold and standards (1mM $NaNO_2$ solution) were serially diluted two-fold in IMDM (supplemented with 10% FCS, 100 U/ml penicillin G, 100 µg/ml streptomycin) in a total volume of 50 µl per well in a flat bottomed 96-well plate (Nunc Maxisorb). 25 µl of Griess Reagent 1 (1% sulfanilamide in 2.5% phosphoric acid) and then 25 µl of Griess Reagent 2 (0.1% napthyl-ethylene-diamine in 2.5 % phosphoric acid) were sequentially added to each well. The plate was incubated at room temperature for 5 minutes to allow the reaction to develop. The colorimetric reactions were read at 540 nm and the reference wavelength at 690 nm using a VersaMax microplate reader. The absorbance reading of the samples (in OD units) was correlated to the nitrite concentration (in mM) as calculated by the standard curve.

2.13. Statistical analysis

For each experiment, statistical analysis of the mouse groups were compared to WT controls (IL-4Rα$^{-/lox}$), using either the Student's t-test or One-way ANOVA followed by the Bonferroni post-test. All graphical representations showed means with error bars representing the standard error of the mean (SEM). A $p < 0.05$ was considered significant (*), and values of $p < 0.01$ (**), $p < 0.001$ (***), $p < 0.0001$ (****) were used to emphasise increasing values of significance. Numbers of experiments are indicated in the figure legends.

IL-4Rα–responsive macrophages/neutrophils provide protection against the onset of *N. brasiliensis*-induced chronic lung pathology

3.1.1 Introduction

Previous studies have clearly demonstrated that *N. brasiliensis* infection causes acute lung pathology [1, 2, 4, 109], which then develops into a chronic inflammatory and emphysemic-like disease [1, 2]. IL-4Rα signalling plays a key role in the resolution of *N. brasiliensis* infections [4, 60, 61] and development of host pathology associated with infection[4, 5]. In this chapter, we focused on how *N. brasiliensis* infection impacts on the associated lung pathology during acute (day 5 p.i.) and chronic (day 42 and 180 p.i.) pulmonary pathology.

During acute lung pathology associated with *N. brasiliensis* infection, animals develop an allergy-like pathology due to the excretory and secretory products (NES) of the parasite which alone can cause asthmatic pathology [2, 3, 109]. This is characterised by increased airway hyperresponsiveness (AHR) and infiltration of predominantly mononuclear inflammatory cells to the peribronchial region of the lung [1, 109]. Additionally, the infected animal develops considerable airway goblet cell hyperplasia and mucus production [4, 116], similar to those seen in experimental murine models of allergy such as the ovalbumin-induced allergic airway inflammation model [3, 210, 211]. In both *N. brasiliensis*-induced acute lung pathology and ovalbumin-induced asthmatic disease, the pathology is reduced in mice deficient in IL-4Rα responsiveness [4, 151]. Furthermore, this pathology is typically related to signalling of IL-13, and to a lesser

extent IL-4, which signal via their respective heterodimeric receptors containing IL-4Rα [6, 16, 212, 213].

In the case of *N. brasiliensis*-induced chronic lung pathology far less is understood of how it is induced and whether IL-4Rα plays a direct role. Indeed, a recent study indicated that IL-4Rα does not influence the development of emphysema in mice [1]. In general, few studies of chronic lung pathology have addressed the influence of TH2-driven immunity in inducing chronic lung pathology. In models of chronic lung inflammation, such as Sendai Virus (SeV) infection which is an influenza model [145] and murine models of spontaneous emphysema [18], Type 2 responses have been associated with driving chronic pulmonary diseases. In SeV it has been demonstrated that chronic IL-13 signalling and the induction of alternatively activated macrophage (AAM) populations in the lung play an important role in driving the onset of COPD [145]. Furthermore, it has been reported that increases in either IL-13 [121] or IFN-γ [143] levels in the lung can induce metalloproteinase-dependent emphysema [119]. These studies indicate that the onset of chronic lung pathology can be either Type 1- or Type 2-driven host responses. The specific mechanisms underlying these two potential immunological factors of pulmonary inflammatory diseases have yet to be explained.

From these previous studies it is apparent that the understanding of how chronic lung pathology develops in an infection model is fragmented [119]. Previous studies have indicated that alternatively activated macrophages (AAM), or M2 monocytes, appear to influence the onset of a range of chronic lung pathology [1, 7, 59, 166, 167, 214]. In the data presented here, we determined whether IL-4Rα responsiveness by macrophages plays a role in the onset of *N. brasiliensis*-induced chronic lung disease.

In order to investigate this question, infectious studies were conducted on IL-4Rα$^{-/lox}$, IL-4Rα$^{-/-}$ and LysM^{Cre}IL-4Rα$^{-/lox}$ mice at days 5, 42 and 180 p.i. and compared to naïve IL-4Rα$^{-/lox}$ control mice. At the defined time points we carried out detailed pathological studies on the lungs of these mice.

Specifically, lung pathology was addressed by assessing the following:

- *Inflammation:* Classification of lymphocytic inflammation is subdivided into severity (quantitative), location (perivascular or peribronchial), early (polar) or late (concentric) and acute or chronic (defined by the predominance of neutrophilic or plasma cell infiltrates, respectively). For example, "early moderate perivascular chronic pulmonary inflammation" describes moderate levels of inflammation associated with blood vessels i.e. small numbers of immune cells, which are predominantly plasma cells, and surrounding blood vessels.

- *Alveolar dilatation* (or distended alveoli, alveolar septa loss, septal disruption or dilatation of distal airspaces): This describes the destruction of alveolar air sacs, due to mechanical damage, resulting in enlarged "spaces" in the lung. This is the classical histological marker of emphysema morphology.

3.1.2 Results:

3.1.2.1 N. brasiliensis infection induces airway hyperresponsiveness (AHR) independently of IL-4Rα-responsiveness.

In order to confirm the development of chronic lung pathology following *N. brasiliensis* infection, AHR was assessed in infected mice at defined points following infection. AHR is associated with asthma [210, 215], COPD [130] and emphysema [1, 130]. Therefore, should AHR increase over time in previously infected animals (irrespective of exposure to a contractile stimulant), it is indicative of the development of a chronic and irreversible lung pathology [1]. AHR was determined as PenH values by whole body plethysmography and was measured in IL-4Rα$^{-/lox}$, IL-4Rα$^{-/-}$ and LysM^{Cre}IL-4Rα$^{-/lox}$ *N. brasiliensis*-infected mice and also uninfected control IL-4Rα$^{-/lox}$ mice. At days 5, 42 and 180 p.i., mice were exposed to the aerosolised airway stimulant β-metacholine (MCh) (10 mg/ml) or PBS (stimulant control).

As expected, naïve IL-4Rα$^{-/lox}$ mice ("Day 0") showed no increase ($p > 0.05$) in airway hyperresponsiveness (PenH values) when challenged with β-metacholine ("+MCh"), compared to unstimulated lungs ("- MCh"; PBS controls). Similarly, there was no change ($p > 0.05$) in PenH values between MCh-challenged mouse groups when compared to PBS-challenged groups at all time points post infection **(Figure 8)**. Additionally, no difference in PenH values was observed between mouse groups at any time point. However, importantly, a positive correlation in increased PenH values compared to time post infection was found in all mouse groups irrespective of MCh challenge. Together, these results showed that *N. brasiliensis* infection induces AHR in an IL-4Rα independent manner.

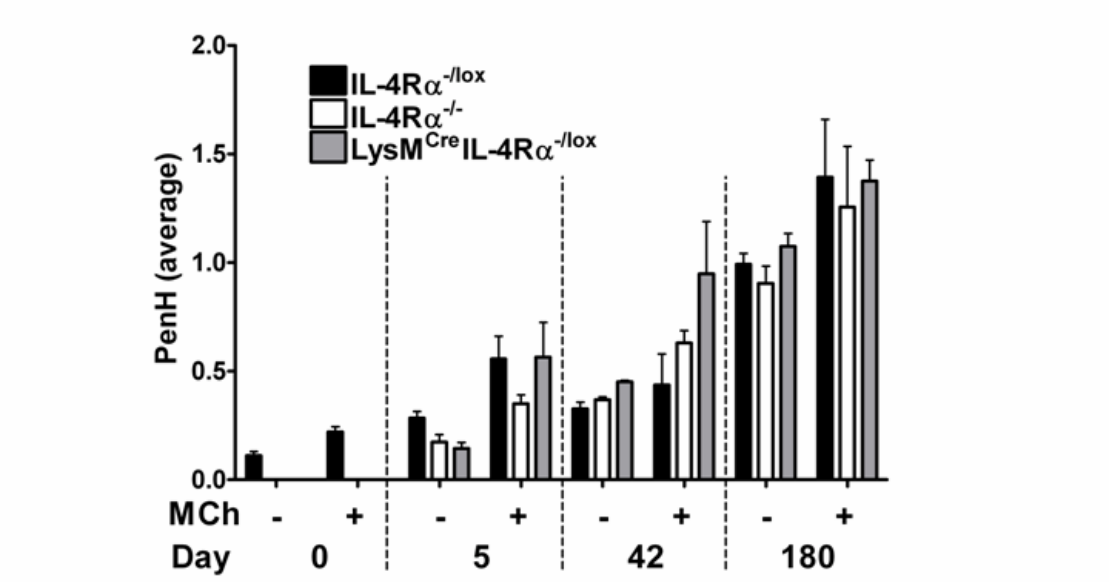

Figure 8: Increase in AHR baseline levels indicate chronic and irreversible lung pathology in *N. brasiliensis*-infected mice. AHR measurements of naïve ("Day 0"), and infected mice with *N. brasiliensis* at 5, 42 and 180 days p.i. AHR was measured using Metacholine (MCh) (10 mg/ml) and a whole body, unrestrained chambered plethysmograph. Enhanced pause (PenH) were averages of the first 5 minutes (normalised against individual baseline readings) after aerosol MCh challenge; n = 5 mice per group (and the same mice were used for each time point); Data is representative of 4 experiments.

3.1.2.2 N. brasiliensis-induced acute and chronic pulmonary pathology is increased in mice deficient for IL-4Rα-responsive macrophages and neutrophils

In order to define the nature of *N. brasiliensis*-induced lung pathology indicated by the increase in AHR, detailed pathological analyses were carried out. Lungs from infected IL-4Rα$^{-/lox}$ and IL-4Rα$^{-/-}$ mice showed similar or equivalent levels both in alveolar dilatation and inflammation at all time points analysed **(Figure 9A, 10 & Table 3)**. Emphysemic-associated alveolar dilatation in lungs from IL-4Rα$^{-/lox}$ and IL-4Rα$^{-/-}$ mice increased from mild (day 5) to moderate by day 42 p.i. and remained chronically moderate throughout the study **(Figure 10A)**. In contrast, in infected

LysM^{Cre}IL-4Rα$^{-/lox}$ mice, alveolar dilatation in lungs was significantly increased ($p < 0.05$) compared to IL-4Rα$^{-/lox}$ (and IL-4Rα$^{-/-}$) mice by day 5 p.i. before it developed to a similar and persistent alveolar dilatation (or emphysemic-like pathology) compared to the other mouse strains **(Figure 10A & Table 3)**.

Inflammation severity was similar between lungs from IL-4Rα$^{-/lox}$ and IL-4Rα$^{-/-}$ mice at all time points analysed **(Figure 9A, 10B & Table 3)**. At 5 days p.i., littermate controls (IL-4Rα$^{-/lox}$) and IL-4Rα$^{-/-}$ mice displayed an obvious mild pulmonary inflammatory response, which decreased during the course of the study, with minimal and diminished pulmonary inflammation evident at 180 days p.i. In contrast, the inflammation scores were consistently and significantly increased ($p < 0.05$ and $p < 0.0001$) in LysM^{Cre}IL-4Rα$^{-/lox}$ mice, compared to both IL-4Rα$^{-/lox}$ and IL-4Rα$^{-/-}$ mice at all time points analysed **(3)**. At day 42p.i., a strong and severe inflammatory disease phenotype was evident in LysM^{Cre}IL-4Rα$^{-/lox}$ lungs, which reduced significantly at 180 days p.i., but was still increased when compared to IL-4Rα$^{-/lox}$ and IL-4Rα$^{-/-}$ lungs at day 180p.i. **(Figure 9A, 10B & Table 3)**.

Microscopic analysis of the lung infiltrating cell populations showed additional differences between the infected mouse groups. In IL-4Rα$^{-/lox}$ mice the infiltrate was granulocytic while in IL-4Rα$^{-/-}$ mice this granulocyte population was absent **(Figure 9A,** yellow arrows**; Table 3)**. In LysM^{Cre}IL-4Rα$^{-/lox}$ mice the sites of inflammation in the lungs showed an increased granulocytic infiltration at day 5 p.i. when compared to IL-4Rα$^{-/lox}$ mice. By day 42 p.i., IL-4Rα$^{-/lox}$ and LysM^{Cre}IL-4Rα$^{-/lox}$ mouse groups showed equivalent levels of granulocytes. It should be noted that in all mouse groups, a reduction in granulocytes was apparent over time at the sites of inflammation,

concomitant with an increase in lymphocytes. The inflammation observed at days 5 and 42 in IL-4Rα$^{-/lox}$ and LysM^{Cre}IL-4Rα$^{-/lox}$ lungs were therefore classified as "acute inflammation" due to a predominantly neutrophilic infiltrate. By 180 days p.i., lung inflammation in both IL-4Rα$^{-/lox}$ and LysM^{Cre}IL-4Rα$^{-/lox}$ mice was classified as "chronic inflammation" due to the predominance of lymphocytes and plasma cells present. Interestingly, in IL-4Rα$^{-/-}$ mice, the observed cellular composition of the lung inflammation at day 5 p.i. was similar to day 42 and 180 days p.i. The inflammation was therefore classified as "chronic inflammation" due to the predominant lymphocytic and plasma cell infiltrate in IL-4Rα$^{-/-}$ mice at all time points in the study.

In agreement with previous studies [1], signs of haemorrhaging, characteristic of hemosiderin-laden macrophages (brown in appearance as a result of hemosiderin deposition from the phagocytosis of erythrocytes and digestion of haemoglobin), were prominent throughout the study. Furthermore, there seemed to be no spatial or quantity differences between the mouse groups studied (data not shown). Signs of pulmonary pathology such as alveolar dilatation, peribronchial and perivascular inflammation, haemorrhaging and AHR, persisted in the chronic stages (day 180 p.i.) in all three mouse groups, even after the parasite had been expelled. This is indicative that *N. brasiliensis* infection could initiate chronic damage to the lung and this is in agreement with previous reports [1, 2]. The pathological evidence of perivascular and peribronchial inflammation, alveolar dilatation and the presence of hemosiderin-laden macrophages, could be explained by worm migration during its life cycle.

In summary, all three mouse groups showed perivascular and peribronchial inflammation, which was composed primarily of lymphocytes. While pulmonary

inflammation was diminished in all three groups at 180 days p.i., the emphysemic-like pathology (alveolar dilatation) and hemosiderin-laden macrophages evidence of haemorrhaging persisted. However, infected LysM^{Cre}IL-4Rα$^{-/lox}$ mice developed increased early (day 5 p.i.) alveolar dilatation and increased pulmonary inflammation at all time points analysed, when compared to IL-4Rα$^{-/lox}$ and IL-4Rα$^{-/-}$ infected mice.

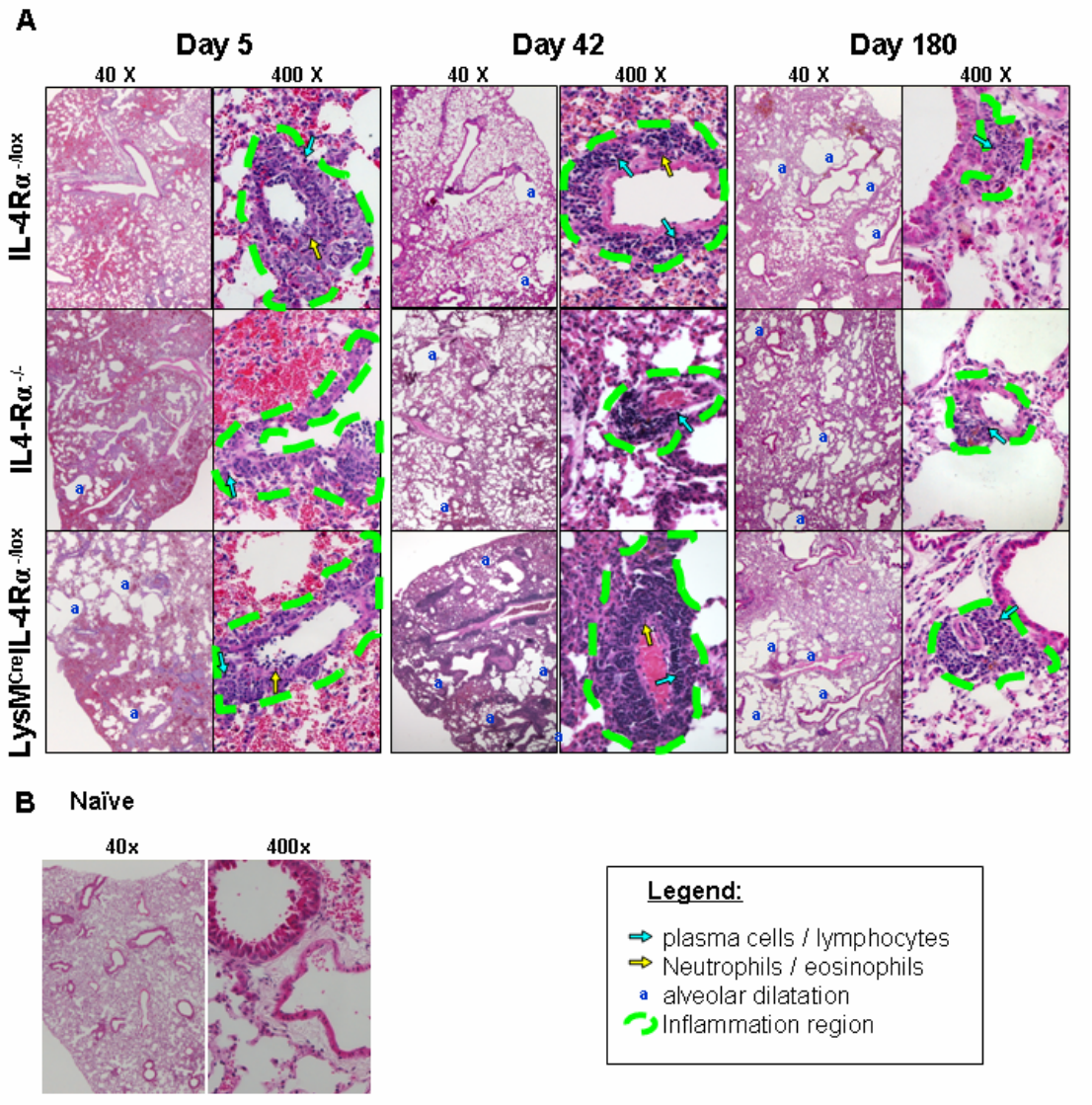

Figure 9: *N. brasiliensis*-infected LysM^{Cre}IL-4Rα$^{-/lox}$ mice demonstrate increased pulmonary inflammation. H&E sections of **(A)** *N. brasiliensis*–infected lungs of IL-4Rα$^{-/-}$, LysM^{Cre}IL-4Rα$^{-/lox}$ and littermate controls (IL-4Rα$^{-/lox}$) at 5, 42 and 180 days p.i. and **(B)** naïve littermate control histological sections. First panels: 40x Magnification; second panels 400x magnification. n = 8-20 mice per group, from 2 to 5 experiments per time point.

Table 3: Summary and scores of pulmonary histopathology induced by *N. brasiliensis*.

	Day 5 p.i.			Day 42 p.i.			Day 180 p.i.		
	IL-4Rα$^{-/lox}$	IL-4Rα$^{-/-}$	LysM^{Cre} IL-4Rα$^{-/lox}$	IL-4Rα$^{-/lox}$	IL-4Rα$^{-/-}$	LysM^{Cre} IL-4Rα$^{-/lox}$	IL-4Rα$^{-/lox}$	IL-4Rα$^{-/-}$	LysM^{Cre} IL-4Rα$^{-/lox}$
Inflammation (Path. score)	Mild (1.4)	Mild (1.3)	Moderate (2.1)	Mild (1.3)	Mild (1.2)	Severe (2.7)	Residual & diminished (0.8)	Residual & diminished (0.9)	Mild (1.3)
Lymphocytic infiltrate	Present	Present	Present	Present	Present	Present	Present	Present	Present
Granulocytic infiltrate	Present	None	High	Present	None	Present	Rare	None	Rare
Alveolar Dilatation (Path. score)	Mild (1.4)	Mild (1.2)	Moderate (2.0)	Moderate (1.6)	Moderate (1.8)	Moderate (2.0)	Moderate (2.0)	Moderate (2.1)	Moderate (2.1)

Information for Table: Inflammation and alveolar dilatation scores were based on severity, as defined in Materials and Methods (2.4). Lymphocytic and granulocytic infiltrates refer to lymphocytes including plasma cells, and neutrophils or eosinophils, respectively, at the site of inflammation (SOI). n = 3–5 mice per group; Data is representative of 2 to 5 experiments per time point, with multiple sections (5 -11) on individual lungs.

Histopathological scoring system key:
0 = none or less than minimal (5%)
1 = minimal to mild
2 = moderate
3 = severe - c.a. 50% or more

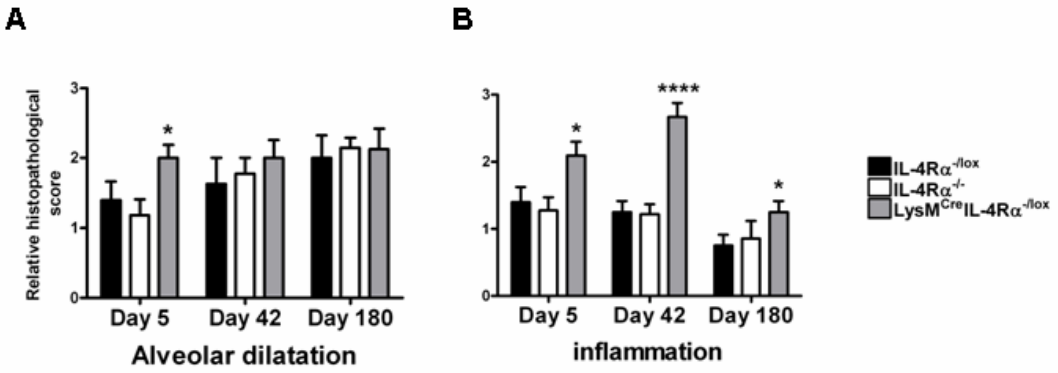

Figure 10: *N. brasiliensis*-infected LysM^{Cre}IL-4Rα$^{-/lox}$ mice demonstrate earlier and increased pulmonary pathology. Relative histological evaluation scores of **(A)** alveolar dilatation and **(B)** inflammation lung pathology on individual *N. brasiliensis*–infected lungs of IL-4Rα$^{-/-}$, LysM^{Cre}IL-4Rα$^{-/lox}$ and littermate controls (IL-4Rα$^{-/lox}$) at 5, 42 and 180 days p.i. Histological sections (H&E) from all lobes of individual mouse lungs were evaluated and graded (0 to 3) with a registered Pathologist (Prof. Govender) using a relative histopathological score as defined in Materials and Methods (modified from Radosevic *et al.* 2007) [195]. n = 8-20 mice per group from 2 to 5 experiments per time point. * $p < 0.05$; **** $p < 0.0001$.

3.1.3 Discussion

In this study we showed that macrophage/neutrophil-specific IL-4Rα deficient mice develop consistently increased pulmonary cellular inflammation following *N. brasiliensis* infection when compared to control mice. We further confirmed previous results that *N. brasiliensis* infection leads to the development of emphysema, which is independent of IL-4Rα-responsiveness [1].

The recent findings by Marsland and colleagues (2008)[1] were the first to show that *N. brasiliensis*-infected mice develop lung emphysema. They also demonstrated that IL-4Rα does not play a role in *N. brasiliensis*-induced emphysema, which was also confirmed in our study since we found no differences between all three groups in AHR and in alveolar dilatation manifestation during the chronic stages (day 42 and 180 p.i.) following *N. brasiliensis* infection.

Although not apparent in the AHR, the increased alveolar dilatation in $LysM^{Cre}$IL-$4R\alpha^{-/lox}$ mice at day 5 p.i. may represent an earlier commitment to the manifestation of emphysema, which may indicate that IL-4Rα-responsive macrophages and/or neutrophils may contribute to prevent destruction of alveolar septa in the early stages of disease manifestation. Our observation of the rapid induction (day 5 p.i.) of alveolar dilatation in the lungs of $LysM^{Cre}$IL-$4R\alpha^{-/lox}$ mice may be explained by: (i) a reduced ability in a population of cells (i.e. AAM) capable of repairing *N. brasiliensis*–induced mechanical damage to the lung [1]; or (ii) increased levels of IL-13 which is associated with metalloproteinase-dependent emphysema[121] and COPD induced by SeV infections [145]; and/or (iii) the increased phagocytosis of denatured

collagen by alveolar macrophages, which further disrupts alveolar wall integrity, resulting in alveolar dilatation [216]. Indeed, increased IL-13 (and IL-4) production [105], following *N. brasiliensis* infection has been shown to be induced by innate NK T-cells [145], which activate macrophages in the lung to become AAMs [165]. These AAMs are able to secrete metalloproteinases [1, 2], and are responsible for collagen and extracellular matrix degradation in the lung [144]. Secretion of metalloproteinases and simultaneous phagocytosis of degraded collagen potentially causes disruption of alveolar septa (or alveolar dilatation), a sign of emphysema [216]. To better define a possible involvement of AAM in the onset of emphysema, further studies are needed to investigate protease and protease inhibitors and other factors involved in emphysema development [119, 140] in relation to IL-4Rα-responsive macrophages. Additional future work could include that the lungs across all mice groups be fixed with formalin at a constant pressure to achieve maximum accuracy in alveolar dilatation analysis.

Pathological analysis indicated that IL-4Rα-responsive macrophages and/or neutrophils are able to down-regulate *N. brasiliensis*-induced lung inflammation. The involvement of IL-4Rα-responsive AAMs in the down-regulation of inflammation has been previously demonstrated in *S. mansoni*–induced pathology, while neutrophils did not play a role in reducing this pathology [59, 72]. However, a contribution by IL-4Rα-responsive neutrophils cannot be excluded, as it is not yet distinguishable whether IL-4Rα-responsive macrophages or neutrophils are involved in the pathology demonstrated here. The underlying cellular interactions that define this regulation of inflammation and subsequent protection are only now starting to be unravelled. Importantly, AAMs are strongly associated with controlling pathological levels of

inflammation by modulating T-cell behaviour [7, 178]. Possibly the most similar demonstration of this to date is the widely reported suppression of T-cell proliferation by AAM populations [7, 72, 170, 178, 217]. From our histological data it could be suggested that such an interaction also occurred in this study. We suggest that the reduced inflammation in IL-4Rα$^{-/lox}$ mice when compared to LysM^{Cre}IL-4Rα$^{-/lox}$ mice is due to the generation of AAM populations controlling the proliferation of pathogenic lymphocytic infiltrates. IL-4Rα$^{-/-}$ mice do not produce AAMs either [163], yet have similar levels of inflammation compared to IL-4Rα$^{-/lox}$ mice. These equivalent levels of inflammation seen between IL-4Rα$^{-/-}$ and IL-4Rα$^{-/lox}$ mice could be as a result of the previously reported disrupted recruitment of lymphocytes to the lung in IL-4Rα$^{-/-}$ mice [4]. However, in LysM^{Cre}IL-4Rα$^{-/lox}$ mice this potentially pathological increase in lymphocyte populations in the lung is unable to be controlled by AAM. To ensure that the there are no differences in the number of *N. brasiliensis* worms migrating through the lung and therefore potentially affecting lung damage and subsequent differences in inflammation, future studies could include assessing the worm burden in the lung at 0, 12, 24 and 48 hours p.i.

To further investigate the role of immunological relevant cells in the onset of early pulmonary inflammation, which could be a potential cause for the development of increased and chronic inflammation in LysM^{Cre}IL-4Rα$^{-/lox}$ mice, a detailed analysis of the lung was performed at day 5 p.i., presented in the following chapter.

Analysis of acute immune responses in *N. brasiliensis*-infected LysM^{Cre}IL-4Rα$^{-/lox}$ lungs that underlie the rapid onset of chronic lung inflammation

3.2.1 Introduction

In the previous chapter (3.1), we established that mice impaired for IL-4Rα-responsiveness by macrophages and neutrophils (LysM^{Cre}IL-4Rα$^{-/lox}$) rapidly developed enhanced lung inflammation when compared to controls. In this chapter we investigated the potential underlying immune mechanisms that may cause this rapid onset of inflammation. This aspect of the current study will focus on the development of the immune response at day 5 p.i., where the earlier onset in pathology was apparent in *N. brasiliensis*-infected LysM^{Cre}IL-4Rα$^{-/lox}$ mice.

It is known that *N. brasiliensis* induces immunological changes in the lung upon infection. These changes are associated with high levels of TH2 cytokines and Type 2 antibody production [97], as well as recruitment to the lung of T-cells [4], eosinophils [218] and basophils [92]. Macrophage populations are also greatly increased and typically of the alternatively activated phenotype [97, 105]. The TH2 cytokine response is characterised primarily by the production of IL-4 and IL-13, in addition to other cytokines such as IL-5, IL-9 and IL-10 [219]. In chronic pulmonary pathology, IL-13 is the TH2 cytokine most commonly associated with the onset of pulmonary diseases such as asthma [212], fibrosis [50] and COPD [145], including emphysema [121]. Important cellular sources of IL-13 include T-cells, eosinophils, basophils and macrophages, all of which are recognised as playing important roles in chronic lung pathology [14, 97, 137,

[145, 153, 212, 220]. These early IL-13 responses, along with T-cell-antigen presenting cell (APC) interactions, can drive T-cell associated chronic lung inflammation. [221].

In our study, microscopic analysis revealed lymphocytic, granulocytic and macrophage infiltrates in the lungs of *N. brasiliensis*-infected mice (Chapter 3.1). In this chapter we examined these immune cell populations and markers of their activity in the lungs of mice at day 5 p.i. to determine why $LysM^{Cre}IL\text{-}4R\alpha^{-/lox}$ mice exhibit such a rapid and early onset of chronic lung inflammation when compared to littermate controls during *N. brasiliensis* infection.

3.2.2 Results:

3.2.2.1 Acute pulmonary inflammation in infected LysM^{Cre}IL-4Rα$^{-/lox}$ mice is associated with increased T-cell numbers and TH2 cytokine responses.

To examine whether the increased inflammatory phenotype in LysM^{Cre}IL-4Rα$^{-/lox}$ mice at day 5 p.i. could be explained by increased numbers of lymphocytes in the lung, the cellular composition of the lungs were analysed by flow cytometry from single-cell suspensions of lung digests in both infected and naïve mice at day 5 p.i.

Quantification by flow cytometry of T-cell populations in the lung, including CD3$^+$, CD3$^+$CD4$^+$ and CD3$^+$CD8$^+$ cells, showed that infected IL-4Rα$^{-/lox}$ and IL-4Rα$^{-/-}$ mice, cell numbers at 5 days p.i. remained similar to those found in naïve mice **(Figure 11A, B & C)**. Interestingly, LysM^{Cre}IL-4Rα$^{-/lox}$ mice showed significant increases in the absolute and relative numbers of CD3$^+$ T-cell populations when compared to the other mouse strains **(Figure 11A)**. This was predominantly due to CD4$^+$ T-cells, as they exceeded approximately twice the number of CD8$^+$ T-cells **(Figure 11B & C)**.

To ascertain whether cytokines were playing a role in the initiation and progression of inflammation, the TH2 cytokines, IL-4 and IL-13, the Th1 cytokine, IFN-γ, and the immunoregulatory cytokine IL-10, were measured *in vitro* after anti-CD3 re-stimulation of collagenase-treated cells from lungs isolated from mice at day 5 p.i. Re-stimulated collagenase-treated cells from infected lungs of IL-4Rα$^{-/lox}$ mice showed increased IL-10, IL-4 and IL-13 secretion, when compared to naïve lung cell preparations **(Figure 11D)**. As expected, IL-4Rα$^{-/-}$ lung cell suspensions had reduced

IL-4 production, but increased IFN-γ production when compared to re-stimulated IL-4Rα$^{-/lox}$ lung cell suspensions. However, lung cell suspensions from LysM^{Cre}IL-4Rα$^{-/lox}$ and IL-4Rα$^{-/lox}$ mice produced similar levels of IFN-γ compared to cells from naïve mice. Interestingly, LysM^{Cre}IL-4Rα$^{-/lox}$ lung cell suspensions produced higher levels of IL-4, IL-13 and IL-10 compared to IL-4Rα$^{-/lox}$ and IL-4Rα$^{-/-}$ re-stimulated lung cell suspensions **(Figure 11D)**.

Indeed, IL-4 and IL-13 measurements after anti-CD3 re-stimulation from isolated CD4^{+} T-cells of the draining mediastinal (MST) lymph nodes (LN), showed that a TH2 response evident in control mice was increased in LysM^{Cre}IL-4Rα$^{-/lox}$ mice, but abrogated in IL-4Rα$^{-/-}$ mice **(Figure 11E)**.

Quantification of B220^{+} B lymphocytes showed that there were no significant differences between B-cell numbers in naïve and infected mice at 5 days p.i. **(Figure 11F)**.

Together, these results show increased pulmonary TH2 cell and cytokine responses in *N. brasiliensis*-infected LysM^{Cre}IL-4Rα$^{-/lox}$ mice at 5 days p.i.

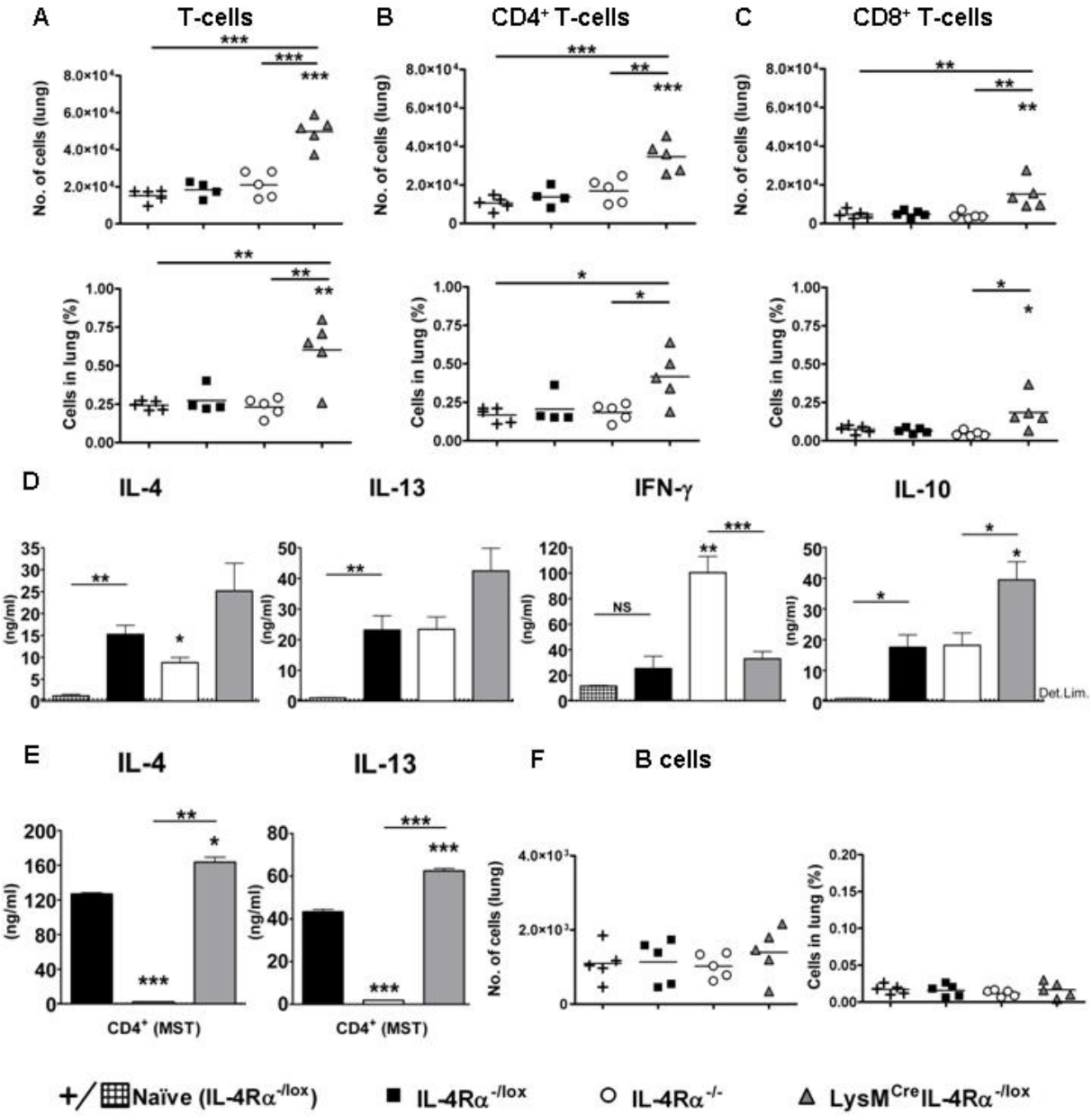

Figure 11: T and B lymphocyte populations and cytokine production in lungs of IL-4Rα$^{-/lox}$, IL-4Rα$^{-/-}$ and LysM^{Cre}IL-4Rα$^{-/lox}$ *N. brasiliensis*-infected mice. (A) CD3$^+$, **(B)** CD3$^+$CD4$^+$ and **(C)** CD3$^+$CD8$^+$ T-cell numbers and percentages, analysed by flow cytometry; and anti-CD3 re-stimulated **(D)** IL-4, IL-13, IFN-y and IL-10 levels in collagenase-treated lung cell suspensions from individual naïve and infected mice. **(E)** Anti-CD3 re-stimulated cytokine production of CD4$^+$ cells (> 80% purity) from pooled mediastinal (MST) lymph nodes. **(F)** B220$^+$ B cell numbers and percentages from naïve and *N. brasiliensis*-infected lungs. All data is at 5 days p.i. (n = 5 mice per group). Data represents individual mice from one experiment, except data for MST cytokines (E) which were from pooled lymph nodes and representative of 3 experiments. Det. Lim.: Detection limit of assay. NS: not significant. * $p < 0.05$, ** $p < 0.01$, *** $p < 0.001$ (compared to IL-4Rα$^{-/lox}$ ■).

3.2.2.2 Normal granulocyte infiltration and activation in LysM^{Cre}IL-4Rα$^{-/lox}$ mice

The granulocyte populations during *N. brasiliensis* infections consist predominantly of neutrophils and eosinophils, both of which can release strong cytotoxic proteins such as myeloperoxidase (MPO) [222] and eosinophil peroxidise (EPO) [14], respectively. Neutrophils, which were defined in previous studies as GR-1^{+}CCR3^{-} and eosinophils (GR-1^{int}CCR3^{+}) [223], were analysed by flow cytometry and by the MPO and EPO assays respectively, to ascertain whether the phenotypic pulmonary inflammation seen in LysM^{Cre}IL-4Rα$^{-/lox}$ mice was associated with changes in granulocyte infiltration and function.

Granulocyte numbers were increased in the lung at day 5 p.i. in all mouse groups **(Figure 12 A).** This granulocyte population consisted predominantly of GR-1^{+}CCR3^{-} neutrophils with no significant differences in numbers between experimental groups (**Figure 12 B(i)**). However analysis of the neutrophil activation and maturation status by MPO assay showed significantly increased MPO levels from IL-4Rα$^{-/lox}$ and LysM^{Cre}IL-4Rα$^{-/lox}$ lungs, but not from IL-4Rα$^{-/-}$ lungs when compared to naïve controls (**Figure 12 B(ii)**).

The number of eosinophils was low in lungs at 5 days p.i. (**Figure 12 C(i)**). Eosinophil infiltration (**Figure 12 C(i)**) and activity, measured by EPO levels (**Figure 12 C(ii)**), was not seen at day 5 p.i in any mouse groups.

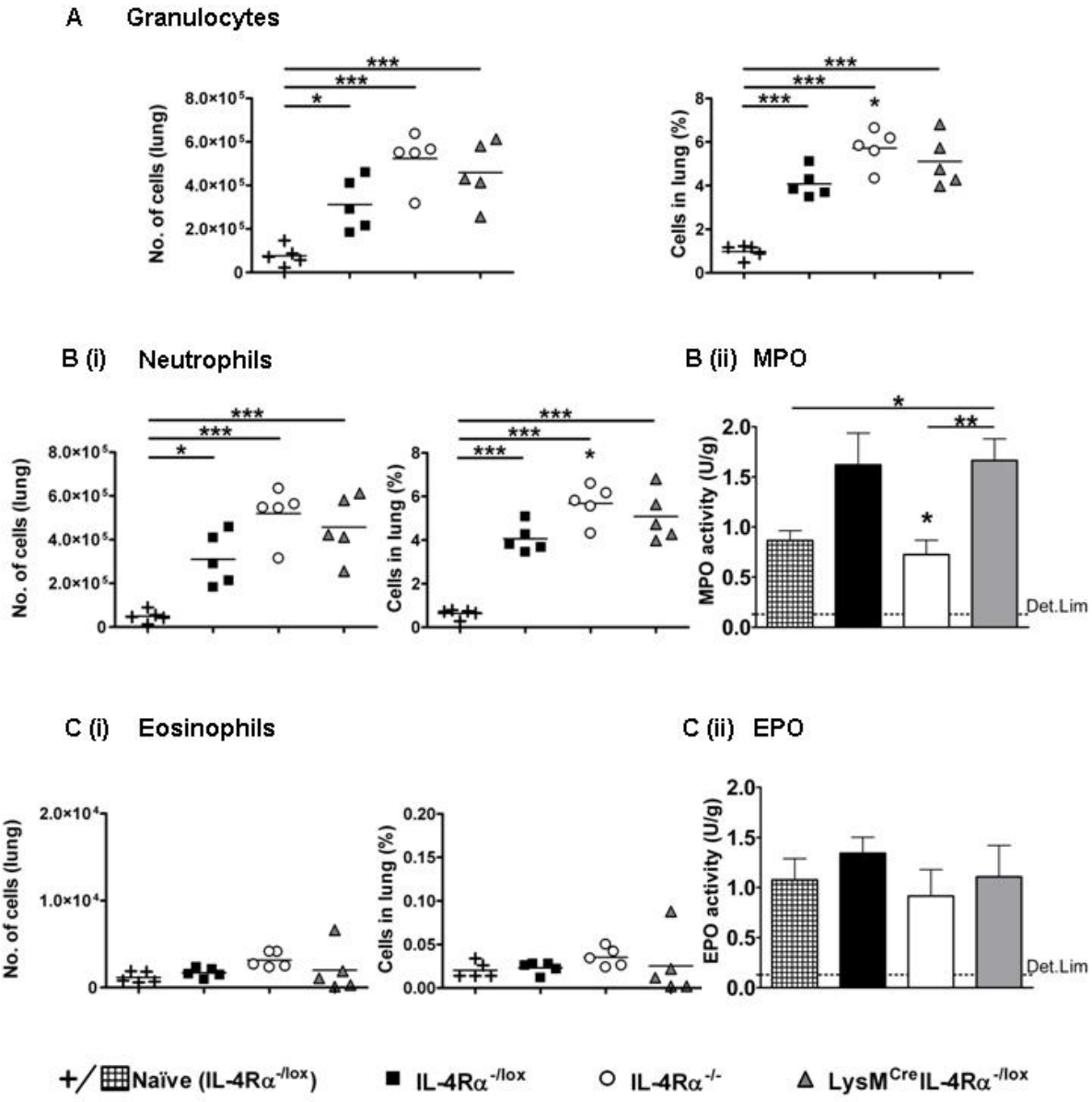

Figure 12: The effects of IL4Rα signalling on granulocyte infiltration and activity in *N. brasiliensis*-infected lungs. Flow cytometry was analysed on whole lung single-cell digests and calculated against total cell counts to give percentages and cell numbers of **(A)** granulocytes **(B)** neutrophils (GR-1^{+},$CCR3^{-}$) and **(C)** Eosinophils (GR-1^{int},$CCR3^{+}$) in the lung. MPO **(B (ii))** and EPO **(C (ii))** were measured as markers of activated neutrophils and eosinophils, respectively, in naïve and *N. brasiliensis*-infected lungs at 5 days p.i. (n = 4-5 mice per group). Data represents individual mice from one experiment. Det. Lim.: Detection limit of assay. * $p < 0.05$; ** $p < 0.01$; *** $p < 0.001$ (compared with IL-4Rα$^{-/lox}$ ■).

3.2.2.3 IL-4Rα-responsiveness affects alveolar macrophage activation

Resident macrophage populations, or alveolar macrophages, are constitutively found in the lung and are the first cells to encounter inhaled pathogens and particles involved in lung diseases [196, 224]. Alveolar macrophages are increased in acute stages of *N. brasiliensis* infections [87] and are chronically present in COPD [123].

In order to identify any changes in alveolar macrophage populations following *N. brasiliensis* infection, these populations were defined as autofluorescent $CD11c^{+}MHCII^{Lo}$ SSC^{HI} cells [196] and quantified from single-cell suspensions of lung digests by flow cytometry. These alveolar macrophages were significantly increased in number in all mouse groups at 5 days p.i. when compared to naïve controls (**Figure 13A**), and the cell number percentages from IL-4Rα$^{-/lox}$ and $LysM^{Cre}$IL-4Rα$^{-/lox}$ mice were significantly elevated compared to IL-4Rα$^{-/-}$ mice (**Figure 13A**).

Nitric oxide synthase-2 (NOS2) and arginase activity in single-cell suspensions of lung digests were assessed as biomarkers for classical or alternatively activated macrophages, respectively. Nitric oxide (NO) or NOS2 activity, measured as nitrite levels, was below detection limit levels in all mouse groups (**Figure 13B**). In contrast, arginase activity, measured as urea production, was significantly increased in infected IL-4Rα$^{-/lox}$ lung cells compared to naïve and the infected mouse groups (**Figure 13C**). However IL-4Rα$^{-/-}$ and $LysM^{Cre}$IL-4Rα$^{-/lox}$ arginase activity was significantly decreased compared to IL-4Rα$^{-/lox}$ levels.

Together, these data show normal pulmonary granulocyte infiltration and activation in LysM^{Cre}IL-4Rα$^{-/lox}$ mice, while IL-4Rα$^{-/lox}$ control mice may have a predominant alternative activation of alveolar macrophages, following in *N. brasiliensis* infection.

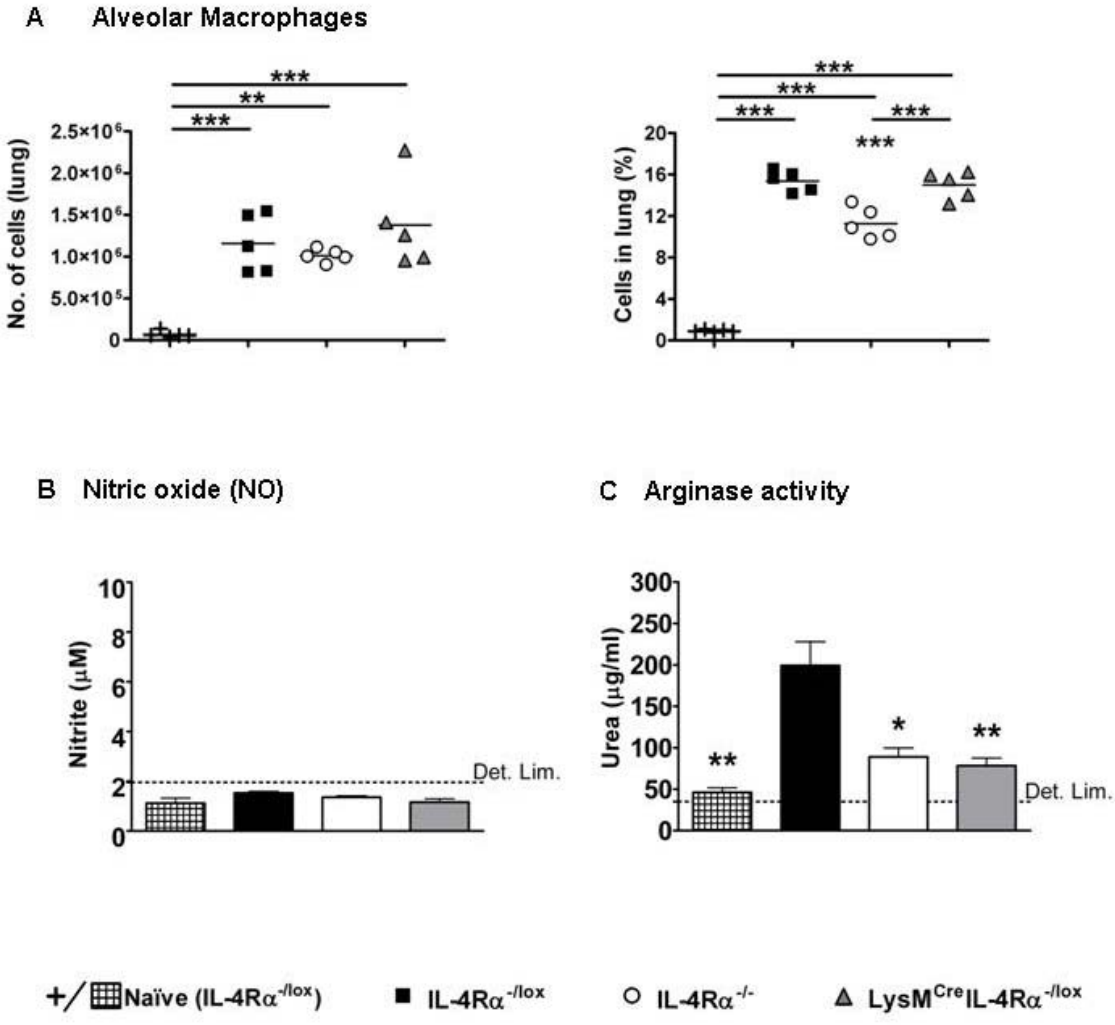

Figure 13: IL-4Rα effects on alveolar macrophage recruitment and function. (A) Numbers and percentages of alveolar macrophages (autofluorescent SSC^{HI} CD11c^{+}) in the lung. **(B)** Nitric oxide (NO) levels and **(C)** Arginase activity measurements in naïve and *N. brasiliensis*-infected lungs at 5 days p.i. (n = 4-5 mice per group). Data represents individual mice from one experiment. Det. Lim.: Detection limit of assay. * $p < 0.05$, ** $p < 0.01$, *** $p < 0.001$ (compared with IL-4Rα$^{-/lox}$ ■).

3.2.3 Discussion:

In this chapter, we further investigated the underlying causes of the increased inflammation observed in *N. brasiliensis*-infected lungs of LysM^{Cre}IL-4Rα$^{-/lox}$ mice at 5 days p.i. (Chapter 3.1). At this early time point, we observed increased pulmonary T-cell numbers in LysM^{Cre}IL-4Rα$^{-/lox}$ mice, with an associated heightened response in TH2 cytokine production of IL-4 and IL-13 and elevated levels of IL-10. The cellular composition of the increased inflammation seen previously in LysM^{Cre}IL-4Rα$^{-/lox}$ mice (Chapter 3.1) was not associated with B-cell, neutrophil, eosinophil and macrophage cell numbers, since these cell populations were unaltered in the lungs of infected mice. Neutrophil and eosinophil activation was also unaffected in LysM^{Cre}IL-4Rα$^{-/lox}$ lungs, as determined by MPO and EPO assays respectively. Additionally, although there were no overall differences in macrophage cell numbers between infected groups, IL-4Rα$^{-/-}$ and LysM^{Cre}IL-4Rα$^{-/lox}$ mice showed reduced arginase activity compared to IL-4Rα$^{-/lox}$ collagenase-treated lung cell suspensions.

Flow cytometry was used to quantify the cellular compositions of lung inflammation. Although analysis of bronchoalveolar lavage (BAL) fluid is an alternative method, the evaluation of cell numbers in the inflamed lung by flow cytometry is a more accurate method, as concluded by previous reports [7, 223]. Additionally, the BAL method excludes inflammatory cells associated with peri-vascular inflammation, while flow cytometry quantifies cells in both peribronchial and peri-vascular inflammation, which were both present in *N. brasiliensis*-induced pulmonary immuno-pathology as observed by our histological examinations (Chapter 3.1).

A previous study by Mearns and colleagues (2008) [4], showed increased numbers of $CD4^+$ T-cells in the lungs of IL-4R$\alpha^{-/lox}$ and IL-4R$\alpha^{-/-}$ *N. brasiliensis*-infected mice at 7 days p.i.. We found at 5 days p.i. significantly increased numbers of $CD4^+$ and $CD8^+$ T-cells, only in the lungs of $LysM^{Cre}$IL-4R$\alpha^{-/lox}$ mice. Since IL-4 can induce $CD8^+$ T-cell proliferation [225], it is not clear at this stage whether the increase in $CD8^+$ T-cells is a pathological response or whether it is merely a consequence of exaggerated levels of IL-4 in infected $LysM^{Cre}$IL-4R$\alpha^{-/lox}$ lungs. Previous studies have shown, particularly in asthma ($CD4^+$) [150] and COPD ($CD8^+$) [152], that increases in the populations of pulmonary T-cell populations correlate strongly with the onset of inflammation. Our data indicates this may also be the case in the *N. brasiliensis*-infected lung and that this significant increase in $CD4^+$ T-cell numbers may underlie the early onset of TH2-driven pulmonary inflammation in $LysM^{Cre}$IL-4R$\alpha^{-/lox}$ mice.

It has been previously shown that $CD4^+$ T-cells in the lung are responsible for the induction of TH2 cytokines, particularly IL-4 and IL-13, during *N. brasiliensis* infection[4]. Analysis of cytokine responses in re-stimulated lung cells in our study, showed that the early onset of chronic inflammatory pathology at day 5 p.i. was associated with increased IL-4, IL-13 and IL-10 production by anti-CD3 stimulated $LysM^{Cre}$IL-4R$\alpha^{-/lox}$ cells when compared to infected mouse groups. IL-13 is a cytokine involved in allergic pulmonary inflammation and several other pathological outcomes [16, 212, 226, 227]. In contrast, IL-10 is commonly referred to as an anti-inflammatory cytokine and is produced by T-cell and non-T-cell populations [228-230]. However, under long-term exposure, IL-10 can induce T and B lymphocyte inflammation in the lung [231]. Therefore, both IL-13 and IL-10 could play a potentially vital role in *N. brasiliensis*-induced chronic lung pathology. For example, the

observed increased IL-4 and IL-13 production from MST $CD4^+$ T-cells may play a role in the induction of TH2 inflammation in the lungs of infected $LysM^{Cre}IL\text{-}4R\alpha^{-/lox}$ mice [4]. In contrast, the increased IL-10 production could be induced in the infected lung in an attempt to counteract and down-modulate the accelerated and increased inflammatory responses present in infected $LysM^{Cre}IL\text{-}4R\alpha^{-/lox}$ lungs at 5 days p.i. [229, 231]. In support of this, it has been reported that elevated IL-10 levels were associated with increased inflammation in $LysM^{Cre}IL\text{-}4R\alpha^{-/lox}$ mice during *S. mansoni* infection, and that increased IL-10 levels could not substitute for IL-4Rα-responsive macrophages in the role of down-modulating inflammation, as seen in our study [59]. Although the histological studies show that the pulmonary inflammation in $LysM^{Cre}IL\text{-}4R\alpha^{-/lox}$ mice does eventually decrease at 180 days p.i. to a mild inflammation level similar to the other infected groups, it is not clear how or if IL-10 is playing a direct role. Hence, further *in vivo* studies by IL-10 neutralisation/supplementation or studies with IL-10 transgenic mice might help to uncover the role of IL-10 following *N. brasiliensis* infections.

Eosinophil cell number and activation by EPO was unaltered compared to naïve mice in all infected mouse groups. While MPO quantifications confirmed histological evaluations (Chapter 3.1) that shared low granulocyte numbers at the sites of inflammation in the lungs of $IL\text{-}4R\alpha^{-/-}$ mice, the neutrophil quantification by flow cytometry did not agree with this data**.** A possible explanation for this may be that microscopic evaluations are based on an activated neutrophilic criteria, while the flow cytometry data presented here encompasses not only activated, but also non-activated progenitor cells ($GR\text{-}1^+CCR3^-$) [223], as there were no significant differences in the amounts of inflammation between $IL\text{-}4R\alpha^{-/-}$ mice and $IL\text{-}4R\alpha^{-/lox}$ control mice.

Additionally, while EPO activity is specific to eosinophils, sources other than neutrophils have been described for MPO, including monocytes [222, 232] and vascular non-haematopoietic cells [233].

Importantly, neutrophil activation and recruitment in LysM^{Cre}IL-4Rα$^{-/lox}$ lungs was not affected, despite disrupted neutrophil (and macrophage) IL-4Rα expression. This may suggest that neutrophil recruitment is dependent on IL-4Rα signalling by cells other than neutrophils and macrophages. Furthermore, this study suggests that it is unlikely that IL-4Rα-responsive neutrophils play a role in controlling *N. brasiliensis*-induced pulmonary immuno-pathology. Instead, IL-4Rα-responsive macrophages seem to play a central role in controlling the increased pulmonary pathology in LysM^{Cre}IL-4Rα$^{-/lox}$ mice (Chapter 3.1), as demonstrated in other helminth studies [59].

AAMs are impaired in LysM^{Cre}IL-4Rα$^{-/lox}$ mice, since they lack IL-4Rα-responsive macrophages [59]. In support of this, we found decreased arginase levels in lung cells at 5 days p.i., indicative of impaired development of AAMs [72, 166, 170]. This, however, needs to be further confirmed by arginase assays and quantitative real-time PCR (qRT-PCR) for *Arg-1* mRNA on isolated alveolar macrophages. It is likely that the absence of IL-4Rα-responsive alternatively activated macrophages are responsible for the observed increased inflammation (Chapter 3.1) and increased CD3$^+$ T-cell numbers in the LysM^{Cre}IL-4Rα$^{-/lox}$ lung, since these AAMs are known to down-modulate inflammation and proliferation of CD4$^+$ T-cells [72, 178, 188, 214]. Additionally, it has been shown that helminth-induced AAMs show anti-proliferative activity of T lymphocytes, through the suppression of the cell cycle (G1 and G2/M phases) in CD4$^+$ T-cells through direct macrophage-T-cell contact [178]. Other possible

mechanisms by which AAMS inhibit T-cell proliferation include factors such as 2/15-lipoxygenase [188], Fizz1 [214] or apoptosis by an arginase-induced mechanism [72, 234]. Therefore, these data together may demonstrate an impaired ability of LysM^{Cre}IL-4Rα$^{-/lox}$ pulmonary macrophages to control exacerbated T-cell proliferation, as a result of these pulmonary macrophages not being able to become alternatively activated. Although these data may support our hypothesis, it should be further tested by performing infected macrophage-T-cell co-culture proliferation studies and macrophage characterization of isolated alveolar macrophages in *N. brasiliensis*-infected lungs.

It is unclear why neither of the IL-4Rα-deficient mouse groups do not have increased NO production in the supernatants of whole lung cell suspensions, since peritoneal macrophages from IL-4Rα$^{-/-}$ and LysM^{Cre}IL-4Rα$^{-/lox}$ mice was found to have increased NO production in a previous study [59]. However, collagenase-treated cell suspensions from infected lungs were used in this study at 5 days p.i. and the low cell number could have an effect on NO production after 5 days. In order to identify if these macrophages were classically activated, future work would include assessing NO production, qRT-PCR on NOS RNA and protein levels of IL-12 on isolated macrophages from the infected lungs of naïve and infected mice.

The question arises why global IL-4Rα$^{-/-}$ mice do not have as exacerbated inflammation and increased pulmonary T-cell numbers compared to LysM^{Cre}IL-4Rα$^{-/lox}$ mice in our study, even though both do not produce IL-4Rα-responsive alternatively activated macrophages [59, 163]. Importantly, IL-4Rα$^{-/-}$ mice lack IL-4Rα on all cells [62, 235] and thus lack IL-4Rα-responsive T-cells as well [4]. As a consequence,

IL-4Rα$^{-/-}$ mice have an impaired TH2 response [4, 60, 235], also confirmed in our study by decreased IL-4 and IL-13 production in MST CD4^{+} T-cells. Additionally, IL-4Rα$^{-/-}$ mice have disrupted recruitment of CD4^{+} T-cells to the lung during *N. brasiliensis* infection [4]. Therefore, in the complete absence of IL-4Rα expression, T-cell recruitment to the lung is severely reduced [57], resulting in the lack of T-cell mediated inflammation in IL-4Rα$^{-/-}$ mice as shown in our study.

Together, these data support previous findings and suggests that AAM are involved in controlling the onset of chronic lung inflammation following *N. brasiliensis* infection as early as day 5 p.i., by suppressing either or both recruitment and proliferation of T-cells [72, 178, 188, 214]. The data further suggests that IL-4Rα-responsive macrophages down-modulate IL-4 and IL-13 cytokine production in the lung and CD4^{+} T-cell IL-4 and IL-13 production in draining lymph nodes following *N. brasiliensis* infection, in agreement with previous studies [2, 105]. In order to further investigate the phenotype of these macrophages and their role in the lung during infection, we carried out a detailed molecular analysis of their gene expression profile in the following Chapter.

Analysis of differential gene expression of alveolar macrophages from naïve and *N. brasiliensis*-infected lungs

3.3.1 Introduction

We established in the previous chapters that mice with disrupted IL-4Rα expression on macrophages and neutrophils ($LysM^{Cre}IL\text{-}4R\alpha^{-/lox}$) rapidly developed enhanced acute and chronic lung inflammation following infection with *N. brasiliensis* as demonstrated by histopathological studies (Chapter 3.1). This increased inflammation was associated with increased numbers of $CD4^+$ and $CD8^+$ T-cells in the lung and increased secretion of TH2 cytokines in $LysM^{Cre}IL\text{-}4R\alpha^{-/lox}$ mice (Chapter 3.2). Though similar numbers of alveolar macrophages (AlvM) were present in the lung, $LysM^{Cre}IL\text{-}4R\alpha^{-/lox}$ lung cell suspensions showed impaired alternative macrophage activation. Together these data suggest that AAMs down-regulate lung inflammation by influencing T-cell responses following *N. brasiliensis* infection. This chapter investigates the differential gene expression patterns of AlvMs in *N. brasiliensis*-infected $IL\text{-}4R\alpha^{-/lox}$, $IL\text{-}4R\alpha^{-/-}$ and $LysM^{Cre}IL\text{-}4R\alpha^{-/lox}$ mice and discusses how variations in gene expression may influence *N. brasiliensis*-induced lung pathology.

Murine AAM activity is typically characterised as IL-4Rα-driven increase in *arginase-1* expression [72, 166-170]. Arginase-1 activity, in AAMs, is associated with repression of NO production, control of TH2 cytokine activity [72] and production of proline [169, 174]. This response is generally associated with anti-inflammatory and tissue repair responses. Other markers of AAMs include increased expression of mannose

receptor (MMR) [165] and chitinase and FIZZ family members (ChaFFs) [171]. ChaFFs include resistin-like molecules such as found in inflammatory zone 1 (FIZZ1; or resistin-like alpha or relmα) [172], chitinase-like molecules such as acidic mammalian chitinase (AMCase) [171] and Ym1 (or chitinase 3-like 3) [172, 173]. These AAMs biomarkers have been associated with the control of helminth-induced inflammation [72, 214]. In particular, AAMs are associated with the inhibition of potentially exacerbated T-cell responses in other helminth studies [72, 178].

Along with these markers are a range of other molecules including chemokines and cytokines that are also associated with AAM function [169, 192, 193]. Secretion of chemokines and cytokines by macrophages is particularly associated with recruitment of cells such as leukocytes and granulocytes by chemotaxis. Of potential relevance in the current study may be the chemokines CXCL9, CXCL10 and CXCL11 which are secreted by AlvMs and are associated with the onset of COPD [139]. Furthermore, CXCL11 (or ITAC) has a dual role as a caM associated chemokine [1, 169, 192, 236, 237].

In the following chapter, preliminary analysis was presented from a macrophage-targeted microarray that could enable further understanding of AAM phenotype and function in the *N. brasiliensis*-infected lung. The expression of 460 target genes were examined possibly associated with alveolar macrophage (AlvM) function (A. Kirby; unpublished data ; Appendix E). From these results data was generated that could help to define how the biology of IL-4Rα-responsive AlvMs in *N. brasiliensis* infections may control the onset of chronic lung inflammation. Importantly, this work may identify potential molecular markers that may underlie the rapid onset of the chronic lung pathology observed in $LysM^{Cre}IL\text{-}4R\alpha^{-/lox}$ mice.

3.3.2 Results:

3.3.2.1 Isolation of Alveolar Macrophages (AlvMs)

In order to analyse gene expression patterns of AlvMs following *N. brasiliensis* infection, a homogenous macrophage population, defined as autofluorescent $CD11c^{+}MHCII^{Lo}$ SSC^{HI} cells [196], were isolated by FACS at days 5, 42 and 180 p.i. (**Figure 14A**). Cytospins of the isolated AlvM samples revealed a homogenous population of macrophages with no discernable differences between the mouse groups or between the time points analysed (**Figure 14B**). An average yield of 80,000 AlvMs were obtained per lung with more than 98% purity (**Table 4**).

3.3.2.2 Preparation of isolated AlvM RNA for chip analysis

Total RNA was extracted from the isolated AlvMs and quantity, quality and integrity of the RNA was assessed using a BioAnalyzer 2100. The yield of extracted RNA ranged between 9 ng and 461 ng per experimental group (**Table 4**). The quality of the isolated RNA was assessed using the 28S:18S rRNA ratio which ranged from 0.3-1.0, while RNA integrity number (RIN) ranged between 4.7 and 7.6 (**Table 4**). Though these numbers were relatively low compared to an optimal rRNA ratio of 2.0 and RIN values above 7, clear 28S and 18S peaks were observed on the chromatograms (data not shown). The low integrity of the RNA may be partly attributed to accidental introduction of RNases during the purification or extraction processes. The RNA was then sent to the laboratory of Dr Alun Kirby (University of York, UK) for RNA

amplification, processing and hybridization to microarrays. All RNA samples were successfully linearly amplified to more than 20-fold amplification prior to hybridization to the microarrays (**Table 4**).

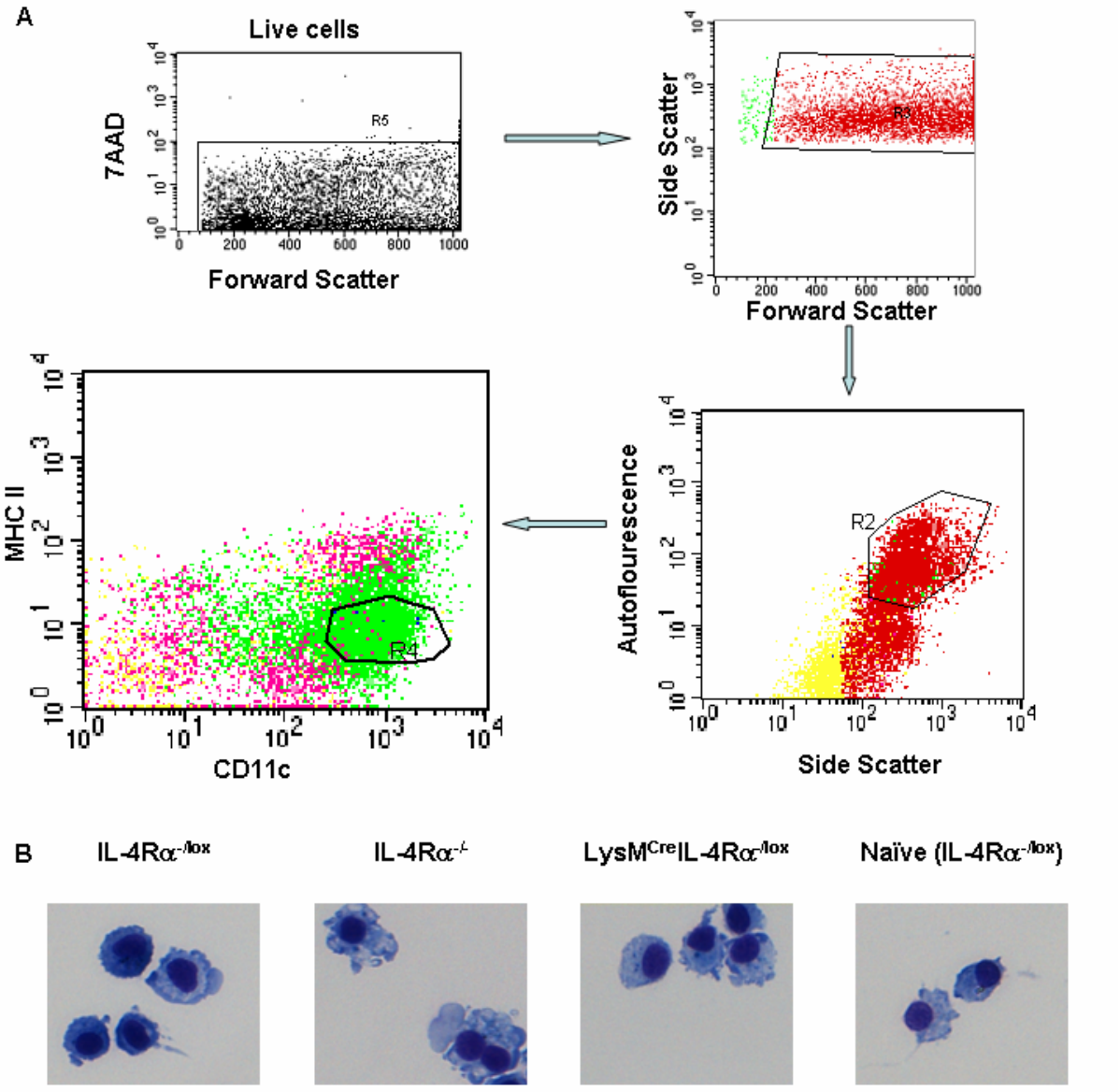

Figure 14: Alveolar macrophage sorting and morphology. (A) Sorting strategy for viable alveolar macrophages (autofluorescent SSC^{Hi} $CD11c^{Hi}$ $MHCII^{Lo}$) [196]. **(B)** Cytospins of sorted (99% purity) alveolar macrophages from gate R4 were stained (Rapiddif Quick) and viewed under a microscope (40x). Pooled lungs (n = 4 -5 mice per group). Representatives of duplicate experiments from all time points analysed.

Table 4: Summary of results of alveolar macrophage (SSC^{Hi},$CD11c^{Hi}$,$MHCII^{Lo}$) isolation, RNA extraction and amplification.

Days p.i.	Mouse Group	no. of cells ($x10^6$)	purity	total RNA amount (ng)	rRNA ratio [28s/18s]	RIN No.	Amplified RNA (ug)[a]	[a] Fold amplification
Day 5	IL4Rα^{flox}	400	99.10%	461	0.6	5.4	9319	20
Day 5	IL4Rα$^{-/-}$	93	99.60%	66	0.6	6.7	6061	92
Day 5	LysM^{cre}IL4Rα^{flox}	560	99.40%	260	0.3	4.7	7069	27
Day 5	Naïve (IL4Rα^{flox})	49	98.30%	26	0.8	7.1	3215	126
Day 5	IL4Rα^{flox}	650	99.40%	48	0.6	4.7	3584	74
Day 5	IL4Rα$^{-/-}$	160	99.70%	9	1.0	7.2	4203	448
Day 5	LysM^{cre}IL4Rα^{flox}	480	99.50%	17	0.8	6.8	4788	280
Day 5	Naïve (IL4Rα^{flox})	430	99.60%	23	0.7	6.4	5251	230
Day 42	IL4Rα^{flox}	98	99.50%	139	0.6	5.8	6065	44
Day 42	IL4Rα$^{-/-}$	84	99.10%	192	0.5	4.9	6266	33
Day 42	LysM^{cre}IL4Rα^{flox}	150	99.10%	129	0.5	5.5	7177	56
Day 42	Naïve (IL4Rα^{flox})	60	99.50%	61	0.6	6.1	3481	57
Day 42	IL4Rα^{flox}	1100	99.00%	11	0.5	7.6	389	34
Day 42	IL4Rα$^{-/-}$	590	99.20%	27	0.5	6.6	1003	37
Day 42	LysM^{cre}IL4Rα^{flox}	630	99.00%	25	0.7	6.9	767	30
Day 42	Naïve (IL4Rα^{flox})	580	99.10%	52	0.9	6.7	2487	48
Day 180	IL4Rα^{flox}	300	99.60%	217	0.7	7.1	5935	27
Day 180	IL4Rα$^{-/-}$	300	99.10%	374	0.6	5.9	7684	21
Day 180	LysM^{cre}IL4Rα^{flox}	300	99.00%	193	0.7	6.9	9475	49
Day 180	IL4Rα^{flox}	400	99.94%	134	0.7	7.3	10604	79
Day 180	IL4Rα$^{-/-}$	400	99.91%	115	0.7	6.5	12980	112
Day 180	LysM^{cre}IL4Rα^{flox}	400	99.80%	140	0.8	7.3	14800	105
Day 180	Naïve (IL4Rα^{flox})	350	99.70%	215	0.7	6.7	10433	49

[a] : Amplification data kindly provided by Dr. Kirby (York, UK)

3.3.2.3 Microarray of alveolar macrophage RNA

Following amplification, RNA was labelled and the reference RNA (Cy3), extracted from naïve unelicited peritoneal macrophages (or NUPM), and test RNA (Cy5) were hybridised onto a targeted microarray chip. All test RNA gene expression values were compared against NUPM reference RNA, $\log_2$ transformed, and expressed as M-values (i.e. $\log_2$ transformed Cy5/Cy3 ratios). Since the M-values of each test sample were compared to an identical, pooled reference RNA from NUPMs, inter- and intra-

group analyses could be carried out by comparing M-values from one group (e.g. infected IL-4Rα$^{-/lox}$) against M-values of another group (e.g. IL-4Rα$^{-/lox}$ naïve), to give the fold change (FC) expression values of the 460 genes analysed (Appendix E). Significantly differentially expressed genes ($p < 0.05$) were identified by a two-tailed, paired T-test that compared mouse groups in both experiments for each gene (as described in Methods and **Figure 7**). Thus a stringent analysis was reached since statistical tests identified only those genes which had similar regulation, but a large enough difference between M-values from both experimental repeats. The microarray analysis of AlvMs, presented below, were analysed for comparisons between: (1.) infected IL-4Rα$^{-/lox}$ vs. naïve IL-4Rα$^{-/lox}$ mice, (2.) IL-4Rα$^{-/-}$ vs. IL-4Rα$^{-/lox}$ mice and (3.) LysM^{Cre}IL-4Rα$^{-/lox}$ vs. IL-4Rα$^{-/lox}$ mice, following *N. brasiliensis* infection for all three time points.

3.3.2.3.1 Effect of N. brasiliensis infection on gene expression in alveolar macrophages (infected IL-4Rα$^{-/lox}$ vs. naïve IL-4Rα$^{-/lox}$)

Preliminary data analysis identified 36 genes that were significantly ($p < 0.05$) differentially expressed (14 at day 5 p.i. and 22 at day 42 p.i.) in AlvMs of infected IL-4Rα$^{-/lox}$ (WT) mice when compared to naïve IL-4Rα$^{-/lox}$ mice (**Figure 15A**). Functional clustering (Appendix E) of these significantly differentially expressed genes revealed the following:

- 5.6% encoded chemokines and their receptors (i.e. *BCA1, CCR5*)
- 5.6% were cytokines and their receptors (*IRF7, TNFR2p75*)
- 11.1% were TLR-related (*TIRAP, RIG-1, TLR7, TLR5*)

- 5.6% were involved in tissue/lung remodelling (*cathepsinS, cathepsinH*)
- 16.7% were involved in signalling (*SMAD4, SOCS2, SOCS3, Wnt7b, Lyn, SMAD6*)
- 27.8% were APC surface receptors or macrophage-related genes (*CIITA, CD1d2, Mr1, DCAR, PIR-A2, FFAR2* (day 5 and 42 p.i.), *CD40L, IgSR, Ym1*).

Of particular interest were genes associated with alternative activation of macrophages and regulation of pulmonary inflammation. Of the analysed genes associated with AAM, significant differences in expression were only found for *Ym1,* [7, 105 172] which was down-regulated at day 42 p.i. in AlvMs of IL-4Rα$^{-/lox}$ mice when compared to naïve IL-4Rα$^{-/lox}$ controls (**Figure 15A**).

Analysis of those genes that were significantly differentially expressed showed 36% of these genes to be associated with inflammation. Of the inflammatory genes, the following genes showed a significant down-regulation in expression in infected IL-4Rα$^{-/lox}$ mice when compared to naïve control mice: *TNFR2p75* [238, 239], *SOCS3* [240], *TIRAP* [241], *FFAR2* [242, 243], *HDAC5* [244], *IRF7* [245], and *cathepsinH* [120]. The following inflammatory genes showed significantly increased expression in IL-4Rα$^{-/lox}$ mice when compared to naïve control mice: *BCA1* [246, 247], *CathepsinS* [120], *BMPR1B* [248], *CCR5* [249], *SOCS2* [240] and the Toll-like receptor (TLR)-related genes *TLR5* [250], *TLR7* [251] and *RIG-I* [252, 253] (**Figure 15A**).

Together, this preliminary analysis may indicate that some of these AlvM genes were involved in host protective functions against pathogens and inflammation control.

3.3.2.3.2 Comparison of the gene expression profiles of IL-4Rα$^{-/-}$ AlvMs vs. IL-4Rα$^{-/lox}$ AlvMs following N. brasiliensis infection

Gene expression profiling between IL-4Rα$^{-/-}$ and IL-4Rα$^{-/lox}$ AlvMs revealed 28 genes out of 460 to be significantly ($p < 0.05$) differentially expressed (8 at day 5p.i., 6 at day 42 p.i. and 14 at 180 days p.i.) (**Figure 15B**). Functional clustering of these significantly differentially expressed genes showed the following:

- 21.4% of the genes encoded chemokines and their receptors (*CXCL16, BRAK, PF4, ITAC, CCR1, IL-8Ra*);
- 3.6% were cytokines (*IL-17B*)
- None were TLR-related
- 7.1% were involved in tissue/lung remodelling (*MMP13*, *cathepsinF*)
- 10.7% were involved in signalling (*RXRg, Dkk-2, Syk*)
- 21.4% were APC surface receptors or macrophage-related genes (*CLIP, PIR-B, PIR-A1, NFAM-1, PILR-a, CD200R1*)
- 10.7% were integrins (*ItgB6, CD51* (days 42 and 180 p.i.))
- 3.6% were associated with apoptosis (*BCL2*).

None of the typical AAM marker genes analysed (*Arg1* [72, 166], *MR* [165], *FIZZ1* [172, 173, 214], *Ym1*[7, 105 172], *MGL1* [189], *PPARγ* [176], nor caM marker gene *Nos2* [166]) showed significant differential expression in AlvMs from infected IL-4Rα$^{-/-}$ mice when compared to AlvMs from infected IL-4Rα$^{-/lox}$ mice at all three time points analysed.

Similar to our previous analysis, significant differential gene expression was found to be strongly associated with genes involved in modulating inflammation. We found

33% of such genes to be associated with inflammation. Of these the following were up-regulated in IL-4Rα$^{-/-}$ AlvMs: *CCR1* [254], *CXCL16* [255], *IL-17B* [256], *CLIP* [257], *BRAK* [258] and *ItgB6* [259]. Down-regulated inflammatory genes in IL-4Rα$^{-/-}$ AlvMs comprised of the following: *IL-8Ra* [260, 261], *ITAC* [139], *CathepsinF* [120] (**Figure 15B**).

Differential expression profiles of isolated AlvMs from infected IL-4Rα$^{-/-}$ mice (compared against infected IL-4Rα$^{-/lox}$ AlvMs) uncovered candidate genes potentially involved in controlling inflammation. Interestingly, none of the genes on the chip which represented known macrophage activation markers were significantly differentially expressed.

3.3.2.3.3 Comparison of the gene expression profiles of LysM^{Cre}IL-4Rα$^{-/lox}$ AlvMs vs. IL-4Rα$^{-/lox}$ AlvMs following N. brasiliensis infection

Comparison of AlvM gene expression profiles between LysM^{Cre}IL-4Rα$^{-/lox}$ and IL-4Rα$^{-/lox}$ mice revealed 33 genes that were significantly ($p < 0.05$) differentially expressed following *N. brasiliensis* infection (6 at day 5p.i., 20 at day 42 p.i. and 7 at 180 days p.i.). The majority (81.8%) of these significant genes were up-regulated in LysM^{Cre}IL-4Rα$^{-/lox}$ AlvMs when compared to IL-4Rα$^{-/lox}$ AlvMs (**Figure 15C**). Functional clustering of these significantly differentially expressed genes revealed the following:

- 6.1% encoded chemokine receptors (*CCR5, IL-8Rb*)
- 6.1% were cytokines (*TNF, IL-1b*)
- 12.1% were TLR-related (*card9* (days 5 and 42 p.i.), *TLR2, NOD2*)

- None were involved in tissue/lung remodelling
- 15.2% were involved in signalling (*RelB* (days 5 and 42 p.i.)*, SOCS3, SOCS1, Dkk-4*)
- 21.2% encoded APC surface receptors or macrophage-related genes (*FFAR2, LAIR1, ICAM-1, Lamp1* (days 5 and 42 p.i.)*, Ym1, SOD2*)
- 9.1% were integrins and lectins (*integrinB7, CD11b, DCIR*).

Of the AAM marker genes analysed, only *Ym1* was up-regulated in infected LysM^{Cre}IL-4Rα$^{-/lox}$ AlvMs when compared to infected IL-4Rα$^{-/lox}$ AlvMs (**Figure 15C**).

Similar to the other two mouse groups, of the 33 significantly differentially expressed genes in LysM^{Cre}IL-4Rα$^{-/lox}$ AlvMs, 48% were involved in regulating inflammation. The gene transcripts for *card9* [262] (at days 5 and 42 p.i.), *CCR5* [249], *SOD2* [263], *TLR2* [264], *TNF* [265], *FFAR2* [242, 243], *DCIR* [266], *IL-1β* [267], *RelB* [268] (at days 5 and 42 p.i.), *SOCS1* [240, 269], *SOCS3* [240] and *TRIM30* [270] were up-regulated; while *ACVR1* [248], *IL8Rb* [271, 272], *Nod2* [273] and *CD11b* [274] were down-regulated in the LysM^{Cre}IL-4Rα$^{-/lox}$ AlvMs when compared to IL-4Rα$^{-/lox}$ AlvMs following infection (**Figure 15C**). Interestingly, *RelB* [268] and *card9* [262], known to promote inflammation, were up-regulated at day 5 p.i. and sustained at day 42 p.i. in LysM^{Cre}IL-4Rα$^{-/lox}$ AlvMs. At this time point (day 42 p.i.), *SOCS1* and *SOCS3*, known to suppress pro-inflammatory cytokine responses [240, 269], were up-regulated. Importantly, strong pro-inflammatory genes, including *TNF* [265]*, IL-1β* [267] and *TLR2* [264], were amongst the significantly up-regulated genes in LysM^{Cre}IL-4Rα$^{-/lox}$ AlvMs. (**Figure 15C**).

Together, these preliminary microarray analyses indicated that AlvMs from infected LysM^{Cre}IL-4Rα$^{-/lox}$ mice portray gene expression profiles associated with control of inflammation as opposed to induction of known AAM-associated genes, similar to the other mouse groups. Furthermore, LysM^{Cre}IL-4Rα$^{-/lox}$ AlvMs showed up-regulation of *TNF* [265] and *IL-1β* [267] cytokine transcripts, indicating a more pronounced pro-inflammatory response compared to control IL-4Rα$^{-/lox}$ AlvMs.

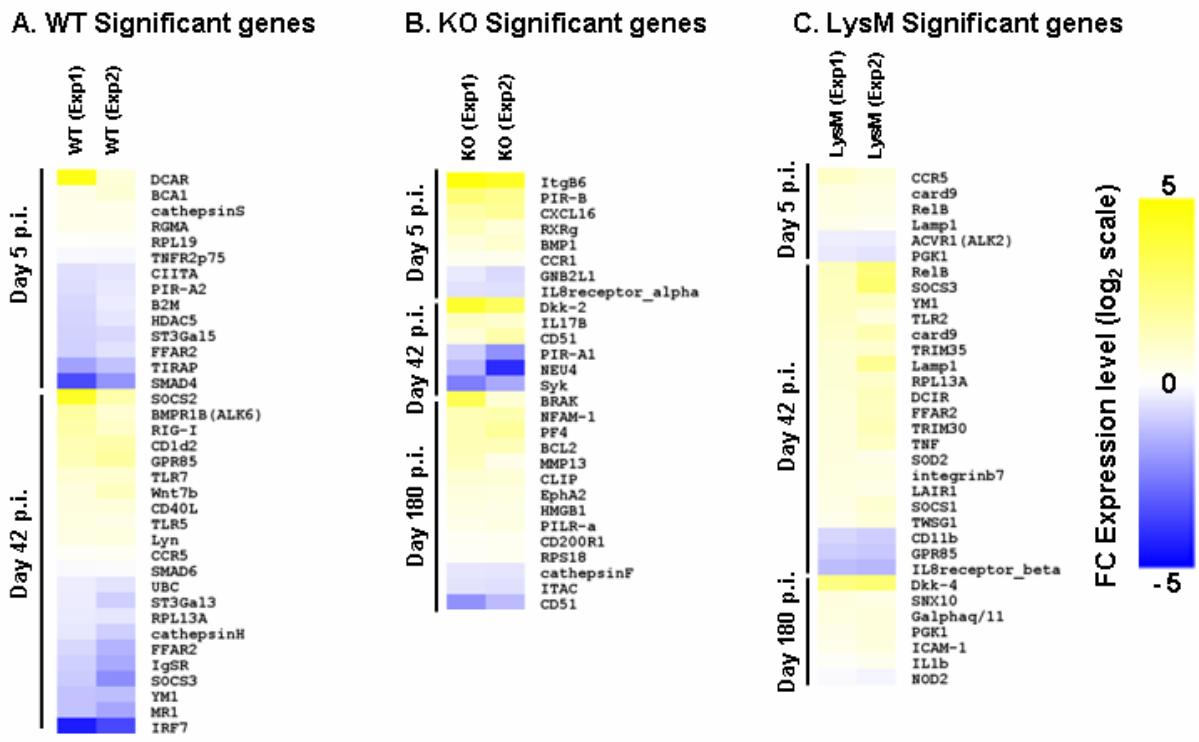

Figure 15: Significant differential expression of Alveolar Macrophage genes following *N. brasiliensis* infection. (A-C) Gene expression heatmaps of significantly ($p < 0.05$) differentially expressed genes in AlvM from infected: **(A)** IL-4Rα$^{-/lox}$ (WT) vs. naïve WT, **(B)** IL-4Rα$^{-/-}$ (KO) vs. WT, **(C)** LysM^{Cre}IL-4Rα$^{-/lox}$ (LysM) vs. WT mice. FC values (log_2 scale), ranked in descending order, were used to generate heatmaps of significantly up-regulated (*yellow*) and down-regulated (*blue*) genes of duplicate biological experiments. The gene symbols used are fully annotated in Appendix E. Exp1, Exp2: biological experiment 1 and biological (repeated) experiment 2. FC: Fold change. Significance could not be determined for WT genes at day 180 p.i., since there was only one naïve (WT) sample.

3.3.3 Discussion:

Based on our findings in the previous chapters, we hypothesized that IL-4Rα-responsive macrophages control *N. brasiliensis*-associated lung inflammation. In a transcriptomics approach, we analysed and compared the expression patterns of AlvMs from *N. brasiliensis*–infected LysM^{Cre}IL-4Rα$^{-/lox}$, IL-4Rα$^{-/-}$ and IL-4Rα$^{-/lox}$ control mice. Data from these preliminary microarray analyses suggests the following:

- A trend for down-regulation of anti-inflammatory-associated genes (i.e. *TNFR2p75*, *SOCS3*) and an up-regulation of genes associated with TLR/MyD88/NF-κB (innate) signalling pathways (*TLR5, TLR7, RIG-I*) and IL-13- and IL-4-induced genes (*CCR5*, *CD1d;* and *SOCS2*) in IL-4Rα$^{-/lox}$ AlvMs isolated from *N. brasiliensis*-infected lungs when compared with naïve IL-4Rα$^{-/lox}$ AlvMs.
- Following *N. brasiliensis* infection, LysM^{Cre}IL-4Rα$^{-/lox}$ AlvMs demonstrated up-regulated pro-inflammatory cytokine gene expression (*TNF* and *IL-1B*) when compared to infected IL-4Rα$^{-/lox}$ AlvMs. Additionally, the IL-13 induced gene, *CCR5*, and genes associated with innate responses, such as the TLR family genes (*card9, RelB, TLR2*) were also up-regulated in LysM^{Cre}IL-4Rα$^{-/lox}$ AlvMs.
- The gene expression profile of IL-4Rα$^{-/-}$ AlvMs differed substantially from the expression profiles of both IL-4Rα$^{-/lox}$ and LysM^{Cre}IL-4Rα$^{-/lox}$ AlvMs.

Taken together, these results indicate that specific disruption of IL-4Rα expression on macrophages (LysM^{Cre}IL-4Rα$^{-/lox}$ AlvMs) results in a heightened expression of genes associated with pro-inflammatory responses.

Interestingly, our analysis did not show the previously reported up-regulation of known AAM-associated markers in IL-4Rα$^{-/lox}$ AlvMs compared to naïve mice. No significant changes in expression of the following AAM associated genes were found: *Arg1* [72, 166], *MR* [165], *FIZZ1* [172, 173, 214], *MGL1* [189] or *PPARγ* [176]. However *Ym1* expression was reduced in AlvMs from infected IL-4Rα$^{-/lox}$ mice, but increased in infected LysM^{Cre}IL-4Rα$^{-/lox}$ AlvMs compared to infected IL-4Rα$^{-/lox}$ AlvMs. Increased *Ym1* expression is generally considered to be associated with induction of AAM [166, 169, 237] and has also been shown to be up-regulated in CD11c^{+} AlvMs during *N. brasiliensis* infection [7]. However, our data indicates that *Ym1* expression could be reduced following *N. brasiliensis* infection and also can be expressed independent of IL-4Rα-responsiveness. In support of this observation, it has recently been demonstrated that *Ym1* (as well as *MR*) expression can be independent of IL-4Rα-responsive macrophages during *S. mansoni*-induced inflammation [275].

Along with the above AAM biomarkers, it has been hypothesized that AAMs have a signature chemokine profile [169, 192, 193]. For example, from this chemokine spectrum, AAMs should have an up-regulation of *IL-8Ra* (*CXCR1*) and *IL-8Rb* (*CXCR2*), while *ITAC* (*CXCL11*) and *CXCL16* should be down-regulated [192, 193]. Again, the proposed AAM biomarker signatures were not evident in our study in AlvMs from IL-4Rα$^{-/lox}$ mice. However, AlvMs from LysM^{Cre}IL-4Rα$^{-/lox}$ mice showed a down-regulation of *IL-8Rb* (at 42 days p.i.), indicating that they could have a caM phenotype. Transcriptome analysis of AlvMs from IL-4Rα$^{-/-}$ mice gave a conflicting result, as the up- and down-regulation of *CXCL16* and *IL-8Ra*, respectively, at day 5 p.i. indicated a caM phenotype, while the down-regulation of *ITAC* at day 180 p.i. indicated an AAM phenotype. These conflicting results may suggest that macrophage activation is not a fixed phenotype, but

are dynamic and could be re-programmed, as shown in previous reports [276]. However, these are only a few genes from a proposed spectrum of numerous chemokines and their corresponding receptors and therefore no conclusions can yet be made.

Of particular importance in this study was our finding that macrophages isolated from *N. brasiliensis*–infected lungs show an IL-4Rα–dependent expression pattern for a range of genes associated with inflammation (**Table 5**), which may explain the rapid onset of inflammation observed in the lungs of LysM^{Cre}IL-4Rα$^{-/lox}$ mice compared to IL-4Rα$^{-/lox}$ mice (Chapter 3.1). These genes included the suppressor of cytokine signalling (SOCS) family and TLR family genes, since their significance were common to both IL-4Rα$^{-/lox}$ and LysM^{Cre}IL-4Rα$^{-/lox}$ AlvMs and have previously been shown to act as regulators of inflammation [240, 268, 277]. The most striking difference we found between LysM^{Cre}IL-4Rα$^{-/lox}$ and IL-4Rα$^{-/lox}$ AlvM gene expression profiles in this study was the significantly up-regulated expression of pro-inflammatory cytokine genes *TNF* [265] and *IL-1β* [267] in LysM^{Cre}IL-4Rα$^{-/lox}$ mice. If confirmed by qRT-PRC and protein analysis, these pro-inflammatory cytokines could play a role in the observed increased pulmonary inflammation in infected LysM^{Cre}IL-4Rα$^{-/lox}$ mice.

The exacerbated TH2 responses in the lungs of infected LysM^{Cre}IL-4Rα$^{-/lox}$ mice (Chapter 3.2) may be explained, in part, by the observed (two-fold) up-regulated expression of *CCR5*, since this chemokine receptor induces IL-13-mediated inflammation [190, 249]. *CCR5* is also induced by IL-13 [249], therefore able to induce a positive feedback loop. However, protein quantification and further intracellular signalling analysis needs to be carried out to confirm if this is the case.

Table 5: Significantly differentially expressed genes associated with inflammatory responses from AlvMs following *N. brasiliensis* infection.

Gene Expression Patterns associated with Promoting Inflammation			
Day p.i.	**IL-4Rα$^{-/lox}$ (vs. naïve)**	**IL-4Rα$^{-/-}$ (vs. WT)**	**LysM^{Cre}IL-4Rα$^{-/lox}$ (vs. WT)**
5	TNFR2p75 [238, 239] ↓ cathepsinS [120, 140] ↑ BCA1 [246, 247] ↑	CCR1 [254] ↑ CXCL16 [255] ↑	card9 [262] ↑ CCR5 [249] ↑
42	SOCS3 [240] ↓ CCR5 [249] ↑ TLR5 [250] ↑ BMPR1B [248] ↑ TLR7 [251] ↑ RIG-I [252, 253] ↑	IL17B [256] ↑	CD11b [274] ↓ SOD2 [263] ↑ TLR2 [264] ↑ TNF [265] ↑ FFAR2 [242, 243] ↑ DCIR [266] ↑ card9 [262] ↑
180	C.N.D.	CLIP [257] ↑ BRAK [258] ↑	IL1b [267] ↑
Gene Expression Patterns associated with Suppressing Inflammation			
Day p.i.	**IL-4Rα$^{-/lox}$ (vs. naïve)**	**IL-4Rα$^{-/-}$ (vs. WT)**	**LysM^{Cre}IL-4Rα$^{-/lox}$ (vs. WT)**
5	TIRAP [241] ↓ FFAR2 [242, 243] ↓ HDAC5 [244] ↓	IL8Ra [260, 261] ↓ ItgB6 [259] ↑	ACVR1 [248] ↓ RelB [268] ↑
42	IRF7 [245] ↓ FFAR2 [242, 243] ↓ cathepsinH [120] ↓ SOCS2 [240] ↑	no genes	IL8Rb [271, 272] ↓ SOCS1 [240] ↑ TRIM30 [270] ↑ SOCS3 [240] ↓ RelB [268] ↑
180	C.N.D.	ITAC [139] ↓ cathepsinF [120] ↓	Nod2 [273] ↓

↑ Up-regulated or ↓ down-regulated genes known to Promote (*red*) or Suppress (*blue*) inflammation. C.N.D. = could not determine; WT: (infected) IL-4Rα$^{-/lox}$.

Genes of the SOCS family that showed macrophage IL-4Rα–dependent differential expression in this study included *SOCS1*, *SOCS2* and *SOCS3*. In macrophages and T-cells, SOCS function by suppressing cytokine signalling through the blocking of cytokine receptor interactions or through degradation of JAK family proteins, which are key cytokine signalling proteins [278]. *SOCS1* is induced by both IFN-γ and IL-4 and can suppress IL-4 signalling via STAT-1 and STAT-6 respectively [269]. Induction of *SOCS3* is IFN-γ- or IL-10-dependent but independent of STAT-1 regulation and also suppresses IL-4 signalling [240, 269]. In contrast, *SOCS2* is induced by IL-4 and exerts its effects in a STAT-6 dependent manner, however it is unclear which cytokine signalling pathways SOCS2 suppresses. Interestingly, macrophages from day 42 p.i. *N. brasiliensis*–infected IL-4Rα$^{-/lox}$ mice showed up-regulation of *SOCS2* in agreement with an IL-4 (and IL-13) dominated immune response (Chapter 3.2). Macrophages from infected LysM^{Cre}IL-4Rα$^{-/lox}$ mice showed up-regulation of *SOCS1* and *SOCS3* at day 42 p.i., which could be a consequence of the absence of IL-4-responsiveness and subsequent induction of the IFN-γ-induced genes, *SOCS1* and *SOCS3* [240]. However, any suppressive activities driven by SOCS1 and SOCS3 may be insufficient in down-modulating inflammation in the lungs of *N. brasiliensis*-infected LysM^{Cre}IL-4Rα$^{-/lox}$ mice, since these mice still displayed significantly higher pathology scores at day 5 and 42 p.i. when compared to IL-4Rα$^{-/lox}$ and IL-4Rα$^{-/-}$ mice (Chapter 3.1).

In addition to SOCS genes, a number of significantly differentially expressed genes were observed which belong to the TLR family. AlvMs from infected IL-4Rα$^{-/lox}$ mice showed up-regulation of *TLR5* [250], *TLR7* [251] and *RIG-I* [252, 253] at day 42 p.i., while *TIRAP* [241] was down-regulated at day 5 p.i. AlvMs from LysM^{Cre}IL-4Rα$^{-/lox}$ mice

showed up-regulation of *card9* [262] and *TLR2* [264] at day 42 p.i., while *Nod2* [273] was down-regulated at day 180 p.i. In contrast, AlvMs from infected IL-4Rα$^{-/-}$ mice did not show significant differential expression of TLR-related genes. Although TLR genes are usually associated with innate immunity and the induction of inflammatory responses [9], they have recently been associated with chronic inflammation [277, 279]. Since necrotic cell death has also been associated with inflammation [279, 280], it has recently been suggested that TLRs could recognise these endogenous ligands from necrotic cells and thus further induce inflammatory responses via TLR signalling [279] . This could be a potential reason for the significant up-regulation of TLR genes at day 42 p.i. However, it does not explain why IL-4Rα$^{-/-}$ AlvMs did not show this similar up-regulation of TLR genes at day 42 p.i., nor does it explain the down-regulation of the other TLR-related genes (*TIRAP* and *Nod2*). Currently, it is not known whether *N. brasiliensis* infections induce TLR expression or signalling. Apart from an asthmatic study which showed that the suppressive effects of NES on OVA-induced asthma was TLR2- and TLR4-independent [281] and a TLR4-responsiveness study to LPS in *N. brasiliensis*-infected mice [282], only a few studies have shown a relationship between pulmonary inflammation and TLR signalling in a TH2 environment (such as asthma [283] and pulmonary virions inducing TH1 and TH2 cytokines [164, 284]). Since TLRs have been associated with inflammation and innate responses, it would be interesting to study this further, if confirmed by qRT-PCR.

Interestingly, significantly differentially expressed genes from IL-4Rα$^{-/-}$ AlvMs were not present in the profile of LysM^{Cre}IL-4Rα$^{-/lox}$ AlvMs, even though both macrophage populations lack IL-4Rα. Besides establishing a unique gene expression profile compared to the other mouse groups analysed, IL-4Rα$^{-/-}$ AlvMs did not show

significant expression of TLR-related genes and SOCS genes. Furthermore, IL-4Rα$^{-/-}$ AlvMs showed significant down-regulation of the caM biomarker *ITAC* (CXCL11), while ITAC was not significantly differentially expressed in the other mouse groups. These results reflect that the global IL-4Rα deficiency in IL-4Rα$^{-/-}$ mice is affected by the many immunological reactions during infection, and emphasizes the importance of studying gene expression using cell specific models. For example, IL-4Rα$^{-/-}$ mice showed a predominantly TH1 cytokine response in the lung while LysM^{Cre}IL-4Rα$^{-/lox}$ mice showed an increased TH2 response in the lung (Chapter 3.2). Furthermore, pulmonary inflammation in IL-4Rα$^{-/-}$ mice was significantly less severe than in LysM^{Cre}IL-4Rα$^{-/lox}$ mice (Chapter 3.1). Therefore, the drastic differences in the gene expression profiles between the IL-4Rα deficient macrophage populations could explain the drastic phenotypic differences in cytokine, physiological and inflammatory responses between IL-4Rα$^{-/-}$ and LysM^{Cre}IL-4Rα$^{-/lox}$ mice.

In summary, gene expression profiling of AlvMs showed significant differentially expressed genes in the infected strains with possible candidate genes involved in the increased inflammation in the lungs of LysM^{Cre}IL-4Rα$^{-/lox}$ mice.

Since a full analysis is beyond the scope of this thesis, future work would include further bioinformatic analysis, experimental repeats, quantification of selected genes by quantitative real-time PCR (qRT-PCR) and functional analysis including *in vitro* siRNA experiments in macrophages. Furthermore, since genes expression levels do not necessarily correlate with protein translation, the protein products of candidate genes will be quantified to establish possible relationships between gene expression and protein translation. Moreover, further experimental repeats are needed to reliably

detect significance and reduce variability (see Appendix E) between biological experiments. Variability can be minimized with more robust quality control procedures to control for biological and technical biases. For example intra- and inter-group fluorescent testing and quality assessment using Expression Console™ Software to test for unusually bright or dim chips, high sensitivity and specificity, correction of fluorescence intensities and assessment of RNA hybridization. Further rigorous bioinformatical analysis could be done to investigate each gene in more detail. This would entail compiling in-depth information for each gene by (i) extensive literature mining - either manually or using software such as MILANO [200], (ii) determining enrichment scores for over- and under-represented gene functions and Gene Ontology annotations using DAVID (Database for Annotation Visualization and Integrated Discovery)[285], (iii) mapping the differentially expressed genes to signalling pathways and constructing protein-protein interaction networks using Ingenuity Pathway Analysis (Ingenuity Systems, www.ingenuity.com).

4. CONCLUSION

In this study we explored the role of IL-4Rα-responsive macrophages in lung pathology resulting from *N. brasiliensis* infection. Our data demonstrated that macrophage-specific IL-4Rα-signalling is important in controlling chronic *N. brasiliensis*-driven lung pathology. The data confirmed previous reports of *N. brasiliensis* infection driving a largely IL-4Rα-independent development of chronic emphysemic-like pathology. Associated with this rapid development of a chronic lung inflammation at 5 days p.i. in LysM^{Cre}IL-4Rα$^{-/lox}$ mice, increased CD4^{+} and CD8^{+} T-cell numbers and increased TH2 cytokine responses were apparent in the lungs of infected LysM^{Cre}IL-4Rα$^{-/lox}$ mice when compared to IL-4Rα$^{-/lox}$ controls and IL-4Rα$^{-/-}$ mice. While macrophage cell numbers and morphology remained unaltered, arginase activity, indicative of alternative activation, was impaired in macrophages from infected LysM^{Cre}IL-4Rα$^{-/lox}$ mice. RNA transcriptomic studies of isolated alveolar macrophages showed a strong up-regulation of IL-13-associated inflammatory chemokine receptor, *CCR5*, and the pro-inflammatory cytokine genes *IL-1B* and *TNF* from LysM^{Cre}IL-4Rα$^{-/lox}$ mice.

Taken together, these data suggest that IL-4Rα-responsive macrophages are important for the down-modulation of pulmonary inflammation and TH2 cytokine responses during *N. brasiliensis* infection. These responses are characteristic of AAM-associated control of inflammation previously described in a range of helminth infection models where transgenic mouse models lacking AAMs demonstrated increased inflammation [59, 72, 214] and increased TH2 cytokine production [72, 214]. For example, *S. mansoni* infection studies in transgenic mice lacking either Relmα/Fizz1 (Retnla$^{-/-}$) [214] or

macrophage-specific Arginase1 ($LysM^{Cre}Arg1^{-/flox}$) [72], which were therefore unable to generate AAM, demonstrated increased inflammation and TH2 cytokine production.

Our microarray analysis of macrophages isolated from lungs of *N. brasiliensis* mice also agrees with our and other's previous findings that *N. brasiliensis* infection leads to the development of macrophage populations with anti-inflammatory properties [7]. Three important findings in our microarray study were of special interest as they suggested a different AAM phenotype to the M2 macrophage:

(i) A large percentage (> 32%) of significantly differentially expressed genes were associated with controlling inflammation.

(ii) A lack of robust AAM biomarkers in IL-4Rα$^{-/lox}$ mice AlvMs and a lack of either AAM or caM biomarkers in $LysM^{Cre}$IL-4Rα$^{-/lox}$ mice.

(iii) Up-regulation of TNF and IL-1B in $LysM^{Cre}$IL-4Rα$^{-/lox}$ mice

Cytokines and chemokines are associated with both macrophage differentiation [192, 193, 236, 286] and chronic inflammatory diseases [287]. Furthermore, TLRs induce chemokine production [287] and are associated with chronic inflammation [279, 287]. Therefore, the observed up-regulation of TLRs, cytokines and chemokines in $LysM^{Cre}$IL-4Rα$^{-/lox}$ mice, could be potential candidate genes involved in the early onset of inflammation in $LysM^{Cre}$IL-4Rα$^{-/lox}$ mice.

AAM-associated biomarkers, such as *Arg1* [72, 166], *MR* [165], *FIZZ1* [172, 173, 214], *MGL1* [189], *PPARγ* [176], have been shown to be up-regulated in lungs or macrophages from *N. brasiliensis*-infected mice. However, in our study, we did not find this up-regulation to be statistically significant in IL-4Rα$^{-/lox}$ mice. We also did not find an up-regulation

of iNOS, IL-12 or any other biomarker of classically activated macrophages in LysM^{Cre}IL-4Rα$^{-/lox}$ (or IL-4Rα$^{-/lox}$) mice. Therefore, it may be possible that the AlvMs in *N. brasiliensis*-infected mice have different characteristics of activation. It has been proposed that there are other sub-types of AAMs, based on biomarkers and functionality from other helminth studies that sub-divides the AAM classification into: M2a, M2b and M2c (outlined in Introduction) [167, 193].

Since we did not find clear differences in Arginase1 regulation or AAM biomarkers in IL-4Rα$^{-/lox}$ AlvMs, but did observe significant increases in TLR and matrix or tissue remodelling genes, this could be indicate that these macrophages may have characteristics that fall under the M2b or M2c classification, rather than the M2a classification (**Figure 16**). The AAM sub-classification M2b refers to macrophages that are involved in TH2 activation and immunoregulation, while M2c AAMs are referred to as "deactivated" macrophages and are involved in tissue remodelling and immunoregulation. These properties of both AAM subtypes were evident in our studies. The activation of macrophages in *N. brasiliensis*-infected LysM^{Cre}IL-4Rα$^{-/lox}$ mice suggest that they could be M2b AAMs as shown by their significant increases in *TNF* and *IL-1β* and TLR-related genes and a lack of up-regulation of caM biomarker genes, such as *NOS2*. However, further experimentation and functional studies are needed to further elucidate the exact properties of LysM^{Cre}IL-4Rα$^{-/lox}$ and IL-4Rα$^{-/lox}$ AlvMs. Since macrophages have such diverse and varied roles in infection and other general functions, it has been suggested that macrophage activation is not a fixed [7] or linear process [167, 193], but rather a dynamic one which could have overlapping properties [237]. This study may indicate that this is the case in *N. brasiliensis*-induced chronic pulmonary pathology.

From the work presented here we have demonstrated a clear requirement for the development of an anti-inflammatory, IL-4Rα-responsive pulmonary macrophage population as playing a key role in the inhibition of the development of *N. brasiliensis*-induced chronic lung inflammation. Moreover, our findings provide an excellent model for future studies on the identification of molecular targets that may control the onset of chronic lung disease. Together, these studies may provide therapeutic targets for treatment and reversal of chronic lung diseases.

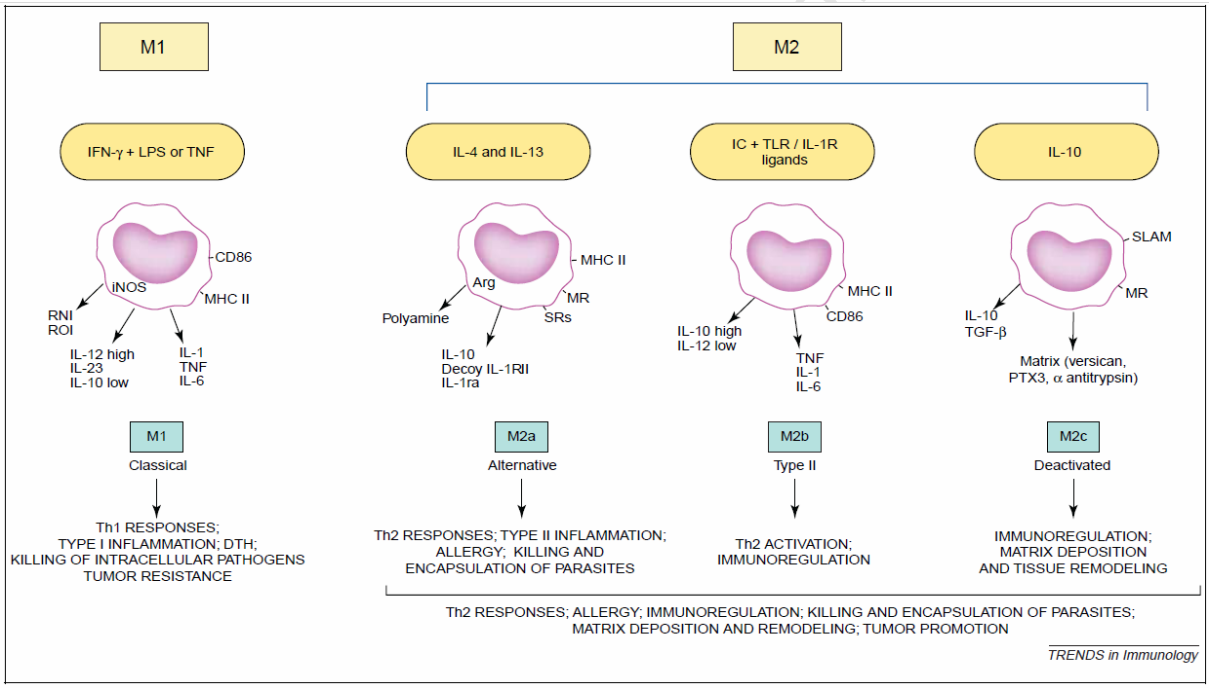

Figure 16: Properties of classically activated macrophages and M2a, M2b and M2c AAM sub-types. Taken from Mantovani *et al.* (2004) [193].

5. FUTURE WORK

The following future work is suggested:

To address the question whether IL-4Rα-responsive AAMs directly control the increase in $CD4^+$ T-cell numbers in the lungs of $LysM^{Cre}IL\text{-}4R\alpha^{-/lox}$ mice, proliferation studies should be carried out [178]. Here pulmonary macrophages and T-cells would be isolated from the lungs of infected mice and naïve control mice and co-cultured. Assessment of T-cell proliferation by CFSE staining (or similar) would establish whether IL-4Rα signalling on macrophages is required to control potentially pathogenic T-cell proliferation.

Other mechanisms suppressing proliferation could be explored including induction of T-cell apoptosis [178, 234] or T-cell responsiveness to arginase [72], which could affect T-cell proliferation. Depletion or the addition of arginine to macrophage/T-cell co-cultures and/or T-cell-only cultures would demonstrate whether macrophage arginase plays a direct role in controlling T-cell proliferation. To determine whether T-cell apoptosis can be induced by macrophages following *N. brasiliensis* infection, TUNEL and AnnexinV staining of $CD4^+$ T-cell populations isolated from lungs of infected mice could be carried out.

IL-10 is known to play a role in controlling inflammation [231] and regulating AAM biomarkers such as Ym1 and Mannose receptor [275]. Therefore, it would be interesting to determine whether IL-10 over-expression can counteract the heightened inflammation seen in $LysM^{Cre}IL\text{-}4R\alpha^{-/lox}$ mice. Interbreeding inducible lung-specific IL-10 transgenic mice that over-express IL-10 in the lung, using the Clara cell

promoter [231], with LysM^{Cre}IL-4Rα$^{-/lox}$ mice may allow to study the effects of IL-10 in the *N. brasiliensis*–induced pulmonary inflammation model.

Of particular interest would be to investigate the roles of the potential candidate genes associated with promoting inflammation, such as *Card9*, or suppressing inflammation such as *SOCS3* and *RelB*. The genes *Card9* and *RelB* were chosen as they were both up-regulated at two time points (5 and 42 days p.i.) in AlvMs from infected LysM^{Cre}IL-4Rα$^{-/lox}$ mice when compared to IL-4Rα$^{-/lox}$ AlvMs, and they were associated with TLR-dependent inflammation. It would be interesting to further investigate the role of *SOCS3* in IL-4Rα–responsive macrophages as it was up-regulated in LysM^{Cre}IL-4Rα$^{-/lox}$ AlvMs and down-regulated in IL-4Rα$^{-/lox}$ AlvMs. Furthermore, it would be interesting to include a naïve LysM^{Cre}IL-4Rα$^{-/lox}$ mouse control group to investigate which genes are pathogen-specific or specific to IL-4Rα signalling in our AlvM expression profile from LysM^{Cre}IL-4Rα$^{-/lox}$ mice. Subsequently, the RNA and protein expression of the candidate genes would first be confirmed by qRT-PCR and western blots respectively, in isolated AlvMs. Studies of these genes using transgenic mice (except for *SOCS3* which is lethal when abrogated [240]), or antibodies which bind and inactivate the proteins, or siRNA studies which inhibit mRNA gene expression, are feasible approaches to determine how these genes influence *N. brasiliensis*-induced chronic lung pathology.

It is envisaged that these investigations will gain further insight into anti-inflammatory mechanisms of AAMs in chronic lung pathology. Such findings are likely to be important in the future development of therapies against chronic lung inflammation.

6. REFERENCES

1. Marsland, B.J., Kurrer, M., Reissmann, R., Harris, N.L. & Kopf, M. Nippostrongylus brasiliensis infection leads to the development of emphysema associated with the induction of alternatively activated macrophages. *European journal of immunology* **38**, 479-488 (2008).
2. Reece, J.J., Siracusa, M.C., Southard, T.L., Brayton, C.F., Urban, J.F., Jr. & Scott, A.L. Hookworm-induced persistent changes to the immunological environment of the lung. *Infection and immunity* **76**, 3511-3524 (2008).
3. Marsland, B.J., Camberis, M. & Le Gros, G. Secretory products from infective forms of Nippostrongylus brasiliensis induce a rapid allergic airway inflammatory response. *Immunology and cell biology* **83**, 40-47 (2005).
4. Mearns, H., Horsnell, W.G., Hoving, J.C., Dewals, B., Cutler, A.J., Kirstein, F. *et al.* Interleukin-4-promoted T helper 2 responses enhance Nippostrongylus brasiliensis-induced pulmonary pathology. *Infection and immunity* **76**, 5535-5542 (2008).
5. Horsnell, W.G., Cutler, A.J., Hoving, J.C., Mearns, H., Myburgh, E., Arendse, B. *et al.* Delayed goblet cell hyperplasia, acetylcholine receptor expression, and worm expulsion in SMC-specific IL-4Ralpha-deficient mice. *PLoS pathogens* **3**, e1 (2007).
6. Marillier, R.G., Michels, C., Smith, E.M., Fick, L.C., Leeto, M., Dewals, B. *et al.* IL-4/IL-13 independent goblet cell hyperplasia in experimental helminth infections. *BMC immunology* **9**, 11 (2008).
7. Siracusa, M.C., Reece, J.J., Urban, J.F., Jr. & Scott, A.L. Dynamics of lung macrophage activation in response to helminth infection. *Journal of leukocyte biology* **84**, 1422-1433 (2008).
8. Male, D., Brostoff, B., Roth, B.D. & Roitt, I. *Immunology*, Edn. 7th Edition. (Elsevier Ltd., Canada; 2006).
9. Akira, S. & Takeda, K. Toll-like receptor signalling. *Nature reviews* **4**, 499-511 (2004).
10. Beutler, B. Innate immunity: an overview. *Molecular immunology* **40**, 845-859 (2004).
11. Hoebe, K., Janssen, E. & Beutler, B. The interface between innate and adaptive immunity. *Nature immunology* **5**, 971-974 (2004).
12. Xiang, M. & Fan, J. Pattern recognition receptor-dependent mechanisms of acute lung injury. *Molecular medicine (Cambridge, Mass* **16**, 69-82 (2010).
13. Alexopoulou, L., Holt, A.C., Medzhitov, R. & Flavell, R.A. Recognition of double-stranded RNA and activation of NF-kappaB by Toll-like receptor 3. *Nature* **413**, 732-738 (2001).
14. Rothenberg, M.E. & Hogan, S.P. The eosinophil. *Annual review of immunology* **24**, 147-174 (2006).
15. Rodriguez-Pinto, D. B cells as antigen presenting cells. *Cellular immunology* **238**, 67-75 (2005).
16. Brombacher, F. The role of interleukin-13 in infectious diseases and allergy. *Bioessays* **22**, 646-656 (2000).
17. Tato, C.M. & O'Shea, J.J. Immunology: what does it mean to be just 17? *Nature* **441**, 166-168 (2006).
18. Kurowska-Stolarska, M., Kewin, P., Murphy, G., Russo, R.C., Stolarski, B., Garcia, C.C. *et al.* IL-33 induces antigen-specific IL-5+ T cells and promotes

allergic-induced airway inflammation independent of IL-4. *J Immunol* **181**, 4780-4790 (2008).
19. Veldhoen, M., Uyttenhove, C., van Snick, J., Helmby, H., Westendorf, A., Buer, J. *et al.* Transforming growth factor-beta 'reprograms' the differentiation of T helper 2 cells and promotes an interleukin 9-producing subset. *Nature immunology* **9**, 1341-1346 (2008).
20. Mosmann, T.R., Cherwinski, H., Bond, M.W., Giedlin, M.A. & Coffman, R.L. Two types of murine helper T cell clone. I. Definition according to profiles of lymphokine activities and secreted proteins. *J Immunol* **136**, 2348-2357 (1986).
21. Szabo, S.J., Kim, S.T., Costa, G.L., Zhang, X., Fathman, C.G. & Glimcher, L.H. A novel transcription factor, T-bet, directs Th1 lineage commitment. *Cell* **100**, 655-669 (2000).
22. Szabo, S.J., Sullivan, B.M., Stemmann, C., Satoskar, A.R., Sleckman, B.P. & Glimcher, L.H. Distinct effects of T-bet in TH1 lineage commitment and IFN-gamma production in CD4 and CD8 T cells. *Science (New York, N.Y* **295**, 338-342 (2002).
23. Zheng, W. & Flavell, R.A. The transcription factor GATA-3 is necessary and sufficient for Th2 cytokine gene expression in CD4 T cells. *Cell* **89**, 587-596 (1997).
24. Kopf, M., Le Gros, G., Bachmann, M., Lamers, M.C., Bluethmann, H. & Kohler, G. Disruption of the murine IL-4 gene blocks Th2 cytokine responses. *Nature* **362**, 245-248 (1993).
25. Mosmann, T.R. & Sad, S. The expanding universe of T-cell subsets: Th1, Th2 and more. *Immunology today* **17**, 138-146 (1996).
26. Murphy, K.M. & Reiner, S.L. The lineage decisions of helper T cells. *Nature reviews* **2**, 933-944 (2002).
27. Forbes, E., van Panhuys, N., Min, B. & Le Gros, G. Differential requirements for IL-4/STAT6 signalling in CD4 T-cell fate determination and Th2-immune effector responses. *Immunology and cell biology* **88**, 240-243 (2010).
28. van Panhuys, N., Tang, S.C., Prout, M., Camberis, M., Scarlett, D., Roberts, J. *et al.* In vivo studies fail to reveal a role for IL-4 or STAT6 signaling in Th2 lymphocyte differentiation. *Proceedings of the National Academy of Sciences of the United States of America* **105**, 12423-12428 (2008).
29. Stumhofer, J.S., Laurence, A., Wilson, E.H., Huang, E., Tato, C.M., Johnson, L.M. *et al.* Interleukin 27 negatively regulates the development of interleukin 17-producing T helper cells during chronic inflammation of the central nervous system. *Nature immunology* **7**, 937-945 (2006).
30. Bettelli, E., Carrier, Y., Gao, W., Korn, T., Strom, T.B., Oukka, M. *et al.* Reciprocal developmental pathways for the generation of pathogenic effector TH17 and regulatory T cells. *Nature* **441**, 235-238 (2006).
31. Ivanov, II, McKenzie, B.S., Zhou, L., Tadokoro, C.E., Lepelley, A., Lafaille, J.J. *et al.* The orphan nuclear receptor RORgammat directs the differentiation program of proinflammatory IL-17+ T helper cells. *Cell* **126**, 1121-1133 (2006).
32. Fontenot, J.D., Gavin, M.A. & Rudensky, A.Y. Foxp3 programs the development and function of CD4+CD25+ regulatory T cells. *Nature immunology* **4**, 330-336 (2003).

33. Kolls, J.K., Kanaly, S.T. & Ramsay, A.J. Interleukin-17: an emerging role in lung inflammation. *American journal of respiratory cell and molecular biology* **28**, 9-11 (2003).
34. Koenders, M.I., Lubberts, E., Oppers-Walgreen, B., van den Bersselaar, L., Helsen, M.M., Di Padova, F.E. *et al.* Blocking of interleukin-17 during reactivation of experimental arthritis prevents joint inflammation and bone erosion by decreasing RANKL and interleukin-1. *The American journal of pathology* **167**, 141-149 (2005).
35. Huang, W., Na, L., Fidel, P.L. & Schwarzenberger, P. Requirement of interleukin-17A for systemic anti-Candida albicans host defense in mice. *The Journal of infectious diseases* **190**, 624-631 (2004).
36. Sakaguchi, S. Naturally arising Foxp3-expressing CD25+CD4+ regulatory T cells in immunological tolerance to self and non-self. *Nature immunology* **6**, 345-352 (2005).
37. Nelms, K., Keegan, A.D., Zamorano, J., Ryan, J.J. & Paul, W.E. The IL-4 receptor: signaling mechanisms and biologic functions. *Annual review of immunology* **17**, 701-738 (1999).
38. Lowenthal, J.W., Castle, B.E., Christiansen, J., Schreurs, J., Rennick, D., Arai, N. *et al.* Expression of high affinity receptors for murine interleukin 4 (BSF-1) on hemopoietic and nonhemopoietic cells. *J Immunol* **140**, 456-464 (1988).
39. Russell, S.M., Keegan, A.D., Harada, N., Nakamura, Y., Noguchi, M., Leland, P. *et al.* Interleukin-2 receptor gamma chain: a functional component of the interleukin-4 receptor. *Science (New York, N.Y* **262**, 1880-1883 (1993).
40. Murata, T., Taguchi, J. & Puri, R.K. Interleukin-13 receptor alpha' but not alpha chain: a functional component of interleukin-4 receptors. *Blood* **91**, 3884-3891 (1998).
41. Kelly-Welch, A.E., Hanson, E.M., Boothby, M.R. & Keegan, A.D. Interleukin-4 and interleukin-13 signaling connections maps. *Science (New York, N.Y* **300**, 1527-1528 (2003).
42. Andrews, A.L., Holloway, J.W., Holgate, S.T. & Davies, D.E. IL-4 receptor alpha is an important modulator of IL-4 and IL-13 receptor binding: implications for the development of therapeutic targets. *J Immunol* **176**, 7456-7461 (2006).
43. LaPorte, S.L., Juo, Z.S., Vaclavikova, J., Colf, L.A., Qi, X., Heller, N.M. *et al.* Molecular and structural basis of cytokine receptor pleiotropy in the interleukin-4/13 system. *Cell* **132**, 259-272 (2008).
44. Obiri, N.I., Debinski, W., Leonard, W.J. & Puri, R.K. Receptor for interleukin 13. Interaction with interleukin 4 by a mechanism that does not involve the common gamma chain shared by receptors for interleukins 2, 4, 7, 9, and 15. *The Journal of biological chemistry* **270**, 8797-8804 (1995).
45. Wills-Karp, M. Interleukin-13 in asthma pathogenesis. *Current allergy and asthma reports* **4**, 123-131 (2004).
46. Ramalingam, T.R., Pesce, J.T., Sheikh, F., Cheever, A.W., Mentink-Kane, M.M., Wilson, M.S. *et al.* Unique functions of the type II interleukin 4 receptor identified in mice lacking the interleukin 13 receptor alpha1 chain. *Nature immunology* **9**, 25-33 (2008).
47. Mikita, T., Campbell, D., Wu, P., Williamson, K. & Schindler, U. Requirements for interleukin-4-induced gene expression and functional characterization of Stat6. *Molecular and cellular biology* **16**, 5811-5820 (1996).

48. Ennaciri, J. & Girard, D. IL-4R(alpha), a new member that associates with Syk kinase: implication in IL-4-induced human neutrophil functions. *J Immunol* **183**, 5261-5269 (2009).
49. Donaldson, D.D., Whitters, M.J., Fitz, L.J., Neben, T.Y., Finnerty, H., Henderson, S.L. *et al.* The murine IL-13 receptor alpha 2: molecular cloning, characterization, and comparison with murine IL-13 receptor alpha 1. *J Immunol* **161**, 2317-2324 (1998).
50. Fichtner-Feigl, S., Strober, W., Kawakami, K., Puri, R.K. & Kitani, A. IL-13 signaling through the IL-13alpha2 receptor is involved in induction of TGF-beta1 production and fibrosis. *Nature medicine* **12**, 99-106 (2006).
51. Andrews, A.L., Nordgren, I.K., Kirby, I., Holloway, J.W., Holgate, S.T., Davies, D.E. *et al.* Cytoplasmic tail of IL-13Ralpha2 regulates IL-4 signal transduction. *Biochemical Society transactions* **37**, 873-876 (2009).
52. Morimoto, M., Zhao, A., Sun, R., Stiltz, J., Madden, K.B., Mentink-Kane, M. *et al.* IL-13 receptor alpha2 regulates the immune and functional response to Nippostrongylus brasiliensis infection. *J Immunol* **183**, 1934-1939 (2009).
53. Shimoda, K., van Deursen, J., Sangster, M.Y., Sarawar, S.R., Carson, R.T., Tripp, R.A. *et al.* Lack of IL-4-induced Th2 response and IgE class switching in mice with disrupted Stat6 gene. *Nature* **380**, 630-633 (1996).
54. Akimoto, T., Numata, F., Tamura, M., Takata, Y., Higashida, N., Takashi, T. *et al.* Abrogation of bronchial eosinophilic inflammation and airway hyperreactivity in signal transducers and activators of transcription (STAT)6-deficient mice. *The Journal of experimental medicine* **187**, 1537-1542 (1998).
55. Kuperman, D., Schofield, B., Wills-Karp, M. & Grusby, M.J. Signal transducer and activator of transcription factor 6 (Stat6)-deficient mice are protected from antigen-induced airway hyperresponsiveness and mucus production. *The Journal of experimental medicine* **187**, 939-948 (1998).
56. Miyata, S., Matsuyama, T., Kodama, T., Nishioka, Y., Kuribayashi, K., Takeda, K. *et al.* STAT6 deficiency in a mouse model of allergen-induced airways inflammation abolishes eosinophilia but induces infiltration of CD8+ T cells. *Clin Exp Allergy* **29**, 114-123 (1999).
57. Mearns, H. in Health Sciences Vol. Masters (Medicine) in Clinical Laboratory Sciences and Immunology (93 pages) (University of Cape Town, Cape Town; 2007).
58. Scales, H.E., Ierna, M.X. & Lawrence, C.E. The role of IL-4, IL-13 and IL-4Ralpha in the development of protective and pathological responses to Trichinella spiralis. *Parasite immunology* **29**, 81-91 (2007).
59. Herbert, D.R., Holscher, C., Mohrs, M., Arendse, B., Schwegmann, A., Radwanska, M. *et al.* Alternative macrophage activation is essential for survival during schistosomiasis and downmodulates T helper 1 responses and immunopathology. *Immunity* **20**, 623-635 (2004).
60. Barner, M., Mohrs, M., Brombacher, F. & Kopf, M. Differences between IL-4R alpha-deficient and IL-4-deficient mice reveal a role for IL-13 in the regulation of Th2 responses. *Curr Biol* **8**, 669-672 (1998).
61. Urban, J.F., Jr., Noben-Trauth, N., Donaldson, D.D., Madden, K.B., Morris, S.C., Collins, M. *et al.* IL-13, IL-4Ralpha, and Stat6 are required for the expulsion of the gastrointestinal nematode parasite Nippostrongylus brasiliensis. *Immunity* **8**, 255-264 (1998).
62. Mohrs, M., Ledermann, B., Kohler, G., Dorfmuller, A., Gessner, A. & Brombacher, F. Differences between IL-4- and IL-4 receptor alpha-deficient

mice in chronic leishmaniasis reveal a protective role for IL-13 receptor signaling. *J Immunol* **162**, 7302-7308 (1999).
63. Mohrs, M., Holscher, C. & Brombacher, F. Interleukin-4 receptor alpha-deficient BALB/c mice show an unimpaired T helper 2 polarization in response to Leishmania major infection. *Infection and immunity* **68**, 1773-1780 (2000).
64. Tachdjian, R., Mathias, C., Al Khatib, S., Bryce, P.J., Kim, H.S., Blaeser, F. *et al.* Pathogenicity of a disease-associated human IL-4 receptor allele in experimental asthma. *The Journal of experimental medicine* **206**, 2191-2204 (2009).
65. Ray, M.K., Fagan, S.P. & Brunicardi, F.C. The Cre-loxP system: a versatile tool for targeting genes in a cell- and stage-specific manner. *Cell transplantation* **9**, 805-815 (2000).
66. Sauer, B. Inducible gene targeting in mice using the Cre/lox system. *Methods (San Diego, Calif* **14**, 381-392 (1998).
67. Gu, H., Marth, J.D., Orban, P.C., Mossmann, H. & Rajewsky, K. Deletion of a DNA polymerase beta gene segment in T cells using cell type-specific gene targeting. *Science (New York, N.Y* **265**, 103-106 (1994).
68. Nieuwenhuizen, N., Herbert, D.R., Lopata, A.L. & Brombacher, F. CD4+ T cell-specific deletion of IL-4 receptor alpha prevents ovalbumin-induced anaphylaxis by an IFN-gamma-dependent mechanism. *J Immunol* **179**, 2758-2765 (2007).
69. Radwanska, M., Cutler, A.J., Hoving, J.C., Magez, S., Holscher, C., Bohms, A. *et al.* Deletion of IL-4Ralpha on CD4 T cells renders BALB/c mice resistant to Leishmania major infection. *PLoS pathogens* **3**, e68 (2007).
70. Kuperman, D.A., Huang, X., Nguyenvu, L., Holscher, C., Brombacher, F. & Erle, D.J. IL-4 receptor signaling in Clara cells is required for allergen-induced mucus production. *J Immunol* **175**, 3746-3752 (2005).
71. Clausen, B.E., Burkhardt, C., Reith, W., Renkawitz, R. & Forster, I. Conditional gene targeting in macrophages and granulocytes using LysMcre mice. *Transgenic research* **8**, 265-277 (1999).
72. Pesce, J.T., Ramalingam, T.R., Mentink-Kane, M.M., Wilson, M.S., El Kasmi, K.C., Smith, A.M. *et al.* Arginase-1-expressing macrophages suppress Th2 cytokine-driven inflammation and fibrosis. *PLoS pathogens* **5**, e1000371 (2009).
73. Cao, Y., Brombacher, F., Tunyogi-Csapo, M., Glant, T.T. & Finnegan, A. Interleukin-4 regulates proteoglycan-induced arthritis by specifically suppressing the innate immune response. *Arthritis and rheumatism* **56**, 861-870 (2007).
74. Gallina, G., Dolcetti, L., Serafini, P., De Santo, C., Marigo, I., Colombo, M.P. *et al.* Tumors induce a subset of inflammatory monocytes with immunosuppressive activity on CD8+ T cells. *The Journal of clinical investigation* **116**, 2777-2790 (2006).
75. Jenkins, S.J. & Allen, J.E. Similarity and diversity in macrophage activation by nematodes, trematodes, and cestodes. *Journal of biomedicine & biotechnology* **2010**, 262609 (2010).
76. Bethony, J., Brooker, S., Albonico, M., Geiger, S.M., Loukas, A., Diemert, D. *et al.* Soil-transmitted helminth infections: ascariasis, trichuriasis, and hookworm. *Lancet* **367**, 1521-1532 (2006).

77. Hotez, P.J., Brindley, P.J., Bethony, J.M., King, C.H., Pearce, E.J. & Jacobson, J. Helminth infections: the great neglected tropical diseases. *The Journal of clinical investigation* **118**, 1311-1321 (2008).
78. Nacher, M. Malaria vaccine trials in a wormy world. *Trends in parasitology* **17**, 563-565 (2001).
79. Su, Z., Segura, M., Morgan, K., Loredo-Osti, J.C. & Stevenson, M.M. Impairment of protective immunity to blood-stage malaria by concurrent nematode infection. *Infection and immunity* **73**, 3531-3539 (2005).
80. Elias, D., Britton, S., Kassu, A. & Akuffo, H. Chronic helminth infections may negatively influence immunity against tuberculosis and other diseases of public health importance. *Expert review of anti-infective therapy* **5**, 475-484 (2007).
81. Yazdanbakhsh, M., Kremsner, P.G. & van Ree, R. Allergy, parasites, and the hygiene hypothesis. *Science (New York, N.Y* **296**, 490-494 (2002).
82. Cooper, P.J., Chico, M.E., Rodrigues, L.C., Ordonez, M., Strachan, D., Griffin, G.E. *et al.* Reduced risk of atopy among school-age children infected with geohelminth parasites in a rural area of the tropics. *The Journal of allergy and clinical immunology* **111**, 995-1000 (2003).
83. Medeiros, M., Jr., Figueiredo, J.P., Almeida, M.C., Matos, M.A., Araujo, M.I., Cruz, A.A. *et al.* Schistosoma mansoni infection is associated with a reduced course of asthma. *The Journal of allergy and clinical immunology* **111**, 947-951 (2003).
84. Yazdanbakhsh, M., van den Biggelaar, A. & Maizels, R.M. Th2 responses without atopy: immunoregulation in chronic helminth infections and reduced allergic disease. *Trends in immunology* **22**, 372-377 (2001).
85. Summers, R.W., Elliott, D.E., Urban, J.F., Jr., Thompson, R. & Weinstock, J.V. Trichuris suis therapy in Crohn's disease. *Gut* **54**, 87-90 (2005).
86. Summers, R.W., Elliott, D.E., Urban, J.F., Jr., Thompson, R.A. & Weinstock, J.V. Trichuris suis therapy for active ulcerative colitis: a randomized controlled trial. *Gastroenterology* **128**, 825-832 (2005).
87. Egwang, T.G., Gauldie, J. & Befus, D. Complement-dependent killing of Nippostrongylus brasiliensis infective larvae by rat alveolar macrophages. *Clinical and experimental immunology* **55**, 149-156 (1984).
88. Ramaswamy, K., De Sanctis, G.T., Green, F. & Befus, D. Pathology of pulmonary parasitic migration: morphological and bronchoalveolar cellular responses following Nippostrongylus brasiliensis infection in rats. *The Journal of parasitology* **77**, 302-312 (1991).
89. Urban, J.F., Jr., Katona, I.M., Paul, W.E. & Finkelman, F.D. Interleukin 4 is important in protective immunity to a gastrointestinal nematode infection in mice. *Proceedings of the National Academy of Sciences of the United States of America* **88**, 5513-5517 (1991).
90. Svetic, A., Madden, K.B., Zhou, X.D., Lu, P., Katona, I.M., Finkelman, F.D. *et al.* A primary intestinal helminthic infection rapidly induces a gut-associated elevation of Th2-associated cytokines and IL-3. *J Immunol* **150**, 3434-3441 (1993).
91. Finkelman, F.D., Shea-Donohue, T., Goldhill, J., Sullivan, C.A., Morris, S.C., Madden, K.B. *et al.* Cytokine regulation of host defense against parasitic gastrointestinal nematodes: lessons from studies with rodent models. *Annual review of immunology* **15**, 505-533 (1997).

92. Voehringer, D., Shinkai, K. & Locksley, R.M. Type 2 immunity reflects orchestrated recruitment of cells committed to IL-4 production. *Immunity* **20**, 267-277 (2004).
93. Anthony, R.M., Urban, J.F., Jr., Alem, F., Hamed, H.A., Rozo, C.T., Boucher, J.L. *et al.* Memory T(H)2 cells induce alternatively activated macrophages to mediate protection against nematode parasites. *Nature medicine* **12**, 955-960 (2006).
94. Ramalingam, T.R., Pesce, J.T., Mentink-Kane, M.M., Madala, S., Cheever, A.W., Comeau, M.R. *et al.* Regulation of helminth-induced Th2 responses by thymic stromal lymphopoietin. *J Immunol* **182**, 6452-6459 (2009).
95. Taylor, B.C., Zaph, C., Troy, A.E., Du, Y., Guild, K.J., Comeau, M.R. *et al.* TSLP regulates intestinal immunity and inflammation in mouse models of helminth infection and colitis. *The Journal of experimental medicine* **206**, 655-667 (2009).
96. Ohnmacht, C. & Voehringer, D. Basophils protect against reinfection with hookworms independently of mast cells and memory Th2 cells. *J Immunol* **184**, 344-350 (2010).
97. Anthony, R.M., Rutitzky, L.I., Urban, J.F., Jr., Stadecker, M.J. & Gause, W.C. Protective immune mechanisms in helminth infection. *Nature reviews* **7**, 975-987 (2007).
98. Maizels, R.M. & Yazdanbakhsh, M. Immune regulation by helminth parasites: cellular and molecular mechanisms. *Nature reviews* **3**, 733-744 (2003).
99. Herbert, D.R., Yang, J.Q., Hogan, S.P., Groschwitz, K., Khodoun, M., Munitz, A. *et al.* Intestinal epithelial cell secretion of RELM-beta protects against gastrointestinal worm infection. *The Journal of experimental medicine* **206**, 2947-2957 (2009).
100. Daly, C.M., Mayrhofer, G. & Dent, L.A. Trapping and immobilization of Nippostrongylus brasiliensis larvae at the site of inoculation in primary infections of interleukin-5 transgenic mice. *Infection and immunity* **67**, 5315-5323 (1999).
101. Turner, J.D., Faulkner, H., Kamgno, J., Cormont, F., Van Snick, J., Else, K.J. *et al.* Th2 cytokines are associated with reduced worm burdens in a human intestinal helminth infection. *The Journal of infectious diseases* **188**, 1768-1775 (2003).
102. Allen, J.E. & Loke, P. Divergent roles for macrophages in lymphatic filariasis. *Parasite immunology* **23**, 345-352 (2001).
103. Allen, J.E. & Maizels, R.M. Immunology of human helminth infection. *International archives of allergy and immunology* **109**, 3-10 (1996).
104. Matsuda, S., Tani, Y., Yamada, M., Yoshimura, K. & Arizono, N. Type 2-biased expression of cytokine genes in lung granulomatous lesions induced by Nippostrongylus brasiliensis infection. *Parasite immunology* **23**, 219-226 (2001).
105. Reece, J.J., Siracusa, M.C. & Scott, A.L. Innate immune responses to lung-stage helminth infection induce alternatively activated alveolar macrophages. *Infection and immunity* **74**, 4970-4981 (2006).
106. Sandler, N.G., Mentink-Kane, M.M., Cheever, A.W. & Wynn, T.A. Global gene expression profiles during acute pathogen-induced pulmonary inflammation reveal divergent roles for Th1 and Th2 responses in tissue repair. *J Immunol* **171**, 3655-3667 (2003).

107. Mohrs, K., Harris, D.P., Lund, F.E. & Mohrs, M. Systemic dissemination and persistence of Th2 and type 2 cells in response to infection with a strictly enteric nematode parasite. *J Immunol* **175**, 5306-5313 (2005).
108. Finkelman, F.D., Shea-Donohue, T., Morris, S.C., Gildea, L., Strait, R., Madden, K.B. *et al.* Interleukin-4- and interleukin-13-mediated host protection against intestinal nematode parasites. *Immunological reviews* **201**, 139-155 (2004).
109. Coyle, A.J., Kohler, G., Tsuyuki, S., Brombacher, F. & Kopf, M. Eosinophils are not required to induce airway hyperresponsiveness after nematode infection. *European journal of immunology* **28**, 2640-2647 (1998).
110. Urban, J.F., Jr., Madden, K.B., Svetic, A., Cheever, A., Trotta, P.P., Gause, W.C. *et al.* The importance of Th2 cytokines in protective immunity to nematodes. *Immunological reviews* **127**, 205-220 (1992).
111. MacDonald, A.S., Araujo, M.I. & Pearce, E.J. Immunology of parasitic helminth infections. *Infection and immunity* **70**, 427-433 (2002).
112. Gause, W.C., Urban, J.F., Jr. & Stadecker, M.J. The immune response to parasitic helminths: insights from murine models. *Trends in immunology* **24**, 269-277 (2003).
113. McKenzie, G.J., Bancroft, A., Grencis, R.K. & McKenzie, A.N. A distinct role for interleukin-13 in Th2-cell-mediated immune responses. *Curr Biol* **8**, 339-342 (1998).
114. Urban, J.F., Jr., Noben-Trauth, N., Schopf, L., Madden, K.B. & Finkelman, F.D. Cutting edge: IL-4 receptor expression by non-bone marrow-derived cells is required to expel gastrointestinal nematode parasites. *J Immunol* **167**, 6078-6081 (2001).
115. Cambridge www.path.cam.ac.uk/partIB_pract/P15/image02.jpg.
116. Cohn, L., Homer, R.J., MacLeod, H., Mohrs, M., Brombacher, F. & Bottomly, K. Th2-induced airway mucus production is dependent on IL-4Ralpha, but not on eosinophils. *J Immunol* **162**, 6178-6183 (1999).
117. Salman, S.K. & Brown, P.J. A study of the pathology of the lungs of rats after subcutaneous or intravenous injection of active or inactive larvae of Nippostrongylus brasiliensis. *Journal of comparative pathology* **90**, 447-455 (1980).
118. Arizono, N., Nishida, M., Uchikawa, R., Yamada, M., Matsuda, S., Tegoshi, T. *et al.* Lung granulomatous response induced by infection with the intestinal nematode Nippostrongylus brasiliensis is suppressed in mast cell-deficient Ws/Ws rats. *Clinical and experimental immunology* **106**, 55-61 (1996).
119. Churg, A. & Wright, J.L. Proteases and emphysema. *Current opinion in pulmonary medicine* **11**, 153-159 (2005).
120. Veillard, F., Lecaille, F. & Lalmanach, G. Lung cysteine cathepsins: intruders or unorthodox contributors to the kallikrein-kinin system? *The international journal of biochemistry & cell biology* **40**, 1079-1094 (2008).
121. Zheng, T., Zhu, Z., Wang, Z., Homer, R.J., Ma, B., Riese, R.J., Jr. *et al.* Inducible targeting of IL-13 to the adult lung causes matrix metalloproteinase- and cathepsin-dependent emphysema. *The Journal of clinical investigation* **106**, 1081-1093 (2000).
122. Di Stefano, A., Caramori, G., Ricciardolo, F.L., Capelli, A., Adcock, I.M. & Donner, C.F. Cellular and molecular mechanisms in chronic obstructive pulmonary disease: an overview. *Clin Exp Allergy* **34**, 1156-1167 (2004).

123. Barnes, P.J. Immunology of asthma and chronic obstructive pulmonary disease. *Nature reviews* **8**, 183-192 (2008).
124. Bhattacharya, S., Srisuma, S., Demeo, D.L., Shapiro, S.D., Bueno, R., Silverman, E.K. *et al.* Molecular biomarkers for quantitative and discrete COPD phenotypes. *American journal of respiratory cell and molecular biology* **40**, 359-367 (2009).
125. Taraseviciene-Stewart, L. & Voelkel, N.F. Molecular pathogenesis of emphysema. *The Journal of clinical investigation* **118**, 394-402 (2008).
126. Pauwels, R.A., Buist, A.S., Calverley, P.M., Jenkins, C.R. & Hurd, S.S. Global strategy for the diagnosis, management, and prevention of chronic obstructive pulmonary disease. NHLBI/WHO Global Initiative for Chronic Obstructive Lung Disease (GOLD) Workshop summary. *American journal of respiratory and critical care medicine* **163**, 1256-1276 (2001).
127. Mathers, C.D. & Loncar, D. Projections of global mortality and burden of disease from 2002 to 2030. *PLoS medicine* **3**, e442 (2006).
128. Barnes, P.J. & Stockley, R.A. COPD: current therapeutic interventions and future approaches. *Eur Respir J* **25**, 1084-1106 (2005).
129. Agusti, A., MacNee, W., Donaldson, K. & Cosio, M. Hypothesis: does COPD have an autoimmune component? *Thorax* **58**, 832-834 (2003).
130. Petty, T.L. COPD: clinical phenotypes. *Pulmonary pharmacology & therapeutics* **15**, 341-351 (2002).
131. Finkelstein, R., Ma, H.D., Ghezzo, H., Whittaker, K., Fraser, R.S. & Cosio, M.G. Morphometry of small airways in smokers and its relationship to emphysema type and hyperresponsiveness. *American journal of respiratory and critical care medicine* **152**, 267-276 (1995).
132. Celli, B.R. Chronic obstructive pulmonary disease: from unjustified nihilism to evidence-based optimism. *Proceedings of the American Thoracic Society* **3**, 58-65 (2006).
133. Schafroth Torok, S. & Leuppi, J.D. Bronchial hyper-responsiveness and exhaled nitric oxide in chronic obstructive pulmonary disease. *Swiss Med Wkly* **137**, 385-391 (2007).
134. Eriksson, S. Pulmonary Emphysema and Alpha1-Antitrypsin Deficiency. *Acta medica Scandinavica* **175**, 197-205 (1964).
135. Feghali-Bostwick, C.A., Gadgil, A.S., Otterbein, L.E., Pilewski, J.M., Stoner, M.W., Csizmadia, E. *et al.* Autoantibodies in patients with chronic obstructive pulmonary disease. *American journal of respiratory and critical care medicine* **177**, 156-163 (2008).
136. Rutgers, S.R., Postma, D.S., ten Hacken, N.H., Kauffman, H.F., van Der Mark, T.W., Koeter, G.H. *et al.* Ongoing airway inflammation in patients with COPD who do not currently smoke. *Thorax* **55**, 12-18 (2000).
137. Gadgil, A. & Duncan, S.R. Role of T-lymphocytes and pro-inflammatory mediators in the pathogenesis of chronic obstructive pulmonary disease. *International journal of chronic obstructive pulmonary disease* **3**, 531-541 (2008).
138. Lee, S.H., Goswami, S., Grudo, A., Song, L.Z., Bandi, V., Goodnight-White, S. *et al.* Antielastin autoimmunity in tobacco smoking-induced emphysema. *Nature medicine* **13**, 567-569 (2007).
139. Stefanska, A.M. & Walsh, P.T. Chronic obstructive pulmonary disease: evidence for an autoimmune component. *Cellular & molecular immunology* **6**, 81-86 (2009).

140. Abboud, R.T. & Vimalanathan, S. Pathogenesis of COPD. Part I. The role of protease-antiprotease imbalance in emphysema. *Int J Tuberc Lung Dis* **12**, 361-367 (2008).
141. Gross, P., Pfitzer, E.A., Tolker, E., Babyak, M.A. & Kaschak, M. Experimental Emphysema: Its Production with Papain in Normal and Silicotic Rats. *Archives of environmental health* **11**, 50-58 (1965).
142. Mahadeva, R. & Shapiro, S.D. Chronic obstructive pulmonary disease * 3: Experimental animal models of pulmonary emphysema. *Thorax* **57**, 908-914 (2002).
143. Wang, Z., Zheng, T., Zhu, Z., Homer, R.J., Riese, R.J., Chapman, H.A., Jr. *et al.* Interferon gamma induction of pulmonary emphysema in the adult murine lung. *The Journal of experimental medicine* **192**, 1587-1600 (2000).
144. Hautamaki, R.D., Kobayashi, D.K., Senior, R.M. & Shapiro, S.D. Requirement for macrophage elastase for cigarette smoke-induced emphysema in mice. *Science (New York, N.Y* **277**, 2002-2004 (1997).
145. Kim, E.Y., Battaile, J.T., Patel, A.C., You, Y., Agapov, E., Grayson, M.H. *et al.* Persistent activation of an innate immune response translates respiratory viral infection into chronic lung disease. *Nature medicine* **14**, 633-640 (2008).
146. Kraft, M. Asthma and chronic obstructive pulmonary disease exhibit common origins in any country! *American journal of respiratory and critical care medicine* **174**, 238-240; discussion 243-234 (2006).
147. Barnes, P.J. Against the Dutch hypothesis: asthma and chronic obstructive pulmonary disease are distinct diseases. *American journal of respiratory and critical care medicine* **174**, 240-243; discussion 243-244 (2006).
148. Marsland, B.J., Nembrini, C., Schmitz, N., Abel, B., Krautwald, S., Bachmann, M.F. *et al.* Innate signals compensate for the absence of PKC-{theta} during in vivo CD8(+) T cell effector and memory responses. *Proceedings of the National Academy of Sciences of the United States of America* **102**, 14374-14379 (2005).
149. Mauad, T. & Dolhnikoff, M. Pathologic similarities and differences between asthma and chronic obstructive pulmonary disease. *Current opinion in pulmonary medicine* **14**, 31-38 (2008).
150. Elias, J. The relationship between asthma and COPD. Lessons from transgenic mice. *Chest* **126**, 111S-116S; discussion 159S-161S (2004).
151. Heinzmann, A. & Deichmann, K.A. Genes for atopy and asthma. *Current opinion in allergy and clinical immunology* **1**, 387-392 (2001).
152. Saetta, M., Di Stefano, A., Turato, G., Facchini, F.M., Corbino, L., Mapp, C.E. *et al.* CD8+ T-lymphocytes in peripheral airways of smokers with chronic obstructive pulmonary disease. *American journal of respiratory and critical care medicine* **157**, 822-826 (1998).
153. Curtis, J.L., Freeman, C.M. & Hogg, J.C. The immunopathogenesis of chronic obstructive pulmonary disease: insights from recent research. *Proceedings of the American Thoracic Society* **4**, 512-521 (2007).
154. Russell, R.E., Thorley, A., Culpitt, S.V., Dodd, S., Donnelly, L.E., Demattos, C. *et al.* Alveolar macrophage-mediated elastolysis: roles of matrix metalloproteinases, cysteine, and serine proteases. *American journal of physiology* **283**, L867-873 (2002).
155. Quint, J.K. & Wedzicha, J.A. The neutrophil in chronic obstructive pulmonary disease. *The Journal of allergy and clinical immunology* **119**, 1065-1071 (2007).

156. Tetley, T.D. Macrophages and the pathogenesis of COPD. *Chest* **121**, 156S-159S (2002).
157. Finkelstein, R., Fraser, R.S., Ghezzo, H. & Cosio, M.G. Alveolar inflammation and its relation to emphysema in smokers. *American journal of respiratory and critical care medicine* **152**, 1666-1672 (1995).
158. Barnes, P.J., Shapiro, S.D. & Pauwels, R.A. Chronic obstructive pulmonary disease: molecular and cellular mechanisms. *Eur Respir J* **22**, 672-688 (2003).
159. Grumelli, S., Corry, D.B., Song, L.Z., Song, L., Green, L., Huh, J. *et al.* An immune basis for lung parenchymal destruction in chronic obstructive pulmonary disease and emphysema. *PLoS medicine* **1**, e8 (2004).
160. Harrison, O.J., Foley, J., Bolognese, B.J., Long, E., 3rd, Podolin, P.L. & Walsh, P.T. Airway infiltration of CD4+ CCR6+ Th17 type cells associated with chronic cigarette smoke induced airspace enlargement. *Immunology letters* **121**, 13-21 (2008).
161. Majo, J., Ghezzo, H. & Cosio, M.G. Lymphocyte population and apoptosis in the lungs of smokers and their relation to emphysema. *Eur Respir J* **17**, 946-953 (2001).
162. Loke, P., Gallagher, I., Nair, M.G., Zang, X., Brombacher, F., Mohrs, M. *et al.* Alternative activation is an innate response to injury that requires CD4+ T cells to be sustained during chronic infection. *J Immunol* **179**, 3926-3936 (2007).
163. Stenzel, W., Muller, U., Kohler, G., Heppner, F.L., Blessing, M., McKenzie, A.N. *et al.* IL-4/IL-13-dependent alternative activation of macrophages but not microglial cells is associated with uncontrolled cerebral cryptococcosis. *The American journal of pathology* **174**, 486-496 (2009).
164. Shirey, K.A., Pletneva, L.M., Puche, A.C., Keegan, A.D., Prince, G.A., Blanco, J.C. *et al.* Control of RSV-induced lung injury by alternatively activated macrophages is IL-4R alpha-, TLR4-, and IFN-beta-dependent. *Mucosal immunology* **3**, 291-300 (2010).
165. Stein, M., Keshav, S., Harris, N. & Gordon, S. Interleukin 4 potently enhances murine macrophage mannose receptor activity: a marker of alternative immunologic macrophage activation. *The Journal of experimental medicine* **176**, 287-292 (1992).
166. Gordon, S. Alternative activation of macrophages. *Nature reviews* **3**, 23-35 (2003).
167. Kreider, T., Anthony, R.M., Urban, J.F., Jr. & Gause, W.C. Alternatively activated macrophages in helminth infections. *Current opinion in immunology* **19**, 448-453 (2007).
168. Bronte, V. & Zanovello, P. Regulation of immune responses by L-arginine metabolism. *Nature reviews* **5**, 641-654 (2005).
169. Martinez, F.O., Helming, L. & Gordon, S. Alternative activation of macrophages: an immunologic functional perspective. *Annual review of immunology* **27**, 451-483 (2009).
170. Varin, A. & Gordon, S. Alternative activation of macrophages: Immune function and cellular biology. *Immunobiology* (2009).
171. Nair, M.G., Gallagher, I.J., Taylor, M.D., Loke, P., Coulson, P.S., Wilson, R.A. *et al.* Chitinase and Fizz family members are a generalized feature of nematode infection with selective upregulation of Ym1 and Fizz1 by antigen-presenting cells. *Infection and immunity* **73**, 385-394 (2005).

172. Nair, M.G., Cochrane, D.W. & Allen, J.E. Macrophages in chronic type 2 inflammation have a novel phenotype characterized by the abundant expression of Ym1 and Fizz1 that can be partly replicated in vitro. *Immunology letters* **85**, 173-180 (2003).
173. Raes, G., De Baetselier, P., Noel, W., Beschin, A., Brombacher, F. & Hassanzadeh Gh, G. Differential expression of FIZZ1 and Ym1 in alternatively versus classically activated macrophages. *Journal of leukocyte biology* **71**, 597-602 (2002).
174. Hesse, M., Modolell, M., La Flamme, A.C., Schito, M., Fuentes, J.M., Cheever, A.W. *et al.* Differential regulation of nitric oxide synthase-2 and arginase-1 by type 1/type 2 cytokines in vivo: granulomatous pathology is shaped by the pattern of L-arginine metabolism. *J Immunol* **167**, 6533-6544 (2001).
175. Wynn, T.A. Fibrotic disease and the T(H)1/T(H)2 paradigm. *Nature reviews* **4**, 583-594 (2004).
176. Ricote, M., Huang, J.T., Welch, J.S. & Glass, C.K. The peroxisome proliferator-activated receptor(PPARgamma) as a regulator of monocyte/macrophage function. *Journal of leukocyte biology* **66**, 733-739 (1999).
177. Zhao, A., Urban, J.F., Jr., Anthony, R.M., Sun, R., Stiltz, J., van Rooijen, N. *et al.* Th2 cytokine-induced alterations in intestinal smooth muscle function depend on alternatively activated macrophages. *Gastroenterology* **135**, 217-225 e211 (2008).
178. Loke, P., MacDonald, A.S., Robb, A., Maizels, R.M. & Allen, J.E. Alternatively activated macrophages induced by nematode infection inhibit proliferation via cell-to-cell contact. *European journal of immunology* **30**, 2669-2678 (2000).
179. Reyes, J.L. & Terrazas, L.I. The divergent roles of alternatively activated macrophages in helminthic infections. *Parasite immunology* **29**, 609-619 (2007).
180. Loke, P., MacDonald, A.S. & Allen, J.E. Antigen-presenting cells recruited by Brugia malayi induce Th2 differentiation of naive CD4(+) T cells. *European journal of immunology* **30**, 1127-1135 (2000).
181. Loke, P., Nair, M.G., Parkinson, J., Guiliano, D., Blaxter, M. & Allen, J.E. IL-4 dependent alternatively-activated macrophages have a distinctive in vivo gene expression phenotype. *BMC immunology* **3**, 7 (2002).
182. MacDonald, A.S., Maizels, R.M., Lawrence, R.A., Dransfield, I. & Allen, J.E. Requirement for in vivo production of IL-4, but not IL-10, in the induction of proliferative suppression by filarial parasites. *J Immunol* **160**, 1304-1312 (1998).
183. Taylor, M.D., Harris, A., Nair, M.G., Maizels, R.M. & Allen, J.E. F4/80+ alternatively activated macrophages control CD4+ T cell hyporesponsiveness at sites peripheral to filarial infection. *J Immunol* **176**, 6918-6927 (2006).
184. Nair, M.G., Guild, K.J. & Artis, D. Novel effector molecules in type 2 inflammation: lessons drawn from helminth infection and allergy. *J Immunol* **177**, 1393-1399 (2006).
185. Smith, P., Walsh, C.M., Mangan, N.E., Fallon, R.E., Sayers, J.R., McKenzie, A.N. *et al.* Schistosoma mansoni worms induce anergy of T cells via selective up-regulation of programmed death ligand 1 on macrophages. *J Immunol* **173**, 1240-1248 (2004).

186. Donnelly, S., O'Neill, S.M., Sekiya, M., Mulcahy, G. & Dalton, J.P. Thioredoxin peroxidase secreted by Fasciola hepatica induces the alternative activation of macrophages. *Infection and immunity* **73**, 166-173 (2005).
187. Flynn, R.J., Mannion, C., Golden, O., Hacariz, O. & Mulcahy, G. Experimental Fasciola hepatica infection alters responses to tests used for diagnosis of bovine tuberculosis. *Infection and immunity* **75**, 1373-1381 (2007).
188. Brys, L., Beschin, A., Raes, G., Ghassabeh, G.H., Noel, W., Brandt, J. *et al.* Reactive oxygen species and 12/15-lipoxygenase contribute to the antiproliferative capacity of alternatively activated myeloid cells elicited during helminth infection. *J Immunol* **174**, 6095-6104 (2005).
189. Raes, G., Brys, L., Dahal, B.K., Brandt, J., Grooten, J., Brombacher, F. *et al.* Macrophage galactose-type C-type lectins as novel markers for alternatively activated macrophages elicited by parasitic infections and allergic airway inflammation. *Journal of leukocyte biology* **77**, 321-327 (2005).
190. Rodriguez-Sosa, M., Satoskar, A.R., Calderon, R., Gomez-Garcia, L., Saavedra, R., Bojalil, R. *et al.* Chronic helminth infection induces alternatively activated macrophages expressing high levels of CCR5 with low interleukin-12 production and Th2-biasing ability. *Infection and immunity* **70**, 3656-3664 (2002).
191. Terrazas, L.I., Montero, D., Terrazas, C.A., Reyes, J.L. & Rodriguez-Sosa, M. Role of the programmed Death-1 pathway in the suppressive activity of alternatively activated macrophages in experimental cysticercosis. *International journal for parasitology* **35**, 1349-1358 (2005).
192. Mantovani, A., Sozzani, S., Locati, M., Allavena, P. & Sica, A. Macrophage polarization: tumor-associated macrophages as a paradigm for polarized M2 mononuclear phagocytes. *Trends in immunology* **23**, 549-555 (2002).
193. Mantovani, A., Sica, A., Sozzani, S., Allavena, P., Vecchi, A. & Locati, M. The chemokine system in diverse forms of macrophage activation and polarization. *Trends in immunology* **25**, 677-686 (2004).
194. Hamelmann, E., Schwarze, J., Takeda, K., Oshiba, A., Larsen, G.L., Irvin, C.G. *et al.* Noninvasive measurement of airway responsiveness in allergic mice using barometric plethysmography. *American journal of respiratory and critical care medicine* **156**, 766-775 (1997).
195. Radosevic, K., Wieland, C.W., Rodriguez, A., Weverling, G.J., Mintardjo, R., Gillissen, G. *et al.* Protective immune responses to a recombinant adenovirus type 35 tuberculosis vaccine in two mouse strains: CD4 and CD8 T-cell epitope mapping and role of gamma interferon. *Infection and immunity* **75**, 4105-4115 (2007).
196. Kirby, A.C., Coles, M.C. & Kaye, P.M. Alveolar macrophages transport pathogens to lung draining lymph nodes. *J Immunol* **183**, 1983-1989 (2009).
197. Nexterion Slide E Protocol. (http://www.isogen-lifescience.com/uploads/X7/-Y/X7-YQBgqztbgz01VkPYqMQ/slidee_short_20031013.pdf).
198. Saeed, A.I., Sharov, V., White, J., Li, J., Liang, W., Bhagabati, N. *et al.* TM4: a free, open-source system for microarray data management and analysis. *Biotechniques* **34**, 374-378 (2003).
199. Brazma, A., Hingamp, P., Quackenbush, J., Sherlock, G., Spellman, P., Stoeckert, C. *et al.* Minimum information about a microarray experiment (MIAME)-toward standards for microarray data. *Nat Genet* **29**, 365-371 (2001).

200. Rubinstein, R. & Simon, I. MILANO--custom annotation of microarray results using automatic literature searches. *BMC Bioinformatics* **6**, 12 (2005).
201. PubMed http://www.ncbi.nlm.nih.gov/entrez/query.fcgi?db=PubMed).
202. Aceview http://www.ncbi.nlm.nih.gov/IEB/Research/Acembly/index.html).
203. OMIM http://www.ncbi.nlm.nih.gov/entrez/query.fcgi?db=OMIM).
204. Gene http://www.ncbi.nlm.nih.gov/entrez/query.fcgi?db=gene).
205. Reumaux, D., de Boer, M., Meijer, A.B., Duthilleul, P. & Roos, D. Expression of myeloperoxidase (MPO) by neutrophils is necessary for their activation by anti-neutrophil cytoplasm autoantibodies (ANCA) against MPO. *Journal of leukocyte biology* **73**, 841-849 (2003).
206. Khalife, J., Capron, M., Grzych, J.M., Bazin, H. & Capron, A. Extracellular release of rat eosinophil peroxidase (EPO) I. Role of anaphylactic immunoglobulins. *J Immunol* **134**, 1968-1974 (1985).
207. Pesce, J., Kaviratne, M., Ramalingam, T.R., Thompson, R.W., Urban, J.F., Jr., Cheever, A.W. *et al.* The IL-21 receptor augments Th2 effector function and alternative macrophage activation. *The Journal of clinical investigation* **116**, 2044-2055 (2006).
208. Corraliza, I.M., Campo, M.L., Soler, G. & Modolell, M. Determination of arginase activity in macrophages: a micromethod. *Journal of immunological methods* **174**, 231-235 (1994).
209. Nickdel, M.B., Roberts, F., Brombacher, F., Alexander, J. & Roberts, C.W. Counter-protective role for interleukin-5 during acute Toxoplasma gondii infection. *Infection and immunity* **69**, 1044-1052 (2001).
210. Wills-Karp, M. Immunologic basis of antigen-induced airway hyperresponsiveness. *Annual review of immunology* **17**, 255-281 (1999).
211. Grunewald, S.M., Werthmann, A., Schnarr, B., Klein, C.E., Brocker, E.B., Mohrs, M. *et al.* An antagonistic IL-4 mutant prevents type I allergy in the mouse: inhibition of the IL-4/IL-13 receptor system completely abrogates humoral immune response to allergen and development of allergic symptoms in vivo. *J Immunol* **160**, 4004-4009 (1998).
212. Muller, U., Stenzel, W., Kohler, G., Werner, C., Polte, T., Hansen, G. *et al.* IL-13 induces disease-promoting type 2 cytokines, alternatively activated macrophages and allergic inflammation during pulmonary infection of mice with Cryptococcus neoformans. *J Immunol* **179**, 5367-5377 (2007).
213. Grunig, G., Warnock, M., Wakil, A.E., Venkayya, R., Brombacher, F., Rennick, D.M. *et al.* Requirement for IL-13 independently of IL-4 in experimental asthma. *Science (New York, N.Y* **282**, 2261-2263 (1998).
214. Nair, M.G., Du, Y., Perrigoue, J.G., Zaph, C., Taylor, J.J., Goldschmidt, M. *et al.* Alternatively activated macrophage-derived RELM-{alpha} is a negative regulator of type 2 inflammation in the lung. *The Journal of experimental medicine* **206**, 937-952 (2009).
215. Leckie, M.J., ten Brinke, A., Khan, J., Diamant, Z., O'Connor, B.J., Walls, C.M. *et al.* Effects of an interleukin-5 blocking monoclonal antibody on eosinophils, airway hyper-responsiveness, and the late asthmatic response. *Lancet* **356**, 2144-2148 (2000).
216. Lucattelli, M., Cavarra, E., de Santi, M.M., Tetley, T.D., Martorana, P.A. & Lungarella, G. Collagen phagocytosis by lung alveolar macrophages in animal models of emphysema. *Eur Respir J* **22**, 728-734 (2003).
217. Schebesch, C., Kodelja, V., Muller, C., Hakij, N., Bisson, S., Orfanos, C.E. *et al.* Alternatively activated macrophages actively inhibit proliferation of

peripheral blood lymphocytes and CD4+ T cells in vitro. *Immunology* **92**, 478-486 (1997).
218. Voehringer, D., van Rooijen, N. & Locksley, R.M. Eosinophils develop in distinct stages and are recruited to peripheral sites by alternatively activated macrophages. *Journal of leukocyte biology* **81**, 1434-1444 (2007).
219. Mowen, K.A. & Glimcher, L.H. Signaling pathways in Th2 development. *Immunological reviews* **202**, 203-222 (2004).
220. Ohnmacht, C. & Voehringer, D. Basophil effector function and homeostasis during helminth infection. *Blood* **113**, 2816-2825 (2009).
221. MacKenzie, J.R., Mattes, J., Dent, L.A. & Foster, P.S. Eosinophils promote allergic disease of the lung by regulating CD4(+) Th2 lymphocyte function. *J Immunol* **167**, 3146-3155 (2001).
222. Nathan, C. Neutrophils and immunity: challenges and opportunities. *Nature reviews* **6**, 173-182 (2006).
223. van Rijt, L.S., Kuipers, H., Vos, N., Hijdra, D., Hoogsteden, H.C. & Lambrecht, B.N. A rapid flow cytometric method for determining the cellular composition of bronchoalveolar lavage fluid cells in mouse models of asthma. *Journal of immunological methods* **288**, 111-121 (2004).
224. Arredouani, M., Yang, Z., Ning, Y., Qin, G., Soininen, R., Tryggvason, K. *et al.* The scavenger receptor MARCO is required for lung defense against pneumococcal pneumonia and inhaled particles. *The Journal of experimental medicine* **200**, 267-272 (2004).
225. Morris, S.C., Heidorn, S.M., Herbert, D.R., Perkins, C., Hildeman, D.A., Khodoun, M.V. *et al.* Endogenously produced IL-4 nonredundantly stimulates CD8+ T cell proliferation. *J Immunol* **182**, 1429-1438 (2009).
226. Kuperman, D.A., Huang, X., Koth, L.L., Chang, G.H., Dolganov, G.M., Zhu, Z. *et al.* Direct effects of interleukin-13 on epithelial cells cause airway hyperreactivity and mucus overproduction in asthma. *Nature medicine* **8**, 885-889 (2002).
227. Wynn, T.A. IL-13 effector functions. *Annual review of immunology* **21**, 425-456 (2003).
228. Tato, C.M. & Cua, D.J. SnapShot: Cytokines I. *Cell* **132**, 324, 324 e321 (2008).
229. Moore, K.W., de Waal Malefyt, R., Coffman, R.L. & O'Garra, A. Interleukin-10 and the interleukin-10 receptor. *Annual review of immunology* **19**, 683-765 (2001).
230. Rubtsov, Y.P., Rasmussen, J.P., Chi, E.Y., Fontenot, J., Castelli, L., Ye, X. *et al.* Regulatory T cell-derived interleukin-10 limits inflammation at environmental interfaces. *Immunity* **28**, 546-558 (2008).
231. Spight, D., Zhao, B., Haas, M., Wert, S., Denenberg, A. & Shanley, T.P. Immunoregulatory effects of regulated, lung-targeted expression of IL-10 in vivo. *American journal of physiology* **288**, L251-265 (2005).
232. Klebanoff, S.J. Myeloperoxidase: friend and foe. *Journal of leukocyte biology* **77**, 598-625 (2005).
233. Meuwese, M.C., Stroes, E.S., Hazen, S.L., van Miert, J.N., Kuivenhoven, J.A., Schaub, R.G. *et al.* Serum myeloperoxidase levels are associated with the future risk of coronary artery disease in apparently healthy individuals: the EPIC-Norfolk Prospective Population Study. *Journal of the American College of Cardiology* **50**, 159-165 (2007).

234. Bronte, V., Serafini, P., Mazzoni, A., Segal, D.M. & Zanovello, P. L-arginine metabolism in myeloid cells controls T-lymphocyte functions. *Trends in immunology* **24**, 302-306 (2003).
235. Muller, U., Stenzel, W., Kohler, G., Polte, T., Blessing, M., Mann, A. *et al.* A gene-dosage effect for interleukin-4 receptor alpha-chain expression has an impact on Th2-mediated allergic inflammation during bronchopulmonary mycosis. *The Journal of infectious diseases* **198**, 1714-1721 (2008).
236. Martinez, F.O., Gordon, S., Locati, M. & Mantovani, A. Transcriptional profiling of the human monocyte-to-macrophage differentiation and polarization: new molecules and patterns of gene expression. *J Immunol* **177**, 7303-7311 (2006).
237. Mosser, D.M. & Edwards, J.P. Exploring the full spectrum of macrophage activation. *Nature reviews* **8**, 958-969 (2008).
238. Carballo, E. & Blackshear, P.J. Roles of tumor necrosis factor-alpha receptor subtypes in the pathogenesis of the tristetraprolin-deficiency syndrome. *Blood* **98**, 2389-2395 (2001).
239. Peschon, J.J., Torrance, D.S., Stocking, K.L., Glaccum, M.B., Otten, C., Willis, C.R. *et al.* TNF receptor-deficient mice reveal divergent roles for p55 and p75 in several models of inflammation. *J Immunol* **160**, 943-952 (1998).
240. Alexander, W.S. & Hilton, D.J. The role of suppressors of cytokine signaling (SOCS) proteins in regulation of the immune response. *Annual review of immunology* **22**, 503-529 (2004).
241. DiPerna, G., Stack, J., Bowie, A.G., Boyd, A., Kotwal, G., Zhang, Z. *et al.* Poxvirus protein N1L targets the I-kappaB kinase complex, inhibits signaling to NF-kappaB by the tumor necrosis factor superfamily of receptors, and inhibits NF-kappaB and IRF3 signaling by toll-like receptors. *The Journal of biological chemistry* **279**, 36570-36578 (2004).
242. Maslowski, K.M., Vieira, A.T., Ng, A., Kranich, J., Sierro, F., Yu, D. *et al.* Regulation of inflammatory responses by gut microbiota and chemoattractant receptor GPR43. *Nature* **461**, 1282-1286 (2009).
243. Sina, C., Gavrilova, O., Forster, M., Till, A., Derer, S., Hildebrand, F. *et al.* G protein-coupled receptor 43 is essential for neutrophil recruitment during intestinal inflammation. *J Immunol* **183**, 7514-7522 (2009).
244. Zhang, L., Wan, J., Jiang, R., Wang, W., Deng, H., Shen, Y. *et al.* Protective effects of trichostatin A on liver injury in septic mice. *Hepatol Res* **39**, 931-938 (2009).
245. Yao, P.L., Tsai, M.F., Lin, Y.C., Wang, C.H., Liao, W.Y., Chen, J.J. *et al.* Global expression profiling of theophylline response genes in macrophages: evidence of airway anti-inflammatory regulation. *Respiratory research* **6**, 89 (2005).
246. De Paepe, B., Creus, K.K. & De Bleecker, J.L. Role of cytokines and chemokines in idiopathic inflammatory myopathies. *Current opinion in rheumatology* **21**, 610-616 (2009).
247. Sellebjerg, F., Bornsen, L., Khademi, M., Krakauer, M., Olsson, T., Frederiksen, J.L. *et al.* Increased cerebrospinal fluid concentrations of the chemokine CXCL13 in active MS. *Neurology* **73**, 2003-2010 (2009).
248. Rosendahl, A., Pardali, E., Speletas, M., Ten Dijke, P., Heldin, C.H. & Sideras, P. Activation of bone morphogenetic protein/Smad signaling in bronchial epithelial cells during airway inflammation. *American journal of respiratory cell and molecular biology* **27**, 160-169 (2002).

249. Ma, B., Liu, W., Homer, R.J., Lee, P.J., Coyle, A.J., Lora, J.M. *et al.* Role of CCR5 in the pathogenesis of IL-13-induced inflammation and remodeling. *J Immunol* **176**, 4968-4978 (2006).
250. de, C.V.G.M., Le Goffic, R., Balloy, V., Plotkowski, M.C., Chignard, M. & Si-Tahar, M. TLR 5, but neither TLR2 nor TLR4, is involved in lung epithelial cell response to Burkholderia cenocepacia. *FEMS immunology and medical microbiology* **54**, 37-44 (2008).
251. Matsushima, H., Yamada, N., Matsue, H. & Shimada, S. TLR3-, TLR7-, and TLR9-mediated production of proinflammatory cytokines and chemokines from murine connective tissue type skin-derived mast cells but not from bone marrow-derived mast cells. *J Immunol* **173**, 531-541 (2004).
252. Imaizumi, T., Hatakeyama, M., Yamashita, K., Yoshida, H., Ishikawa, A., Taima, K. *et al.* Interferon-gamma induces retinoic acid-inducible gene-I in endothelial cells. *Endothelium* **11**, 169-173 (2004).
253. Kawaguchi, S., Ishiguro, Y., Imaizumi, T., Mori, F., Matsumiya, T., Yoshida, H. *et al.* Retinoic acid-inducible gene-I is constitutively expressed and involved in IFN-gamma-stimulated CXCL9-11 production in intestinal epithelial cells. *Immunology letters* **123**, 9-13 (2009).
254. Gao, J.L., Wynn, T.A., Chang, Y., Lee, E.J., Broxmeyer, H.E., Cooper, S. *et al.* Impaired host defense, hematopoiesis, granulomatous inflammation and type 1-type 2 cytokine balance in mice lacking CC chemokine receptor 1. *The Journal of experimental medicine* **185**, 1959-1968 (1997).
255. Yamauchi, R., Tanaka, M., Kume, N., Minami, M., Kawamoto, T., Togi, K. *et al.* Upregulation of SR-PSOX/CXCL16 and recruitment of CD8+ T cells in cardiac valves during inflammatory valvular heart disease. *Arteriosclerosis, thrombosis, and vascular biology* **24**, 282-287 (2004).
256. Yamaguchi, Y., Fujio, K., Shoda, H., Okamoto, A., Tsuno, N.H., Takahashi, K. *et al.* IL-17B and IL-17C are associated with TNF-alpha production and contribute to the exacerbation of inflammatory arthritis. *J Immunol* **179**, 7128-7136 (2007).
257. Takahashi, K., Koga, K., Linge, H.M., Zhang, Y., Lin, X., Metz, C.N. *et al.* Macrophage CD74 contributes to MIF-induced pulmonary inflammation. *Respiratory research* **10**, 33 (2009).
258. Starnes, T., Rasila, K.K., Robertson, M.J., Brahmi, Z., Dahl, R., Christopherson, K. *et al.* The chemokine CXCL14 (BRAK) stimulates activated NK cell migration: implications for the downregulation of CXCL14 in malignancy. *Experimental hematology* **34**, 1101-1105 (2006).
259. Huang, X.Z., Wu, J.F., Cass, D., Erle, D.J., Corry, D., Young, S.G. *et al.* Inactivation of the integrin beta 6 subunit gene reveals a role of epithelial integrins in regulating inflammation in the lung and skin. *The Journal of cell biology* **133**, 921-928 (1996).
260. Catusse, J., Liotard, A., Loillier, B., Pruneau, D. & Paquet, J.L. Characterization of the molecular interactions of interleukin-8 (CXCL8), growth related oncogen alpha (CXCL1) and a non-peptide antagonist (SB 225002) with the human CXCR2. *Biochemical pharmacology* **65**, 813-821 (2003).
261. Lippert, U., Artuc, M., Grutzkau, A., Moller, A., Kenderessy-Szabo, A., Schadendorf, D. *et al.* Expression and functional activity of the IL-8 receptor type CXCR1 and CXCR2 on human mast cells. *J Immunol* **161**, 2600-2608 (1998).

262. Wu, W., Hsu, Y.M., Bi, L., Songyang, Z. & Lin, X. CARD9 facilitates microbe-elicited production of reactive oxygen species by regulating the LyGDI-Rac1 complex. *Nature immunology* **10**, 1208-1214 (2009).
263. Shilo, S., Pardo, M., Aharoni-Simon, M., Glibter, S. & Tirosh, O. Selenium supplementation increases liver MnSOD expression: molecular mechanism for hepato-protection. *Journal of inorganic biochemistry* **102**, 110-118 (2008).
264. Yu, N., Zhang, S., Zuo, F., Kang, K., Guan, M. & Xiang, L. Cultured human melanocytes express functional toll-like receptors 2-4, 7 and 9. *Journal of dermatological science* **56**, 113-120 (2009).
265. Lundblad, L.K., Thompson-Figueroa, J., Leclair, T., Sullivan, M.J., Poynter, M.E., Irvin, C.G. *et al.* Tumor necrosis factor-alpha overexpression in lung disease: a single cause behind a complex phenotype. *American journal of respiratory and critical care medicine* **171**, 1363-1370 (2005).
266. Eklow, C., Makrygiannakis, D., Backdahl, L., Padyukov, L., Ulfgren, A.K., Lorentzen, J.C. *et al.* Cellular distribution of the C-type II lectin dendritic cell immunoreceptor (DCIR) and its expression in the rheumatic joint: identification of a subpopulation of DCIR+ T cells. *Annals of the rheumatic diseases* **67**, 1742-1749 (2008).
267. Zheng, H., Fletcher, D., Kozak, W., Jiang, M., Hofmann, K.J., Conn, C.A. *et al.* Resistance to fever induction and impaired acute-phase response in interleukin-1 beta-deficient mice. *Immunity* **3**, 9-19 (1995).
268. Li, Q. & Verma, I.M. NF-kappaB regulation in the immune system. *Nature reviews* **2**, 725-734 (2002).
269. Dickensheets, H., Vazquez, N., Sheikh, F., Gingras, S., Murray, P.J., Ryan, J.J. *et al.* Suppressor of cytokine signaling-1 is an IL-4-inducible gene in macrophages and feedback inhibits IL-4 signaling. *Genes and immunity* **8**, 21-27 (2007).
270. Shi, M., Deng, W., Bi, E., Mao, K., Ji, Y., Lin, G. *et al.* TRIM30 alpha negatively regulates TLR-mediated NF-kappa B activation by targeting TAB2 and TAB3 for degradation. *Nature immunology* **9**, 369-377 (2008).
271. Nomellini, V., Faunce, D.E., Gomez, C.R. & Kovacs, E.J. An age-associated increase in pulmonary inflammation after burn injury is abrogated by CXCR2 inhibition. *Journal of leukocyte biology* **83**, 1493-1501 (2008).
272. Thatcher, T.H., McHugh, N.A., Egan, R.W., Chapman, R.W., Hey, J.A., Turner, C.K. *et al.* Role of CXCR2 in cigarette smoke-induced lung inflammation. *American journal of physiology* **289**, L322-328 (2005).
273. Joosten, L.A., Heinhuis, B., Abdollahi-Roodsaz, S., Ferwerda, G., Lebourhis, L., Philpott, D.J. *et al.* Differential function of the NACHT-LRR (NLR) members Nod1 and Nod2 in arthritis. *Proceedings of the National Academy of Sciences of the United States of America* **105**, 9017-9022 (2008).
274. Medoff, B.D., Seung, E., Hong, S., Thomas, S.Y., Sandall, B.P., Duffield, J.S. *et al.* CD11b+ myeloid cells are the key mediators of Th2 cell homing into the airway in allergic inflammation. *J Immunol* **182**, 623-635 (2009).
275. Dewals, B.G., Marillier, R.G., Hoving, J.C., Leeto, M., Schwegmann, A. & Brombacher, F. IL-4Ralpha-independent expression of mannose receptor and Ym1 by macrophages depends on their IL-10 responsiveness. *PLoS neglected tropical diseases* **4**, e689 (2010).
276. Mylonas, K.J., Nair, M.G., Prieto-Lafuente, L., Paape, D. & Allen, J.E. Alternatively activated macrophages elicited by helminth infection can be reprogrammed to enable microbial killing. *J Immunol* **182**, 3084-3094 (2009).

277. Ospelt, C. & Gay, S. TLRs and chronic inflammation. *The international journal of biochemistry & cell biology* **42**, 495-505 (2010).
278. Larsen, L. & Ropke, C. Suppressors of cytokine signalling: SOCS. *Apmis* **110**, 833-844 (2002).
279. Drexler, S.K. & Foxwell, B.M. The role of toll-like receptors in chronic inflammation. *The international journal of biochemistry & cell biology* **42**, 506-518 (2010).
280. Edinger, A.L. & Thompson, C.B. Death by design: apoptosis, necrosis and autophagy. *Current opinion in cell biology* **16**, 663-669 (2004).
281. Trujillo-Vargas, C.M., Werner-Klein, M., Wohlleben, G., Polte, T., Hansen, G., Ehlers, S. *et al.* Helminth-derived products inhibit the development of allergic responses in mice. *American journal of respiratory and critical care medicine* **175**, 336-344 (2007).
282. Balic, A., Smith, K.A., Harcus, Y. & Maizels, R.M. Dynamics of CD11c(+) dendritic cell subsets in lymph nodes draining the site of intestinal nematode infection. *Immunology letters* **127**, 68-75 (2009).
283. Dong, L., Li, H., Wang, S. & Li, Y. Different doses of lipopolysaccharides regulate the lung inflammation of asthmatic mice via TLR4 pathway in alveolar macrophages. *J Asthma* **46**, 229-233 (2009).
284. Abplanalp, A.L., Morris, I.R., Parida, B.K., Teale, J.M. & Berton, M.T. TLR-dependent control of Francisella tularensis infection and host inflammatory responses. *PloS one* **4**, e7920 (2009).
285. Dennis, G., Jr., Sherman, B.T., Hosack, D.A., Yang, J., Gao, W., Lane, H.C. *et al.* DAVID: Database for Annotation, Visualization, and Integrated Discovery. *Genome biology* **4**, P3 (2003).
286. Wang, Y., Wang, Y.P., Zheng, G., Lee, V.W., Ouyang, L., Chang, D.H. *et al.* Ex vivo programmed macrophages ameliorate experimental chronic inflammatory renal disease. *Kidney international* **72**, 290-299 (2007).
287. Zeytun, A., Chaudhary, A., Pardington, P., Cary, R. & Gupta, G. Induction of cytokines and chemokines by Toll-like receptor signaling: strategies for control of inflammation. *Critical reviews in immunology* **30**, 53-67 (2010).

APPENDIX A: General Media Recipes and Equipment used

This Appendix contains recipes for media and buffers used in the project which were obtained from shared laboratory protocols and documentation.

Digestion Buffer.
0.002g DNase I (Roche Germany)
0.0200g g Collagenase Type IV (Gibco-Invitrogen)
Dissolve reagents in 150 ml DMEM (containing 100U/ml penicillin G, 100µg/ml streptomycin). Filter sterilize with a 0.22µM filter and store at 4°C for up to 7 days.

ELISA Blocking Buffer
20g Powder Milk
0.2g NaN_3
Dissolve reagents in a final volume of 1000ml 1X PBS and store at 4ºC.

ELISA Dilution Buffer
10g BSA
0.2g NaN_3
Dissolve the above reagents in a final volume of 1000ml of 1xPBS and store at 4ºC.

ELISA Washing Buffer (20 X)
20g KCL
20g $KH_2HPO_4.2H_2O$
800g NaCl
50ml Tween-20
100ml 10% NaN_3
Make up to 5L with ddH_2O and store at room temperature. Dilute in 1:20 in ddH_2O.

ELISA Substrate Buffer (for horseradish peroxidase conjugates)
Peroxidase Substrate Solution B (Roche Diagnostics GmbH, Mannheim, Germany)
TMB Peroxidase Substrate Solution A (Roche Diagnostics GmbH)
Just before use, mix equal volumes of TMB Peroxidase Substrate (Solution A) with Peroxidase Substrate Solution B.

Griess Reagent 1
1g sulfanilamide
100ml 2.5% phosphoric acid
Dissolve 1g sulfanilamide in 100ml 2.5% phosphoric acid. Cover bottle in foil to protect from light and store at 4°C.

Griess Reagent 2
0.1g napthyl-ethylene-diamine
100ml 2.5 %phosphoric acid
Dissolve 0.1g napthyl-ethylene-diamine in 100ml 2.5% phosphoric acid. Cover bottle in foil to protect from light and store at 4°C.

1 X Phosphate Buffered Saline (PBS)
8g NaCl
0.2g KCl
1.44g Na_2HPO_4
0.24g KH_2PO_4
Weigh out reagents and dissolve in 900ml of ddH_2O and adjust pH to 7.4. Bring final volume to 1000ml and filter sterilize with a 0.22µM filter.

Red Cell Lysis Buffer
8.34g NH_4Cl
0.037g EDTA
1.0g $NaHCO_3$
Dissolve reagents in 1000ml ddH_2O. Filter sterilize (0.22µM) and store at 4 or 25^oC.

Equipment, Reagents and suppliers

Equipment	Supplier
Maxisorb 96 well ELISA plates	Nalge Nunc International, Naperville, IKL,USA
VersaMax microplate reader	Molecular Devices Corporation, Sunnyvale, CA, U.S.A
0.22µM filter	Millipore Corporation, Bedford, USA

Reagent or Kit	Supplier
3,3',5,5'-tetramethylbenzidine (TMB)	Roche Diagnostics GmbH, Mannheim, Germany
Bovine Serum Albumin (fraction V)	Roche Diagnostics GmbH, Mannheim, Germany
Dulbecco's Modified Eagle's Medium (DMEM) for Cell Culture	Gibco, Invitrogen Corporation, Carlsbad, CA, USA
Foetal Calf Serum (FCS)	Delta Bioproducts, Johannesburg, Gauteng Province, South Africa
Penicillin G and Streptomycin Solution (100X)	Gibco, Invitrogen Corporation, Carlsbad, CA, USA
Peroxidase Substrate (Solution B)	Roche Diagnostics GmbH, Mannheim, Germany
TMB Peroxidase Substrate (Solution A)	Roche Diagnostics GmbH, Mannheim, Germany
Triton-X100	BDH Chemicals Ltd., Poole, England

APPENDIX B: FACS Antibodies

Antibody	Conjugation	Dilution Factor	Type	Company	Catalogue No.
CD4	Biotin	1:160	Rat IgG2b	Home-grown	
CD3e	FITC	1:640	Hamster IgG1	Home-grown	
CD8a	PE	1:160	Rat IgG2a	BD-pharmingen	553033
B220	FITC	1:160	Rat IgG2b	Home-grown	
GR-1	FITC	1:80	Rat IgG2b	BD-pharmingen	553125
CCR3	PE	1:80	Rat IgG2a	R&D system	FAB729P
CD11c	PE	1:160	Hamster IgG1	BD-pharmingen	553802
MHC II	Biotin	1: 200	Rat IgG2a	Home-grown	
FcγRII/III	purified	1%	Rat IgG2b	BD-pharmingen	553141
SpA-PerCP	PerCP	1:600	N/A	BD-pharmingen	554067
SpA-APC	APC	1:400	N/A	BD-pharmingen	340130
Isotype	PE	1:200	Hamster IgG1	BD-pharmingen	554711
Isotype	PE	1:80	Rat IgG2b	BD-pharmingen	556925
Isotype	FITC	1:80	Rat IgG2b	BD-pharmingen	553988
CD8 (Ly2)	purified	1:200	Rat IgG2a	Home-grown	
CD11b (MAC1)	purified	1:800	Rat IgG2b	Home-grown	
GR-1	Purified	1:100	Rat IgG2b	Home-grown	
FcγRII/III	purified	1:400	Rat IgG2bκ	Home-grown	
B220	purified	1:200	Rat IgG2b	Home-grown	

APPENDIX C: Flow Cytometry Gating Strategies

The gating strategies of cellular quantifications in the lung in Chapter 3.2 are given below, showing positive controls. Refer to Methods (Section 2.5.2) and Appendix B for methodology and antibody details.

1.) **T-cells**
Cells were labelled with anti-CD3-FITC, anti-CD4-Biotin (with streptavidin (SpA)-PerCP) and anti-CD8-PE antibodies, and gated as follows:

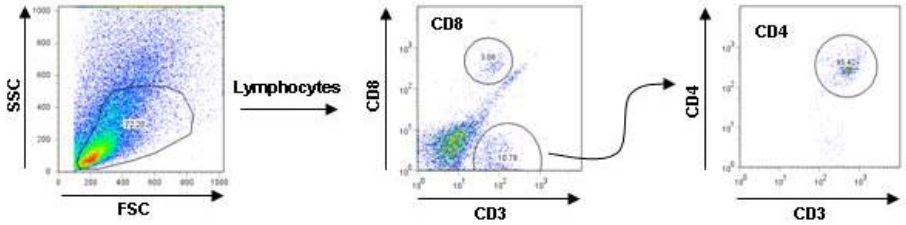

2.) **B-cells**
Cells were labelled with anti-B220-FITC antibodies and gated as follows:

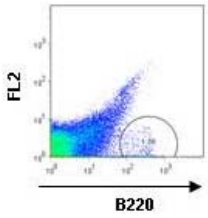

3.) **Neutrophils and Eosinophils**
Cells were labelled with anti-GR-1-FITC and anti-CCR3-PE antibodies. The following gating strategies were used to differentiate between neutrophils (GR-1^{+}CCR3^{-}) and eosinophils (CCR3^{+}GR-1^{int}).

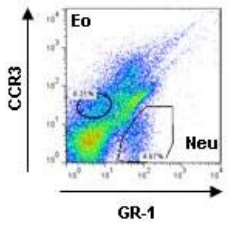

4.) **Alveolar Macrophages**
Cells were labelled with anti-CD11c-PE and anti-MHCII-Biotin (and SpA-PerCP) antibodies and defined as autofluorescent (AF^{+}) SSC^{hi} $CD11c^{+}$ $MHCII^{Lo/+}$.

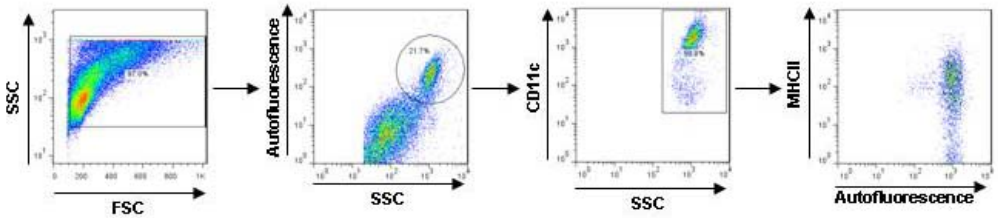

APPENDIX D: Cytokine ELISA Antibodies

	Capture	Detection	Standard	Sensitivity
IL-4	**1:500**	**1:1000**	**250ng/ml**	**10 pg/ml**
Type	Rat anti-mouse	Biotinylated Rat anti-mouse	Recombinant	
Company & Clone	BD-pharmingen BVD4-1D11	BD-pharmingen BVD6-24G2	Pepro Tech EC LTD London	
IL-13	**1:500**	**1:500**	**100ng/ml**	**46 pg/ml**
Type	Rat anti-mouse	Biotinylated Rat anti-mouse	Recombinant	
Company & Clone	R&D Systems, Germany 38213.11	R&D Systems, Germany	BD Biosciences	
INF-γ	**1:500**	**1:1000**	**100ng/ml**	**46 pg/ml**
Type	Rat anti-mouse	Biotinylated Rat anti-mouse	Recombinant	
Company & Clone	BD-pharmingen R4-6A2	BD Biosciences XMG1.2	BD Biosciences	
IL-10	**1:500**	**1:1000**	**100ng/ml**	**120 pg/ml**
Type	Rat anti-mouse	Biotinylated Rat anti-mouse	Recombinant	
Company & Clone	BD-pharmingen JES5-2A5	BD Biosciences SXC-1	BD Biosciences	

APPENDIX E: Gene details and Microarray analysis

The gene symbols (in alphabetical order), their full names and aliases, functional clustering and accession numbers (all provided by Alun Kirby) which were used in microarray analysis of 460 genes, and their associated Fold Change (FC) values (Log_2 scale). Columns represent FC values from individual experiments, with one biological repeat. WT: infected vs naïve IL-4Rα$^{-/lox}$; KO: infected IL-4Rα$^{-/-}$ vs infected IL-4Rα$^{-/lox}$; LysM: infected LysM^{Cre}IL-4Rα$^{-/lox}$ vs infected IL-4Rα$^{-/lox}$. Raw values which were below detection limit were omitted (empty FC squares).

Gene Symbol	Full name(s) and Aliases	Functional Clustering	Accession No. (major)	WT Day5		WT Day42		WT Day180		KO Day5		KO Day42		KO Day180		LysM Day5		LysM Day42		LysM Day180	
28SRNA	ribosomal protein S28 (Rps28)	House keeping	NM_016844	0.6	-0.6	0.5	1.0	-0.2	0.1	-0.6	-0.3	0.0	-1.1	1.6	0.5	-0.5	0.4	-0.2	-0.5	-0.3	0.9
ABCB2	transporter 1, ATP-binding cassette B, TAP1	APC	NM_013683		-2.5			3.6	0.2		2.2		-0.5	-2.8			-0.1		0.6		0.5
ABCB3	transporter 2, ATP-binding cassette B, TAP2	APC	NM_011530	-1.3	-0.8			-2.3	-1.6		1.1		-1.3	1.5	-0.1		0.1		-0.6	0.8	0.4
ACVR1 (ALK2)	activin A receptor, type I	BMPs	NM_001110204	-0.5	-0.7	0.2	0.8	-0.9	0.0	-0.7	0.1	0.0	-0.6	1.1	0.6	-0.3	-0.3	0.5	-0.5	1.3	0.2
ACVR2A	activin A receptor, type IIA	BMPs	NM_007396	-0.1	-0.1	0.1	-0.4		1.1		0.2	0.9	-0.1		0.6	0.2	-0.3	1.8	0.6		0.2
ACVR2B	activin A receptor, type IIB	BMPs	NM_007397		-1.0		-3.8	0.8			4.3		3.5	-2.0					-0.7		
ACVRL1	activin A receptor type II-like 1 (ALK1)	BMPs	NM_009612		-2.0	-0.7	-0.2	2.4	-1.1		4.8		0.6	-2.6	-1.2			-3.0	1.9	-2.7	0.6
AhR	aryl-hydrocarbon receptor (Ahr)	Signalling	NM_013464	0.3		3.8	-0.7	0.8	-0.4			-0.7	-0.4	-1.9	0.1	2.4		-2.9		-0.2	-0.2
ALDOA	aldolase A, fructose-bisphosphate (ALDOA)	House keeping	NM_007438	0.5	0.5	0.2	0.8	0.0	-1.4	-0.5	-1.0	-0.3	-0.8	-0.6	1.3	-1.0	-0.3	-0.2	-0.3	0.6	0.9
ALOX12	arachidonate 12-lipoxygenase (Alox12)	Other (enzyme)	NM_007440		-1.1	3.6	-3.0	-0.3	-2.8		2.2	-2.5	1.1	-1.0	2.3		-3.2	-3.0	1.8	-0.6	1.6
ALOX15	arachidonate 15-lipoxygenase (Alox15), 12-LO, L-12LO, Alox12l	Other (enzyme)	NM_009660	0.4	-0.7	0.3	-1.2	0.0	0.4	-0.6	1.2	0.2	1.9	2.2	0.9	-0.1	0.5	-0.1	1.8	0.3	0.9
ANAC019	Arabidopsis NAC domain containing protein 19	Negative	NM_104167		-4.0		3.9		1.4		4.2		-1.0		-0.5				1.7		-1.4
Arg1	arginase, liver (Arg1)	Macrophage related	NM_007482		0.1	-1.2	-0.2	-0.2	-0.1	0.4	0.3	-0.3	-0.4	-0.3	-0.2	-1.4	-0.9	1.8		-0.4	0.1
ARGHDIA	Rho GDP dissociation inhibitor (GDI) alpha (ARHGDIA)	House keeping	NM_133796	-4.5	1.4	-3.3	-0.4	-1.3	-1.2		0.5	1.3		0.5	0.9		-0.4	2.1	-1.6	1.1	0.5
AT1G62250	Arabidopsis thaliana unknown protein (AT1G62250)	Negative	NM_104905		-2.2		2.5	-5.4	-1.4		3.3	-3.1	3.9	4.2	4.1			-0.6			0.9
AT1G75170	Arabidopsis thaliana transporter (AT1G75170)	Negative	NM_001036207		-0.7	2.7	0.2	1.1	0.7		3.8	-1.9	2.2	0.9				-2.5			-1.1
AT1G76370	Arabidopsis thaliana protein kinase, putative	Negative	NM_106286		-1.4		-1.5		0.8		2.7		-0.8		1.1		-0.4		3.0		0.6
AT2G43280	Arabidopsis thalianaFAR1 family protein	Negative	NM_129890	-2.3	-1.6	6.0		-2.7		5.1	2.4	0.2	-0.1	-0.8		4.7	-1.3	-0.3	-1.3	-0.6	
B2M	beta-2-microglobulin (B2M)	House keeping	NM_009735	-0.7	-0.4	0.3	-3.0	1.0	0.0	0.7	0.0	-0.3	3.3	-0.6	0.6	0.7	0.2	0.5	3.0	-0.4	0.5
b-actin	actin, beta	House keeping	NM_007393	0.9	-0.1	0.7	0.3	0.4	-0.8	-0.1	-0.5	-0.5	0.3	-0.7	1.0	-0.6	-0.1	-0.3	0.0	-0.1	0.6

BAMBI	BMP and activin membrane-bound inhibitor (Bambi)	BMPs	NM_026505	0.6	-0.4			-3.5			1.2			0.8			-0.8		-1.9	0.3	
BAX	BCL2-associated X protein (Bax)	Apoptosis	NM_007527	-0.7	0.3	0.7	0.6	0.7	0.0	-0.5	-0.2	-0.3	-0.1	-0.1	0.6	1.2	-1.2	-0.5	0.0	0.1	0.2
BCA1	CXCL13	Chemokine	NM_018866	0.5	0.8	-0.6	-3.0	0.7	-0.5	0.4	1.1	0.3	2.8	-1.3	0.7	0.4	1.1	0.6	2.7	-1.6	0.4
BCL10	B-cell leukemia/lymphoma 10 (Bcl10)	Apoptosis	NM_009740		-0.9	1.5		-1.4	-0.9		1.9	0.2	-0.8	1.1	0.2			-3.9	-1.2	0.9	0.6
BCL2	B-cell leukemia/lymphoma 2 (Bcl2)	Apoptosis	NM_009741		-1.1			0.6	0.9		2.6		-1.7	1.4	1.4		0.5		-0.9	0.5	
BIK	BCL2-interacting killer (Bik)	Apoptosis	NM_007546		-0.8				-2.6		1.7				6.7		-1.9		-3.3		3.8
BMP1	bone morphogenetic protein 1 (Bmp1), Tolloid	BMPs	NM_009755	-0.2	-0.8	0.4	-0.2	-0.1	-0.6	0.7	1.0	-0.2	0.1	-0.8	1.3	-0.5	0.1	-0.5	0.4	-0.8	1.0
BMP2	bone morphogenetic protein 2 (Bmp2)	BMPs	NM_007553	-1.6	-0.3		1.5	-0.7	-2.9		0.6	0.4	-3.7	0.6	6.4	0.8	-0.8	1.1	-0.8	-0.1	-1.3
BMP4	bone morphogenetic protein 4 (Bmp4)	BMPs	NM_007554	-0.2	-0.1	-0.4	-1.1		-1.8		-0.1	-0.1	0.8				0.4	0.7	1.0		0.9
BMP5	bone morphogenetic protein 5 (Bmp5)	BMPs	NM_007555	-0.2	-0.4	0.7	3.4	1.4	3.2		1.2	-1.2	-1.6	2.4	0.7			1.1	-3.2	2.2	0.4
BMP6	bone morphogenetic protein 6 (Bmp6)	BMPs	NM_007556				-1.4		-3.2				1.5		3.7				2.5		2.7
BMP7	bone morphogenetic protein 7 (Bmp7)	BMPs	NM_007557	-0.6	-0.3			-2.5			1.5	-0.5		0.9				-0.1	-1.3		
BMPR1A	bone morphogenetic protein receptor, type 1A, ALK3	BMPs	NM_009758	-0.9	0.3	0.6	-1.5	-1.5	-2.3	0.2	-0.3	-0.2	1.3	-0.6	1.6	-0.3	0.1	-0.3	1.4	0.9	2.2
BMPR1B	bone morphogenetic protein receptor, type 1B, ALK6	BMPs	NM_007560	-0.5	-1.0	1.9	0.9	-2.7	0.9		0.2	-0.2	-0.6	3.6	-0.4	-1.3	-0.6	0.4	-0.1	3.3	-0.2
BMPR2	bone morphogenic protein receptor, type II	BMPs	NM_007561		-1.7				2.7		2.2		-0.5		1.2				2.3		-0.1
BRAK	CXCL14	Chemokine	NM_019568		0.3		0.3	-6.3	-2.6	-1.4	0.7			3.4	0.8		-3.2		0.8	-1.7	-0.6
BTLA	B and T lymphocyte associated, BTLA1, CD272	Cytokine receptor	NM_001037719		0.6	2.4	1.8				2.6	1.0	3.4					-0.1	-0.1		
C5aR	complement component 5a receptor 1 (C5AR1)	Surface receptor	NM_007577		-3.3	1.5		-5.0			2.8	1.2	-0.7	3.6			1.1	0.3	-0.2	2.3	
CAC2	acetyl co-enzyme A carboxylase biotin carboxylase	Negative	NM_122927	-0.2	-0.3	0.3	1.4	-0.7	-0.6		0.5	0.6	-0.6	0.4	0.4	-2.3	-0.8	-0.2	-0.9	0.7	0.5
card9	caspase recruitment domain family, member 9 (Card9)	TLR related	NM_001037747	-0.3	-0.2	-1.1	-2.0	-1.0	-0.1		0.1	-0.1	1.5	-0.4	0.6	0.6	0.5	1.0	1.5	-0.3	0.3
Caspase1	caspase 1 (Casp1) IL-1B converting enzyme	Apoptosis	NM_009807	-0.3	-0.3	0.1	-1.8	-0.8	-0.3	0.2	0.1	0.2	2.0	1.0	0.4	-0.9	0.2	0.0	2.0	0.4	0.3
Caspase2	apoptosis-related cysteine peptidase (CASP2)	Apoptosis	NM_007610	0.4	-0.5	0.3	-0.1	0.1	-1.0	-2.2	0.2	0.0	-0.2	0.1	0.6		-0.7	-0.1	0.3	-0.2	0.5
Caspase3	caspase 3, apoptosis-related cysteine peptidase	Apoptosis	NM_009810		-1.7		1.1				2.6	1.1									
Caspase7	caspase 7, apoptosis-related cysteine peptidase	Apoptosis	NM_007611		-1.6	1.8		-5.3			2.1	2.5	-1.1	1.1						-2.5	
Caspase8	apoptosis-related cysteine peptidase, MCH5, FLICE	Apoptosis	NM_009812		-0.9			-2.4	-1.5		1.6		-1.0	2.0	0.5		-0.5		0.7	2.0	-0.2
Caspase9	apoptosis-related cysteine peptidase (CASP9)	Apoptosis	NM_015733		-1.1		1.5		-1.3		1.6		-1.0		-1.2		-0.2		1.7		
cathepsinB	cathepsin B	Cathepsin	NM_007798	0.9	0.1	0.8	-0.9	-0.6	-1.5	-0.8	-0.3	0.0	0.7	0.1	0.6	-0.5	0.1	-0.4	0.9	0.2	0.9
cathepsinD	cathepsin D	Cathepsin	NM_009983	0.6	0.7	-0.4	0.5	0.1	-1.0	0.5	-0.8	-0.3	0.0	-1.3	0.6	0.1	0.2	-0.4	0.0	0.5	0.1
cathepsinF	cathepsin F	Cathepsin	NM_019861	0.3	0.9	-0.9	-0.7	-0.3	-0.5		0.5	-2.1	-1.2	-0.5	-0.5		-0.4	-0.4	-6.5	0.4	0.2
cathepsinH	cathepsinH	Cathepsin	NM_007801	-0.4	0.4	-0.5	-0.9	0.1	-0.5	0.4	-0.1	-0.4	1.2	-0.5	0.1	-0.4	-0.1	0.5	1.0	0.1	0.4
cathepsinK	cathepsin K (CTSK)	Cathepsin	NM_007802	0.2	0.0	-1.1	0.4	-0.6	-0.6		0.0	-0.5	0.0	0.1	0.8	0.7	0.0	0.9	0.0	0.9	0.2
cathepsinL	cathepsin L	Cathepsin	NM_009984	0.5	0.6	0.5	-0.4	0.0	-0.6		-0.5	-0.2	0.7	-0.5	0.1	-0.8	0.1	0.0	0.4	0.4	0.2
cathepsinS	cathepsin S	Cathepsin	NM_021281	0.4	0.4	0.7	-1.1	0.4	-0.4	-0.3	-1.0	-0.5	1.4	-0.7	0.6	-0.1	-0.1	-0.2	1.2	-0.1	0.5
cathepsinZ	cathepsin Z	Cathepsin	NM_022325	0.1	1.4	-0.5	-1.1	-0.1	-0.5	-0.3	-0.8	-0.3	1.1	-0.7	0.6	-0.6	-0.3	0.7	1.7	-0.2	0.1
CCL1	CCL1	Chemokine	NM_011329	2.0	0.0	1.6	-0.4		1.5	-0.9	1.5		1.9		0.7	-4.0	-2.4	1.3			1.0
CCR1	CCR1	Chemokine receptor	NM_009912	0.4	-0.5	0.4	1.3	-0.4	-1.0	0.3	0.4	0.3	-0.5	0.6	1.0	-0.6	-0.4	0.0	-1.0	0.8	0.6
CCR2	CCR2	Chemokine receptor	NM_009915	-0.2	-0.6	3.0	1.6		-0.5		1.3	-2.1	-0.3		0.2	1.0	1.2	-1.7	-0.3		-0.6

CCR3	CCR3	Chemokine receptor	NM_009914		-0.8		0.0		-1.0		2.1	0.1	0.7				-0.4	-1.3	0.8		1.4
CCR4	CCR4	Chemokine receptor	NM_009916	-2.9	-1.3	1.2		-0.9	0.1		1.9	-0.2	0.8	0.1	0.0	3.4	-1.7	-0.3	-1.0	0.1	-0.6
CCR5	CCR5	Chemokine receptor	NM_009917	-0.7	-0.6	0.2	0.3	0.0	-0.2	0.7	0.0	-0.4	0.2	-0.3	1.0	1.1	0.7	0.0	0.3	-0.4	0.4
CCR6	CCR6	Chemokine receptor	NM_009835	0.5	-0.2	0.2	1.5	-0.3	0.0	-1.4	0.4	-0.1	-0.6	0.0	-0.3	-0.1	-0.2	-0.4	-0.4	-0.3	-0.5
CCR7	CCR7	Chemokine receptor	NM_007719	1.1	-0.5	0.1	2.6	-0.9	-1.7		1.2	0.3	-1.5	0.3	0.9	-2.8	-0.4	0.3	-1.0	0.3	0.8
CCR8	CCR8	Chemokine receptor	NM_007720	-0.4	-0.9		1.9	0.0	-2.2		0.3	2.0	-1.5	0.0	1.9	-1.3	0.2	3.1	-0.5	-0.5	1.4
CD115	colony stimulating factor 1 receptor (Csf1r), Fms, CD115	Surface receptor	NM_001037859		-0.7				-1.8		1.8		-6.9		0.9				-5.3		-0.7
CD11b	CR3, CR3A, MAC1, Cd11b, integrin alpha M (Itgam)	Integrin	NM_001082960		0.6	0.3					2.2	-0.8					-1.2	-0.8	-1.0		-0.7
CD11c	Integrin alpha x, CD11c	Integrin	NM_021334	-2.0		-0.8		1.0		2.2		-0.2	0.6	-0.2		-0.3		0.2		0.8	
CD123	interleukin 3 receptor, alpha (low affinity) (IL3RA), CD123	Cytokine receptor	NM_008369	-0.1	0.3	-1.0	-0.9	-0.8	-0.6	0.3	-0.3	0.0	1.1	-0.2	0.8	0.5	0.6	0.1	1.2	-0.1	0.1
CD14	CD14 molecule (CD14)	Macrophage related	NM_009841	-0.7	1.0	-0.3	-2.5	-1.0	-1.0	0.8	0.1	-0.4	2.0	-0.4	1.0	0.8	0.1	0.4	2.7	0.2	0.9
CD18	Cd18, Lfa1, integrin beta 2 (Itgb2)	Integrin	NM_008404	0.4	-0.2	-0.4	-1.8	-0.4	-0.9	-1.7	-0.2	-0.4	1.5	-0.2	0.5	-0.5	0.1	0.6	1.7	0.1	0.4
CD1d1	CD1d1 antigen (Cd1d1)	APC	NM_007639	-1.4	-0.1	1.3	0.9	0.1	-0.3		1.0	-0.2	0.0	0.0	-0.1	1.3	0.2	0.3	0.0	0.7	-0.2
CD1d2	CD1d2 antigen (Cd1d2)	APC	NM_007640		0.6	1.5	1.7	-1.7	-1.0		0.7	0.6	-0.6	0.7	0.3		-1.6	-0.1	-0.1	1.8	0.2
CD200	CD200 antigen (Cd200)	Surface receptor	NM_010818	-0.1	-0.8	1.0	-1.4	-0.6	-0.7	-3.4	-0.7	-0.9	0.9	0.5	0.9	0.5	-0.9	-0.1	1.0	-0.5	0.7
CD200R1	CD200 receptor 1 (Cd200r1)	Surface receptor	NM_021325	-0.8	0.2	0.4	0.6	0.3	0.0	-0.4	-0.2	0.0	-0.4	0.2	0.3	0.9	-0.1	-0.2	-0.3	0.3	0.0
CD200R2	Cd200 receptor 2 (Cd200r2)	Surface receptor	NM_206535	0.9	-1.3				-2.3		1.8		-0.9		1.7						4.0
CD200R3	Cd200 receptor 3 (Cd200r3)	Surface receptor	NM_001128132	0.1	-0.3	0.2	-2.0	-0.3	-0.2	-0.4	0.0	0.0	2.1	0.6	0.3	-1.1	0.2	-0.2	2.2	-0.1	0.3
CD200R4	Cd200 receptor 4 (Cd200r4)	Surface receptor	NM_207244		-1.4	1.5	1.4	-0.4	-3.5		2.0	-0.6	-1.0	0.0	2.0			-0.1		-2.0	2.7
CD205	lymphocyte antigen 75, CD205, CLEC13B, DEC-205	Surface receptor	NM_013825	-2.7	-0.8			-2.7	-1.6		2.3		-0.5	1.7	-0.5		-2.2		-0.5	1.7	-0.3
CD32	Fc fragment of IgG, low affinity IIb, receptor (CD32)	Surface receptor	NM_001077189	0.5	-0.3	0.5	-1.8	0.3	-0.6	0.1	-0.1	0.1	1.9	-0.2	0.5	0.1	0.0	-0.7	1.9	0.0	0.2
CD33	CD33, p67, SIGLEC3, SIGLEC-3	Lectin	NM_001111058	-1.4	-0.9		5.5	0.2	-1.8		1.4		-1.8	-2.1	3.8	1.9					1.4
CD36	CD36 molecule (thrombospondin receptor)	Surface receptor	NM_007643	-2.9	-1.2	-1.5		-0.1	0.2	5.0	2.2	3.4	-1.5	2.2	0.6	3.2	0.8	2.1	-0.9	2.4	

CD4	CD4 molecule (CD4)	Surface receptor	NM_013488		0.0	0.3	3.6	-1.8	-0.6		1.4	-1.9	-0.8	-0.1	0.4		-0.5	0.1		0.8	0.2
CD40	CD40, TNF receptor superfamily member 5	APC	NM_011611		-1.4	-1.2		-0.8			3.0	3.0	-1.1	0.0			-0.5	1.7	-2.9	-0.7	
CD40L	IGM, IMD3, Ly62, TRAP, gp39, CD154, Cd40l,HIGM1, Ly-62, T-BAM, Tnfsf5	Surface receptor	NM_011616	-2.8	0.7	0.6	0.7	-1.7	-1.8		-0.1		-1.1	0.6	3.7		-0.8	0.3	-0.1	0.7	0.1
CD44	CD44 molecule (Indian blood group)	Surface receptor	NM_009851		2.2		0.0		0.5	-0.6	0.6	1.5	1.1		-0.5	-2.4	-4.4	1.1	-1.2		-1.3
CD47	CD47 antigen (Rh-related antigen, integrin-associated signal transducer) (Cd47)	Apoptosis	NM_010581	0.1	-0.3	0.3	-1.6	0.3	-0.6	0.6	0.2	-0.2	1.6	-0.2	0.6	0.6	0.2	-0.4	1.7	0.2	0.2
CD48	CD48, BCM1, BLAST, Bcm-1, BLAST1, SLAMF2	Surface receptor	NM_007649		-0.7	-0.5	1.8	-4.2	-0.3	0.0	0.9	-0.9		2.7	1.3		0.7	0.4			-1.3
CD51	integrin, alpha V (vitronectin receptor alpha, CD51)	Integrin	NM_008402	0.1	0.1	0.9	0.9	1.0	1.4	4.4	1.4	0.7	1.7	-2.1	-1.3	2.3				-0.7	-1.9
CD61	integrin, beta 3 (platelet glycoprotein IIIa, CD61)	Integrin	NM_016780	-0.1	0.6	-0.5	0.3	-3.2	-3.3	-0.6	-0.6	0.8	-0.7	0.2	1.1	-0.1	-0.3	0.4	-0.6	0.4	-2.0
CD68	CD68, GP110, SCARD1, macrosialin	Macrophage related	NM_009853	-0.6	1.2	-0.8	-2.5	-0.1	-0.7	0.6	0.0	0.4	2.0	-0.6	0.3	0.5	0.0	0.8	2.2	0.0	0.5
CD8	CD8alpha (CD8a)	Surface receptor	NM_001081110		1.3	-0.4	-3.1	0.2			0.2	-0.4		-0.6				0.3	-1.5	0.0	
CD80	CD80 molecule (CD80)	APC	NM_009855	0.4	-0.7	-0.3	2.3	-1.9	-0.1		1.2	1.3	-0.8	1.5	-0.2	-1.5	0.0	0.4	-0.3	0.4	-0.3
CD84	CD84, LY9B	Surface receptor	NM_013489	0.7	-0.4	0.3	0.1	-1.2	-1.5	-0.8	-0.2	0.4	0.1	-0.2	0.9	-0.8	0.2	0.1	0.2	-0.1	0.7
CD86	CD86 molecule, B70, B7-2	APC	NM_019388		-0.9			-3.2	-2.2		2.2		-0.2	2.3	0.8		0.0	-5.6	-0.8	0.9	-1.1
CHORDIN	chordin (Chrd)	BMPs	NM_009893	-0.1	-0.8	1.1	-1.4	0.5	-0.6	-1.0	1.8	-1.5	1.9	-0.8	0.7	-0.5	1.2	-0.7	1.8	-1.2	0.4
CIITA	MHC classII transactivator	APC	NM_007575	-0.6	-0.5	-0.5	-0.6	-0.1	0.0	0.5	0.8	0.0	1.3	0.8	1.2	0.1	0.6	0.3	1.7	0.3	0.9
CLEC1b	C-type lectin domain family 1, member B, CLEC2	Lectin	NM_019985	6.5	-0.1		1.1	0.6	0.4	-0.5	3.5	2.3		0.2	2.5	-1.8	0.0	1.9	-0.1	-1.2	-0.7
CLIP	CD74, major histocompatibility complex, class II invariant chain	APC	NM_001042605	-0.4	-0.2	0.4	-1.1	-1.1	-0.7	-2.1	-0.4	-0.5	0.7	0.9	0.8	0.8	-1.1	0.7	0.5	-0.2	0.6
cYc	interleukin 2 receptor, gamma,CD132, commongammachain	Cytokine receptor	NM_013563	-0.2	0.4	-0.5	-0.7	-0.8	-0.5	-1.3	-0.2	-0.5	0.4	0.3	-0.2	-0.1	0.1	0.6	0.7	0.3	0.2
CV2	BMPER, Cv2, CRIM3, CROSSVEINLESS	BMPs	NM_028472				-1.4	2.3	0.3				1.7	-3.5	0.3				2.7		-0.9
CRP	C-reactive protein, pentraxin-related (Crp)	Other (acute phase)	NM_007768		-0.8	3.3					1.7	0.9	-2.3	0.1			-0.6	-0.3		-0.8	-4.8
CTACK	CCL27	Chemokine	NM_001048179	-1.0	0.2		-1.0				1.5					6.0		-1.9	3.6		
CX3CR1	CX3CR1	Chemokine receptor	NM_009987		-1.5		2.6		1.6		1.0	3.1				1.0		3.3	2.7		-2.0
CXCL16	CXCL16	Chemokine	NM_023158	0.1	-2.6	1.9	1.4			1.7	2.1	0.9	0.2			-1.3	1.8	-1.2	-1.7		
DAP12	TYRO protein tyrosine kinase binding protein (Tyrobp) Ly83 DAP12 KARAP	TLR related	NM_011662	1.7	2.1	-1.0	-0.1	-0.6	-2.4	0.7	-1.2		-0.2	0.0	0.7		-9.0	-0.4	-0.4	2.5	0.6
DCAR	DCAR, Aplra2, Clec4b, mDcar2, DCARbeta	Surface receptor	NM_027218	4.6	0.8	0.0	-0.2			0.5	0.1	-0.7	-0.4	-0.4	4.0		-0.4	-0.2	0.3	-0.2	-0.9
DCAR1	C-type lectin domain family 4, member b2 (Clec4b2) Aplra1, mDCAR1 APC lectin-like receptor A1	Lectin	NM_001004159	-0.4	0.6	-0.8	-0.5	-0.8	-0.5	-0.2	-0.4	-0.3	0.2	0.3	0.6	-0.1	0.1	0.6	0.6	0.6	-0.6

DCIR	C-type lectin domain family 4, member a, DCIR, LLIR, DDB27, CLECSF6	Lectin	NM_011999	-0.6	0.4	-0.7	-1.6	0.0	-0.4	1.2	-0.8	-0.5	1.4	-0.7	0.1	0.5	-0.3	0.8	1.3	-0.1	0.1
DC-SIGN	CD209, CLEC4L, DC-SIGN, DC-SIGN1,	Lectin	NM_133238		-3.2		2.4				5.2							1.8			
Dectin-1	C-type lectin domain family 7, member A	Lectin	NM_020008	0.2	-0.3	-0.2	1.4	0.4	-0.5	0.5	-0.4	0.7	-1.5	-0.8	0.5	-0.3	0.4	0.3	-1.5	0.1	0.0
Dectin2	C-type lectin domain family 4, member n, CLECSF10	Lectin	NM_020001	-0.3	0.4	-0.3	0.4	0.7	-0.4	0.3	0.0	-0.1	0.0	-1.7	0.9	0.1	0.0	0.2	0.0	0.1	-0.1
Dkk-1	dickkopf homolog 1 (Xenopus laevis) (Dkk1)	Signalling	NM_010051	0.4	-0.6	-0.3	1.1	-0.7	-1.1	-5.4	0.5	1.3	0.0	-0.4	0.6	0.1	0.9	1.0	0.0	-0.7	0.6
Dkk-2	dickkopf homolog 2 (Xenopus laevis) (Dkk2)	Signalling	NM_020265		1.6			1.8	-1.5			4.1	3.2	-2.2	2.1			-0.4	1.4	1.1	1.5
Dkk-3	dickkopf-3 (dkk-3 gene)	Signalling	NM_015814		-3.6	-1.9	-2.5	3.0	1.9		5.6		0.5	-3.0	0.7			0.5	1.6		0.9
Dkk-4	dickkopf homolog 4 (Xenopus laevis) (Dkk4)	Signalling	NM_145592	-0.1	0.4	-0.4	-0.4	-5.0	-5.5		-0.4		-0.2	2.6	7.0		0.0	1.6	0.3	2.5	2.8
DR3	tumor necrosis factor receptor superfamily, member 25, TR3, Wsl, DDR3, LARD, APO-3, TRAMP, WSL-1,	Apoptosis	NM_033042	0.2	-0.7	0.4	-0.9	-0.2	-0.5	-0.8	-0.1	0.5	1.1	-0.2	1.3	-0.1	0.2	-0.3	1.3	-0.3	0.6
DR5	tumor necrosis factor receptor superfamily, member 10b (Tnfrsf10b) Ly98 KILLER TRICKB TRAILR2	Apoptosis	NM_020275	-1.2	-1.1	0.8		1.0	0.3		2.0	0.6	-1.0	0.9	-0.5	1.7	0.2	-0.4	-3.2	0.7	
DR6	tumor necrosis factor receptor superfamily, member 21, DR6, death receptor 6	Apoptosis	NM_178589	0.0	-0.9	0.0	-0.3	-0.6	-0.3	-0.2	0.6	0.0	1.0	0.6	1.1	0.1	0.9	0.2	1.2	0.3	0.5
EFNA1	ephrin A1 (Efna1)	Ephrin	NM_010107		-0.3		1.8	0.9	3.2		2.5		-0.9	-1.8	-2.0						-2.7
EFNA1	ephrin A3 (Efna3)	Ephrin	NM_010108	-1.2	0.1		1.4		-1.3		1.7	-0.6	-0.9				-1.0	-0.1	-1.5		
EFNA2	ephrin A2 (Efna2)	Ephrin	NM_007909	0.4	-1.1		3.5	-1.5	-1.1		1.8	1.2	-0.6	1.2	0.4		-0.1	2.6	-1.8	0.7	
EFNA4	ephrin A4 (Efna4)	Ephrin	NM_007910	0.1	-0.7	-0.6	0.9	-1.7	-1.3		0.5	1.2	-0.8	0.9	0.5	0.0	-0.1	2.1	-0.6	0.4	-0.1
EFNA5	ephrin A5 (Efna5)	Ephrin	NM_207654	-1.5	-0.3	0.5	-1.8	1.2	0.8	1.2	0.8	-0.5	2.4	-0.7	0.7	1.0	1.0	-1.1	2.2	-0.4	0.3
EFNB1	ephrin B1 (Efnb1)	Ephrin	NM_010110	-1.7	-1.3	2.0	5.0	-1.7	0.4		2.0	0.4	-0.1	1.9	3.2	2.3	-0.3	-0.1	-0.5	1.4	-0.2
EFNB2	ephrin B2 (Efnb2)	Ephrin	NM_010111		-0.3	1.1		-1.6	-0.8		2.6	2.0	-1.7	3.0	2.6		-1.6	0.7	2.3	0.1	1.5
EFNB3	ephrin B3 (Efnb3)	Ephrin	NM_007911	-2.3	-0.7	0.4	-1.4	-1.6	-2.5		2.0	1.5	-0.6	2.1	3.6	0.8	-0.5	-0.1	-0.1	0.1	
ELC	CCL19	Chemokine	NM_011888		-1.1		0.2	1.8	-1.1		1.6			-2.4	2.4		-0.7		1.7	-6.2	-0.4
ENA78	CXCL5, LIX, GCP-2, Scyb5, Scyb6, ENA-78, AMCF-II	Chemokine	NM_009141	1.4	-0.9	-4.2	-1.0	-2.3	-0.4	0.8	0.9		-0.3	1.2	-0.9		-0.1	4.2		0.3	-1.6
Endoglin	CD105, Endoglin	BMPs	NM_007932	1.4	0.4	0.2	0.2	-0.9	-1.5	-0.8	-0.5	-0.4	-1.0	0.1	1.3	-0.2	-0.3	0.4	-0.6	-0.4	1.0
Eotaxin	CCL11	Chemokine	NM_011330		-1.5		1.0	0.0	-2.2		2.9			-9.5	0.2		-5.6		4.5		-0.7
Eotaxin-2	CCL24	Chemokine	NM_019577	-0.3	1.2	-0.1	-2.6	-0.5	-0.9	0.5	0.1	1.0	2.4	-0.1	0.6	0.5	0.1	0.7	2.4	-0.4	1.0
Eotaxin-3	CCL26	Chemokine	NM_0010134 12		0.0	-3.7		2.4	2.0		2.2	5.4	2.5	-2.5	-0.3		0.0	1.5		1.7	-0.7
EphA1	Eph receptor A1 (Epha1)	Eph Family	NM_023580		0.0			0.9	-1.8		2.1			-2.1	1.8	4.7				-2.6	0.5
EphA2	Eph receptor A2 (Epha2)	Eph Family	NM_010139	0.0	0.3	1.0	0.6	-0.5	-0.6	0.1	0.4	0.3	-1.1	0.6	0.6	-1.2	0.1	0.1	-0.4	-0.3	0.3
EphA3	Eph receptor A3 (Epha3)	Eph Family	NM_010140		4.2		-0.5	0.6	-0.8		-1.2			0.6	3.0				0.4	1.1	0.7
EphA4	Eph receptor A4 (Epha4)	Eph Family	NM_007936	1.5	-0.2		1.5		-0.9	-2.1	1.7	3.7			2.0		-0.4	-0.7	-1.2		3.5
EphB1	EPH receptor B1 (EPHB1)	Eph Family	NM_173447		-1.9		1.1		3.8		1.5				1.3		-3.8		-0.2		0.4
EphB2	EPH receptor B2 (EPHB2)	Eph Family	NM_010142		-1.5		2.9		0.3		2.5		0.8		1.3		-0.5		0.9		-0.2
EphB4	EPH receptor B4 (EPHB4)	Eph Family	NM_010144		0.0		1.2	2.4			1.9			-1.9			-4.0	6.0	1.4	-2.2	
F4/80	egf-like module containing, mucin-like, hormone receptor-like 1 (EMR1), Ly71, F4/80	Macrophage related	NM_010130	0.4	-0.3	0.2	-1.5	-1.0	-1.6	-0.6	0.4	1.2	1.1	-0.3	1.3	-0.1	0.5	0.5	1.5	-0.4	1.2
FADD	Fas (TNFRSF6)-associated via death domain (Fadd)	Apoptosis	NM_010175		-0.5		2.5	-6.5			1.9		-3.2	6.3			-0.9		-1.0	4.9	
Fas	Fas (TNF receptor superfamily, member 6), APT1, CD95, FAS1, APO-1	Apoptosis	NM_007987		0.0		1.2	-1.8	-1.5		1.3			1.5	0.4		1.8		-0.1	1.1	0.6

Fas-L	Fas ligand (TNF superfamily, member 6) (FASLG) CD178, CD95L	Apoptosis	NM_010177		-0.2	2.0	-2.8	-0.2			2.1	-2.5	-0.8	-1.1				-2.4			
FcgRIII	Fc receptor, IgG, low affinity III (Fcgr3)	Surface receptor	NM_010188		-1.8	0.5	0.5	2.1			4.3	-0.2	1.7	-2.1			1.4	0.0			
FcGRIV	Fc receptor, IgG, low affinity IV (Fcgr4)	Surface receptor	NM_144559	1.2	-0.2	0.6	-0.6	-0.1	-0.2	-0.7	-0.6	-0.3	0.4	-0.3	0.9	-1.0	0.1	-0.3	0.5	-0.5	0.6
FcRe	Fc receptor, IgE, high affinity I, alpha	Surface receptor	NM_010184	0.6	0.8	-0.5	-0.4	0.1	-1.1	0.4	-0.8	-0.2	0.9	-1.4	0.6	-0.1	0.1	-0.3	0.9	0.5	0.3
FFAR2	free fatty acid receptor 2; FFA2R, GPR43	Surface receptor	NM_146187	-0.9	-0.6	-0.7	-1.5	0.1	-0.7	0.5	-0.3	-0.3	1.5	-0.2	0.1	0.2	0.3	0.7	1.3	0.0	0.1
FGF-1	fibroblast growth factor 1 (Fgf1)	Cytokine	NM_010197	0.8		2.1		2.3	1.1			-1.4	2.1	-1.2	0.6	2.0		-0.9	1.9	-0.5	0.3
FGF-2	fibroblast growth factor 2 (Fgf2)	Cytokine	NM_008006		-0.4			3.3	1.9		1.6			1.2						-6.2	-3.5
FGF-5	fibroblast growth factor 5 (Fgf5)	Cytokine	NM_010203	-0.6	-0.9	-0.1		2.1	-1.5		2.2			-4.5	1.5		1.1	-2.2			1.2
FIZZ1	resistin like alpha (Retnla) Fizz1 RELMa RELMalpha	Macrophage related	NM_020509	0.5	2.1	1.0	-3.0	0.3	-0.9	-0.5	-1.0	-0.5	2.9	-0.7	0.9	0.0	-0.1	-0.5	2.8	-1.2	0.7
Fractalkine	CX3CL1	Chemokine	NM_009142	0.2	1.7	-1.3	0.2	-0.3		-0.6	0.6		0.0	0.1		3.3	-0.2	-0.2	-1.5		
FURIN	furin (paired basic amino acid cleaving enzyme), SPC1, PCSK3, FUR, PACE	BMPs	NM_011046	-1.1	0.2		0.6	-1.4	-0.2		1.3		-0.6	0.1	1.0	0.0	-0.6		0.6	-0.2	0.0
FV1	Friend virus susceptibility 1 (Fv1)	TRIM Family	NM_010244		0.1	-0.4	0.6	-7.4	-0.4		1.0	-0.5	-2.4	6.3			-1.2	-0.3	-0.4	5.4	0.0
Fzd5	frizzled homolog 5 (Drosophila) (Fzd5)	Signalling	NM_022721	1.1	0.1	-0.7	0.0	-0.6	-0.7	-1.0	-0.3	1.0	0.0	0.0	0.9	-0.5	0.5	0.9	0.1	0.1	0.3
GAIP	regulator of G-protein signaling 19 (RGS19)	GPR	NM_026446	-1.3	-0.7	0.7	2.7	1.6	-2.7		1.2	1.7	-0.5	-2.8	1.2		1.6	1.9	-0.8	-2.9	-2.2
Galphai1	guanine nucleotide binding protein (G protein), alpha inhibiting activity polypeptide 1 (GNAI1)	GPR	NM_010305		0.7	-0.7		-1.4	2.3		1.9	-0.1	0.9	0.5	-3.8		-0.6	0.1	-0.5	-0.5	-3.3
Galphai2	guanine nucleotide binding protein (G protein), alpha inhibiting activity polypeptide 2 (GNAI2)	GPR	NM_008138	-0.6	-0.3	0.0	-0.7	0.8	0.1		0.3	-0.1	1.8	-0.1	0.2	-0.6	-1.1	-0.1	1.2	-0.2	-0.1
Galphai3	guanine nucleotide binding protein (G protein), alpha inhibiting activity polypeptide 3 (GNAI3)	GPR	NM_010306	0.6	-1.9	1.2		0.0	-0.5		2.9	0.1	-0.6	0.1	0.0	1.8	-0.1	-1.2	-0.2	-0.1	4.1
Galphaq/11	guanine nucleotide binding protein (G protein), alpha 11 (Gq class) (GNA11)	GPR	NM_010301	0.3	0.7	0.5		-0.7	-0.9		1.3	0.2	-1.3	0.4	0.9	-0.7	-4.1	-1.6	-1.7	0.6	0.7
GAPDH	glyceraldehyde-3-phosphate dehydrogenase (GAPDH)	House keeping	NM_008084	0.8	0.2	0.0	-0.6	-0.2	-1.1	-1.1	-0.3	0.8	0.6	0.6	0.8	-0.2	0.1	-0.3	1.0	-0.1	1.0
GCP2	CXCL6	Chemokine	NM_030712	-0.8	0.7	-0.2	1.0	1.2	2.3	1.1	0.4			-3.2	-2.3		-1.0	1.8	0.2	-3.5	-4.6
G-CSF	colony stimulating factor 3 (granulocyte) (CSF3)	Cytokine	NM_009971	-6.5	0.0		-0.9				0.9		1.5			7.6					-1.6
GMCSF	CSF2 (granulocyte-macrophage), GMCSF, CSF2	Cytokine	NM_009969	-0.2		-1.1	0.3	1.2	-0.2	3.7			-0.3	-1.4	0.3	2.3		0.2	-0.6	0.5	0.0
GMCSFR	colony stimulating factor 2 receptor, alpha, low-affinity, GMCSFR	Cytokine receptor	NM_009970	3.0	0.0	0.6	0.7				1.2		-2.8	3.7	5.1		-0.7	0.8		4.1	1.4
GNB2L1	guanine nucleotide binding protein (G protein), beta polypeptide 2 like 1 (Gnb2l1)	House keeping	NM_008143	0.4	0.0	0.3	0.1	0.3	-1.1	-0.4	-0.7	-0.2	-0.5	-0.4	0.1	0.1	-0.1	-0.4	-0.1	-0.1	0.9
GPCR160	G protein-coupled receptor 160, GPCR1, GPCR150	GPR	NM_001134385	0.5	-0.2	0.6	0.9	-1.1	-1.0	-0.6	-0.3	0.2	-0.7	0.3	1.1	0.0	0.0	0.0	-0.6	0.3	0.7
GPR15	G protein-coupled receptor 15 (GPR15)	GPR	XM_916786	-0.2	-1.3	-0.7	1.3	-1.5	-2.4	-2.0	1.7	0.3	0.1	0.1	0.8	-1.4	-0.2	1.4	0.4	0.1	0.5
GPR33	G protein-coupled receptor 33, pseudogene in human	GPR	NM_008159	0.1	-1.6	0.0	0.5		-1.0		1.0	0.7	-0.6		0.7	0.3	0.0	1.3	-0.5		-0.1

GPR34	G protein-coupled receptor 34, GPR34	GPR	NM_011823		-0.9	-0.4	-2.7				2.3	0.9	-1.5				-3.2				
GPR85	G protein-coupled receptor 85	GPR	NM_145066	-0.3	-1.1	1.4	1.9	0.6	-0.5		1.1	0.2	-1.5	-0.9			-1.1	-1.0	-1.1	-3.2	
GREMLIN	gremlin 1 (Grem1)	BMPs	NM_011824	-1.6	-0.3	-0.6	0.8				0.5		-0.7				-0.1	1.0	-1.8		0.7
GREMLIN2	Grem2, Prdc, FLJ21195, CKTSF1B2, DAND3	BMPs	NM_011825	-0.1	-0.3	0.4	0.7				0.8		-1.0	1.2			0.0	0.1	-1.6	1.2	-1.7
GROa	CXCL1	Chemokine	NM_008176	1.1	0.4	-0.4	-1.7	-0.8	-0.8	0.5	-0.3	-0.3		0.2	0.8	0.9	-0.1	0.3	2.2	-0.5	0.3
GROb	CXCL2	Chemokine	NM_009140	-0.3	1.4	-0.9	-2.2	-0.9	-0.6	0.8	-0.8	-0.1	2.6	0.3	0.7	0.0	-0.1	0.8	3.1	-0.3	0.2
GROg	CXCL3	Chemokine	NM_203320	0.0	0.7	-0.8	-2.4	-1.5	-0.7	0.7	-0.7	0.7	2.0	0.4	0.8	0.1	-0.3	0.8	2.1	0.2	0.5
GUSB	glucuronidase, beta (GUSB)	House keeping	NM_010368	-0.1	0.4	0.5	3.6	0.3	-1.4	0.3	1.7	1.0	-1.6	-0.8	1.6	0.9	-0.1	0.6	-3.0	0.3	1.1
HDAC2	histone deacetylase 2 (Hdac2)	Gene expression	NM_008229	1.0	-0.9	1.9	1.6	-1.9	-1.4		1.2	0.6	0.3	1.3	0.7		-0.3	0.6	-0.8	1.2	0.3
HDAC3	histone deacetylase 3 (Hdac3)	Gene expression	NM_010411	1.3	0.4		4.4	-2.9	-1.2		0.0			2.4	-0.1	1.5	-3.1			2.8	0.4
HDAC5	histone deacetylase 5 (Hdac5)	Gene expression	NM_001077696	-0.8	-0.5	0.3	0.5	-1.1	-0.9		1.0	0.4	-0.5	0.6	0.4	0.2	-0.5	0.2	-0.5	0.2	-0.7
Helicard	IFN induced helicaseC domain 1 (Ifih1),Hlcd, MDA5	TLR related	NM_027835		-3.0	2.7	1.9	2.6	1.4		4.1	-1.6	3.6	-6.4	-1.0			-2.8			-1.9
HIF1a	hypoxia inducible factor 1, alpha subunit (Hif1a)	Gene expression	NM_010431		-1.1	4.0		-2.4	-1.5		3.5	-2.7	1.8	0.0			-0.4		-1.1	0.3	-0.5
HIF1N	hypoxia-inducible factor 1, alpha subunit inhibitor Hif1an	Gene expression	NM_176958	2.4	-1.4	-0.6	-1.4	-4.7	-9.3	0.5	2.7	-0.2	1.3	4.0	###	-1.4	-0.6	-0.1	2.3	0.3	7.9
HMGB1	high mobility group box 1 (Hmgb1)	Gene expression	NM_010439	0.3	-0.1	0.5	-0.9	-0.5	-0.4	-1.2	0.3	-0.5	1.2	0.6	0.5	-0.1	0.4	-1.0	1.5	0.2	0.5
HMOX1	heme oxygenase (decycling) 1 (Hmox1)	Other (enzyme)	NM_010442	-0.7	1.3	0.7	-1.8	0.5	0.1	-0.8	-0.8	-0.6	1.7	-0.1	0.1	-0.1	-0.6	-0.2	2.2	0.1	0.1
HMOX2	heme oxygenase (decycling) 2 (Hmox2)	Other (enzyme)	NM_010443	0.3	-0.4	0.4	0.1	1.0	0.1	-3.9	0.2	-0.4	-0.3	-0.3	0.4	-4.0	0.3	-0.4	0.2	-0.4	0.3
HPRT1	hypoxanthine phosphoribosyltransferase 1 (Lesch-Nyhansyndrome) (HPRT1)	House keeping	NM_013556	-1.0	0.2	-0.2	-1.4	0.0	-0.2	1.0	-0.2	0.2	1.4	-0.4	0.5	0.1	0.4	0.0	1.3	0.6	0.2
HRK	harakiri, BCL2 interacting protein (only BH3 domain)	Apoptosis	NM_007545	0.2	0.0	1.3	0.3	-0.8	-0.9		0.5	-0.8	0.0	0.6	1.4	-0.5	-1.0	0.3	0.4	0.1	1.0
HSP90AB1	heat shock protein 90kDa alpha (cytosolic), class B member 1 (HSP90AB1)	House keeping	NM_008302	0.0	-0.2	-0.7	-2.3	-0.5	-0.7	-1.0	0.1	0.2	2.2	-0.1	0.5	-0.2	0.4	1.0	2.3	0.0	0.3
ICAM-1	intercellular adhesion molecule 1 (CD54, ICAM1)	Surface receptor	NM_010493	0.4	0.4	0.1	-0.2	7.2	6.3	-4.1	-0.6	0.3	0.8	-0.4	0.2	-1.0	0.0	0.3	0.7	0.4	0.6
IFNa	interferon alpha 2, IFNA, INFA2	Cytokine	NM_010503	0.4	-1.0			-1.8	0.3	-5.7	1.1		1.6	1.1	1.0	1.9					-0.6
IFNa6	interferon, alpha 6 (IFNA6)	Cytokine	NM_206871	1.6	0.7	5.5	1.3		0.6		0.2	-0.1				2.7	-1.7	-0.1	-0.4		2.8
IFNaR1	interferon (alpha and beta) receptor 1 (Ifnar1) Ifar, Ifrc, CD118	Cytokine receptor	NM_010508	-0.5	-0.1	1.0	-0.7		-1.8	5.2	1.3	0.0	1.1		0.6	2.6		-2.7			-0.4
IFNb	interferon, beta 1, fibroblast (IFNB1)	Cytokine	NM_010510	1.1	1.8		0.0	1.1	3.9		-0.5	-0.4	1.0	1.2	-3.2	2.1	-3.1	0.1	0.1	-0.2	
IFNg	interferon, gamma (IFNG)	Cytokine	NM_008337	-8.2	-0.1		-0.4	-1.6	-0.2	###	1.3	1.8	-3.6	2.5		###	-3.1	2.4		1.5	-1.1
IFNgR1	interferon gamma receptor 1 (IFNGR1)	Cytokine receptor	NM_010511	0.8	-2.0	0.5	1.0	-1.1	-1.1	-2.3	0.4	0.1	-1.4	0.9	0.2	-0.3	0.3	-0.1	-0.9	0.4	0.9

IFNgR2	interferon gamma receptor 2	Cytokine receptor	NM_008338	-1.8	-0.3	0.3	-1.2	0.6	-0.6	0.8	1.1	-0.4	1.9	-0.8	0.9	0.2	0.6	-0.5	1.4	-0.1	0.5
IgSR	Fc receptor-like S, scavenger receptor (Fcrls) IgSR Msr2 Fcrh2 FGP2 MMAN-g	Macrophage related	NM_030707	-1.1	0.4	-0.9	-1.7	-0.3	-0.2	0.8	-0.1	-0.6	1.7	-0.4	1.1	0.4	0.4	0.8	1.8	-0.5	0.4
IKBb	IKB-beta, nuclear factor of kappa light polypeptide gene enhancer in B-cells inhibitor, beta (Nfkbib)	Signalling	NM_010908	0.7	0.2	0.4	0.1	-0.3	-0.6		0.1	0.3	-0.4	0.6	1.1	-0.6	-0.1	0.3	-0.2	0.4	1.1
IKK2b	inhibitor of kappaB kinase beta (Ikbkb), IKK2, IKK-2, IKK[b], IKKbeta	Signalling	NM_010546					0.8	3.7				0.0		-2.7				-5.3	2.3	-3.2
IL10	interleukin 10 (IL10)	Cytokine	NM_010548			0.8	1.1					-1.0	1.1	-0.3	0.8			-0.7		-0.6	-0.1
IL10Ra	interleukin 10 receptor, alpha, CD210A	Cytokine receptor	NM_008348		0.4	-0.1		0.5	1.8		2.5		1.0	-0.8	-1.4	-1.3		-0.6	2.6		-2.9
IL10Rb	interleukin 10 receptor, beta (IL10RB)	Cytokine receptor	NM_008349	0.9	-1.2	3.1	0.5			-4.2	1.1		-1.8	1.2		-1.9	0.2	2.6	-2.3	1.7	
IL12p35	interleukin 12A, p35,	Cytokine	NM_008351	0.8	-2.0		1.5			3.0	2.9					1.6		-1.8			
IL12p40	interleukin 12B, p40)	Cytokine	NM_008352		-1.7			-4.3	-1.2		2.6		0.9	3.0						3.6	-0.1
IL12Rb1	interleukin 12 receptor, beta 1 (IL12RB1)	Cytokine receptor	NM_008353			-1.6		1.0	-0.6			2.3	0.7	-0.7	0.6			2.8	0.1	0.3	-0.3
IL12Rb2	interleukin 12 receptor, beta 2 (IL12RB2)	Cytokine receptor	NM_008354				-0.5	0.4	-0.2				0.4	-1.7	2.7	2.5			1.4	-0.3	-0.4
IL13	interleukin 13 (IL13)	Cytokine	NM_008355	-0.6	-0.2	0.7	0.5	0.4	-1.2	0.7	-0.2	0.0	-0.5	-0.4	1.5	-0.4	0.0	0.2	-0.2	-0.7	1.2
IL13Ra1	interleukin 13 receptor, alpha 1, CD213a1	Cytokine receptor	NM_133990						-1.3				2.4		1.8				1.9		0.8
IL13Ra2	interleukin 13 receptor, alpha 2 (IL13RA2), CD213a2	Cytokine receptor	NM_008356		-0.9		-0.6	2.5	1.4		2.5			-1.1	0.1	6.0	-1.3			1.6	-1.1
IL17A	interleukin 17A (Il17a)	Cytokine	NM_010552		-0.8						1.4			-0.8			-3.5			-3.9	
IL17B	interleukin 17B (Il17b)	Cytokine	NM_019508	0.3	-0.4	1.0	-1.0	3.4	2.4	2.9	2.7	1.2	1.0	-0.1	2.8		2.9	1.3	-1.9	-0.8	2.8
IL17F	interleukin 17F (Il17f)	Cytokine	NM_145856		-0.5	-2.1	0.7				2.7	0.0	1.7	-0.2			0.1	-0.2			
IL18	interleukin 18 (IL18)	Cytokine	NM_008360	0.1	0.7	-0.4	0.4	0.2	-1.2	0.7	0.0	0.3	-0.2	-1.3	0.9	0.7	0.3	0.8	0.0	-0.5	0.4
IL18R1	interleukin 18 receptor 1 (Il18r1)	Cytokine receptor	NM_008365		-2.0	1.6		1.2			2.1	-0.9		-0.2				-3.6	1.2	-6.9	
IL1b	interleukin 1, beta (IL1B)	Cytokine	NM_008361	0.5	2.6	-0.8	-2.6	-0.6	-1.5	0.1	-1.3	-0.8	2.6	-1.0	1.2	-0.6	-0.9	0.6	2.6	0.2	0.3
IL1R	interleukin 1 receptor, type I (IL1R1)	Cytokine receptor	NM_008362		0.1	0.2	-1.3	-1.3	-1.5		1.2		-0.3	0.7			-0.9	1.5		0.7	
IL1RA	interleukin 1 receptor antagonist, IRAP, IL1F3, IL1RA	Cytokine receptor	NM_031167	0.0	0.5	-0.4	-1.9	-0.3	-0.8	1.5	0.4	0.3	1.4	0.0	0.3	-0.3	-0.3	1.0	1.6	-0.2	0.0
IL21	interleukin 21 (IL21)	Cytokine	NM_021782	0.8	-1.5		-0.1			5.4	3.6	-1.4	0.6	-1.4		3.6	1.3	-2.1	-4.3		
IL23p19	interleukin 23, alpha subunit p19 (IL23A)	Cytokine	NM_031252		0.4		-3.3	0.5	-1.1		0.9			-1.5						-3.4	1.5
IL23R	interleukin 23 receptor (IL23R)	Cytokine receptor	NM_144548		-0.8			2.7			2.2		1.9	-0.2			1.8	0.6	1.8	0.1	
il27ra	interleukin 27 receptor, alpha	Cytokine receptor	NM_016671		-2.2	-2.4					2.4		-4.1					-0.8			

IL2Ra	interleukin 2 receptor, alpha chain (Il2ra)	Cytokine receptor	NM_008367	-2.1	0.1	-0.2	-0.3	0.3	-0.5	1.2	1.1	0.4	1.1	-0.6	0.7	0.7	0.6	0.5	0.6	-0.1	0.4
IL4	interleukin 4 (IL4)	Cytokine	NM_021283		0.4	-4.9		2.3			1.4	5.2	0.3	-3.5				1.9			
IL4Ra	interleukin 4 receptor, CD124, IL4RA	Cytokine receptor	NM_001008700		-1.3	1.5	1.9	2.3	-0.2		2.8	-2.0	2.6	-2.5	0.3		0.5	-2.0		0.3	-0.3
IL6	interleukin 6 (interferon, beta 2) (IL6)	Cytokine	NM_031168		0.3		-1.4		2.8		0.2				-1.8				-2.5		-0.8
IL8Ra	CXCR1	Chemokine receptor	NM_178241	0.3	0.1	0.0	-1.2	-0.2	-0.5	-0.6	-0.6	-0.9	1.2	-0.4	0.7	-1.2	0.4	0.3	1.6	-0.2	0.2
IL8Rb	CXCR2,CD128, CXCR2, IL8RA, CDw128, Cmkar2, Gpcr16, IL-8Rh, IL-8rb, mIL-8RH	Chemokine receptor	NM_009909	0.2	-0.6	0.8	1.3	-0.1	0.0	-2.3	0.1	-0.7	-1.6	0.6	0.4	-0.1	-2.1	-1.3	-1.4	0.4	0.0
INHbA	inhibin beta-A (Inhba)	Signalling	NM_008380		-0.2		0.7	-1.0	1.2		0.9			1.2	0.1				-0.7	-1.0	4.3
integrinb7	integrin, beta 7 (ITGB7)	Integrin	NM_013566		1.0	-0.8	-0.4	-2.2	-1.4		0.7	0.0	-1.2	0.7			-0.2	0.6	0.6	-1.2	1.3
intrgrinaE	integrin, alpha E, CD103	Integrin	NM_172944		-1.4	0.3			-1.0			-1.4	1.7		1.2	0.5		-1.0	0.6		-0.5
IP10	CXCL10	Chemokine	NM_021274		1.6	-1.8	-1.2		-1.7		0.1	0.7	0.6		1.9			0.4	0.1		1.2
IRAK1	interleukin-1 receptor-associated kinase 1 (Irak1)	Signalling	NM_008363		-2.0			-3.2			4.9	1.8	1.3	-0.8			-3.3	-0.1			
IRAK4	interleukin-1 receptor-associated kinase 4 (Irak4)	Signalling	NM_029926		-2.3	-4.7	0.6	2.2			3.2	2.3		0.3				2.3		0.3	
IRAK-M	interleukin-1 receptor-associated kinase 3 (Irak3)	Signalling	NM_028679		-0.4			1.4	0.1		4.0		0.5	-5.1	-0.1				1.0		
IRF3	interferon regulatory factor 3 (Irf3)	Signalling	NM_016849	0.5	-0.4	0.9	2.2	-2.2			-0.2	-2.0		0.8		2.2	-0.8	0.4	-2.1	0.7	
IRF7	interferon regulatory factor 7 (IRF7)	Cytokine	NM_016850			-4.4	-3.6		-4.4			4.5			5.3	2.5		1.3			
ITAC	CXCL11	Chemokine	NM_019494	-0.5	0.5	-1.8	0.4	0.4	0.4		1.0	-0.2	-0.4	-0.5	-0.6		0.9	0.5	3.1	-0.1	
Itchy	itchy, E3 ubiquitin protein ligase (Itch)	Signalling	NM_008395		-1.5				1.8		2.4		1.4		-2.0				-1.8		-2.6
ItgA5	integrin alpha 5 (fibronectin receptor alpha) (Itga5)	Integrin	NM_010577			-1.6			2.4		1.8	4.4	1.6		-1.8		-0.4	2.1	-0.9		-3.0
ItgB5	integrin beta 5 (Itgb5)	Integrin	NM_010580		0.7	-3.7			0.0		3.1	4.8	3.1		0.2			2.2			0.1
ItgB6	integrin beta 6 (Itgb6)	Integrin	NM_021359	-5.1	-1.2		-1.9		-0.7	4.7	4.3		1.0		0.8	2.8					-1.0
JAK1	Janus kinase 1 (Jak1)	Signalling	NM_146145		1.7	0.0	1.5		-1.6		2.1		1.8		2.5		-1.0				0.2
JAK2	Janus kinase 2 (Jak2)	Signalling	NM_008413		-0.8	-2.9		0.2	-0.1		4.1	1.6		-3.7	0.2	1.8		2.5	1.9	1.3	-4.7
JAK3	Janus kinase 3 (Jak3)	Signalling	NM_010589		-1.1						1.7		0.2				0.0				
KCR	Kupffer cell c-type lectin receptor	Lectin	NM_016751		1.3		1.6				2.3								-1.0		
LAIR1	leukocyte-associated Ig-like receptor 1 (Lair1)	Surface receptor	NM_001113474	0.7	0.1	-0.1	0.3	-0.5	-1.2	-0.9	-0.5	0.1	0.1	0.9	1.0	-1.1	-0.4	0.6	0.5	-0.1	0.8
Lamp1	lysosomal-associated membrane protein 1 (Lamp1)	Macrophage related	NM_010684	-0.1	0.2	-0.7	-2.4	-0.1	-0.7	0.5	-0.4	-0.3	2.0	-0.8	0.8	0.4	0.3	0.8	2.1	-0.2	0.5
LAMP-2CD107b	lysosomal-associated membrane protein 2, LAMP2, LAMPB, CD107b	Macrophage related	NM_001017959	-1.0	0.3	-0.2	-2.3	-0.1	-0.8	0.6	0.5	-0.1	2.2	-0.9	0.6	0.4	0.7	0.2	1.9	-0.1	0.8
Langerin	CD207, Langerin	Lectin	NM_144943		0.0	-0.9	2.0	3.4	0.2		3.3	2.8	2.4	-3.2	0.8			-0.6	-1.6	0.0	-0.2
LDHA	lactate dehydrogenase A (LDHA)	House keeping	NM_010699	0.9	0.1	0.5	0.1	1.2	-0.9	-0.4	-0.6	-0.9	-0.1	-0.7	1.0	-0.3	0.1	-0.4	0.1	-0.1	1.1
LeptinR	leptin receptor (LEPR)	Surface receptor	NM_146146	-1.0	-0.2	-0.4	-3.2	-0.4	-0.5	1.1	-0.1	-0.4	3.0	-0.4	0.8	1.0	0.8	0.3	3.4	-0.6	0.5
LIGHT	TNF (ligand) superfamily, member 14, CD258, LIGHT	Cytokine	NM_019418	0.2	0.0	0.2	0.4	-1.7	-1.5	-0.2	0.3	0.5	-1.4	0.6	1.0	0.1	0.0	-0.2	-0.1	-0.6	0.5
LTbR	lymphotoxin beta receptor (TNFR superfamily, member 3)	Cytokine receptor	NM_010736		-0.6		1.8	2.4		0.2	2.5		0.4	-2.8		4.0			1.9		

Ly49B	killer cell lectin-like receptor subfamily A, member 2, KLRA2	Surface receptor	NM_008462	-0.3	-0.7	0.8	0.3	-0.7	-0.8	-0.4	0.3	-0.1	0.2	0.6	1.8	-0.3	0.4	-1.7	0.5	0.0	1.2
Lymphotaxin	CXCL1	Chemokine	NM_008510	3.5	-1.2		0.8				0.7		3.3		3.0		-1.1	4.0	0.0		0.2
LTA	lymphotoxin alpha (TNF superfamily, member 1)	Cytokine	NM_010735	-1.1	-0.4	-0.4	-0.1	-0.5	-0.5	0.9	-0.1	-0.1	1.1	-0.9	0.8	1.0	1.2	-0.4	1.5	-0.1	-0.2
LTB	lymphotoxin beta (TNF superfamily, member 3)	Cytokine	NM_008518		-1.4	-3.1					3.2	1.3	-0.3				2.0	0.4	2.2		
Lyn	Yamaguchi sarcoma viral (v-yes-1) oncogene homolog (Lyn)	Signalling	NM_001111096		0.5	0.5	0.6	-2.2	-1.2	-6.3	1.5	-0.5		2.1			-0.3	0.6	-0.9	2.0	0.3
M6P-R (CIMPR)	mannose-6-phosphate receptor, cation dependent, insulin-like growth factor 2 receptor, MPRI, CD222,	Macrophage related	NM_010515	-1.0	-1.4	2.6	-0.4		0.3	0.6	1.7		-1.7				-0.3	0.6	1.1		0.0
MARCO	macrophage receptor with collagenous structure, MARCO, SCARA2	Macrophage related	NM_010766	0.4	1.3	0.7	0.1	-0.6	-0.9	-0.3	0.3	0.1	-0.4	0.0	0.2	-2.9	-0.1	-0.1	-0.3	0.0	0.4
MCL	C-type lectin domain family 4, member D	Lectin	NM_010819	0.0	-1.1	-0.5	-1.6	1.2	0.3	-1.1	0.4	-0.1	2.0	-0.3	0.2	-0.1	0.8	0.8	2.1	-0.1	0.0
Mcl-1	myeloid cell leukemia sequence 1 (BCL2-related)	Apoptosis	NM_008562	0.1	0.2	-0.1	0.0	-0.4	-1.6	-0.4	-0.2	0.2	-0.3	-0.2	1.4	-0.2	0.2	0.0	-0.1	0.4	1.0
MCP1	CCL2	Chemokine	NM_011333		0.4	1.9	1.8	-3.1	-4.1		2.9			0.2	1.2			-2.9	0.3	-0.2	
MCP2	CCL8	Chemokine	NM_021443	-0.4	0.4		-0.3			-0.7	0.2						-1.9	3.2			
MCP3	CCL7	Chemokine	NM_013654	-0.9	0.8		0.8			0.0	0.7		2.8	-1.2	-3.2	4.7	-2.0	0.8		-0.2	-3.2
MDC	CCL22	Chemokine	NM_009137	1.0	0.5	0.4	-0.2	-0.7	-1.6	-0.3	0.0	-0.2	-0.3	0.0	1.0		0.1	0.0	0.2	0.1	-1.8
MEC	CCL28	Chemokine	NM_020279					0.6	0.1					-3.0	0.1				2.6		-0.6
MerTK	c-mer proto-oncogene tyrosine kinase (MERTK)	Signalling	NM_008587	-1.5			0.4	0.9	-1.2	4.5			-0.3	-1.7	1.5	4.5			-4.3	-0.5	1.3
MGL1	macrophage galactose N-acetyl-galactosamine specific lectin 1 (Mgl1), Mgl, CD301a	Lectin	NM_010796	-0.2	0.1		5.0				1.5		-5.6				-1.2	0.6			-1.4
MICL_CLL-1	C-type lectin domain family 12, member A	Lectin	NM_177686		0.2		2.2	-2.1	0.1		0.6		-1.5	3.0	2.0	2.2		0.5	2.2	3.0	2.4
MIF	macrophage migration inhibitory factor (Mif)	Chemokine	NM_010798	0.8	0.1	-0.1	0.7	0.2	-0.5	-0.8	-0.4	0.1	-0.4	0.9	0.9	-1.3	-0.5	0.4	-0.1	0.1	0.8
MIG	CXCL9	Chemokine	NM_008599	-2.0	0.0		0.5	-1.6	-2.3		0.3		-2.3	0.7	0.5		-2.2			-0.5	1.4
Mincle	C-type lectin domain family 4, member E	Lectin	NM_019948	0.7	-0.8	0.6	0.1	-1.6	-3.2		1.5	0.1	-1.2	0.4	2.6		0.4	0.5	-0.9	0.2	2.4
MIP1aS	CCL3	Chemokine	NM_011337	-1.0	-0.3	-0.9	-2.8	-0.6	-0.6	1.0	-0.2	-0.2	2.5	-0.2	0.6	1.0	0.8	0.7	3.0	-0.6	0.6
MIP1b	CCL4	Chemokine	NM_013652	-2.0	-0.7	-0.3	-1.8	-1.3	-1.1		0.7	-0.6	1.8	-0.2	0.6	2.2	-0.3	0.8	1.8	-0.3	0.2
MIP3a	CCL20	Chemokine	NM_016960	-0.1	-0.8	0.7	-0.1	-0.3	-0.7	-0.4	0.4	-0.4	0.7	0.2	1.9	-0.4	0.4	-1.7	1.0	-0.3	1.1
MMP12	matrix metallopeptidase 12 , macrophage metalloelastase; macrophage elastase	MMP/TIMP	NM_008605	-0.2	-0.8		-0.5				0.4	-0.3	2.0	-1.4	0.0	1.0		-0.6	0.3	-0.3	0.1
MMP13	matrix metallopeptidase 13 (Mmp-13), Clg, Mmp1	MMP/TIMP	NM_008607		-0.2						1.9	-0.5		1.3	0.4		1.1	-0.3	0.7	0.7	0.5
MMP14	matrix metallopeptidase 14 (Mmp14)	MMP/TIMP	NM_008608		-1.0						2.5	1.1	-1.8	0.4				0.2		-0.6	-1.8
MMP9	matrix metallopeptidase 9 (gelatinase B, MMP9)	MMP/TIMP	NM_013599		-2.8				-3.7		2.7	-3.5					-0.9	-2.8			6.4
MR1	MRC1 mannose receptor, C type 1, CD206, CLEC13D	Lectin	NM_008625	0.1	0.3	-1.2	-1.7	-0.9	-1.2		2.0	-0.9		0.2				-0.8		0.3	0.0
Mr1	major histocompatibility complex classI-related (Mr1)	APC	NM_008209		-0.4	1.2		-3.1	-2.7	1.1	0.1	-0.4	1.8	-0.2	1.1	0.2	0.0	0.9	2.1	0.0	0.6
MRC2	mannose receptor, C type 2 (Mrc2)	Lectin	NM_008626	0.7	0.1	-0.4	0.4	0.5	0.6	0.2	0.6	-0.6		-0.2	-2.8	-2.4	-0.3	0.8	1.0	0.3	-0.2
MyD88	myeloid differentiation primary response gene (88)	TLR related	NM_010851	-0.1	0.1	0.0	-1.0	-1.0	-1.2		-0.2	-2.4	0.7	0.5	0.9	-1.0	0.0	0.5	0.9	0.2	0.1
NAP2	CXCL7, LDGF, MDGF, TGB1, CTAP3, Scyb7, LA-PF4,	Chemokine	NM_023785	-0.9	-1.3	1.4	-0.6	-0.3	-0.3	0.1	1.2	-0.4	1.3	-0.1	0.5	0.6	1.5	-1.8	1.5	-0.3	-0.3
NEU1	neuraminidase 1, sialidase 1; lysosomal sialidase	Sialidase	NM_010893	-2.2	0.9	0.0		-2.5	-4.3	2.3	0.9	-4.2	-2.7	-0.8	1.6		-3.4	0.4	-1.3	0.5	-0.5
NEU2	neuraminidase 2, brain sialidase; cystolic sialidase	Sialidase	NM_015750	-0.3	-0.5	0.0	0.2	-1.0	-1.4	0.8	0.0	-0.5	-0.3	0.2	1.8	-0.5	0.6	-0.4	0.0	0.5	1.3
NEU3	neuraminidase 3 (Neu3) membrane sialidase	Sialidase	NM_016720		-0.4	-2.4	3.3	0.5		0.0	2.4	0.9				-2.9		1.4	0.8		
NEU4	sialidase 4 (Neu4)	Sialidase	NM_173772	-1.1	-1.8	-0.9		1.0	-1.7	4.6	1.1	-1.4	-4.2	-2.7		2.9		-0.2			

NFAM-1	Nfat activating molecule with ITAM motif 1, CNAIP	Surface receptor	NM_028728	-0.9	-1.5	-0.6	-2.5	-0.1	0.0	0.5	0.6	-0.2	2.7	1.5	1.6	0.8	0.5	0.7	2.4	1.0	1.5
NLRP3	NLR family, pyrin domain containing 3 (Nlrp3), Cias1	Apoptosis	NM_145827			0.3	-1.1						1.6					-1.0			
NOD1	nucleotide-binding oligomerization domain 1	TLR related	NM_172729	-3.7	-0.9	-1.7	0.0	0.3	0.0	3.2	2.3	3.1	0.7	0.2	0.3		1.0				-0.5
NOD2	nucleotide-binding oligomerization domain containing 2(Nod2), Nlrc2, Card15	TLR related	NM_145857	-2.0	-0.6	0.0	-0.8	0.7	-0.2	1.0	1.5	-0.2	1.5	-0.8	0.6	0.4	0.9	-0.1	1.0	-0.1	-0.2
NOGGIN	noggin (Nog)	BMPs	NM_008711		-0.8	-1.9	-2.3	0.7	-0.5		2.9	1.5	1.6	-1.9	0.4			0.3	0.3	0.4	-0.3
NONO	non-POU domain containing, octamer-binding (NONO)	House keeping	NM_023144	0.9	0.4	0.3	1.6	1.8	0.9	-1.0	-0.3	0.3	-1.2	0.1	0.3	-0.7	-0.1	-0.3	-1.0	-0.4	0.6
NOS2	nitric oxide synthase 2, inducible (Nos2)	Macrophage related	NM_010927	0.3	-0.7		2.6	2.2	-5.1		2.4			-3.2			0.2				5.3
Nramp1	solute carrier family 11 (proton-coupled divalent metal ion transporter) member1 (Slc11a1),Bcg,Ity,Lsh	Macrophage related	NM_013612		-0.9	-0.7	-0.3	1.0	0.6	-0.3	1.7	0.4	-0.9	-1.0	-1.1	-0.6	0.0	1.3	-0.2	-0.1	0.0
Nramp2	solute carrier family 11 (proton-coupled divalent metal ion transporter) member2(Slc11a2),DCT1,DMT1	Macrophage related	NM_008732		-0.7		-1.3		-1.9	-0.3	1.7				2.7				2.7		2.1
P2Y12	purinergic receptor P2Y, G-protein coupled 12, P2RY12	Surface receptor	NM_027571	-4.3	-0.1	2.3	2.1	0.1	-0.6		0.8	-0.1	-0.8	-0.3	-0.1	6.9	-1.3	-0.9	-0.6	-0.4	-1.0
P2Y13	purinergic receptor P2Y, G-protein coupled 13, P2RY13 GPCR1, GPR94, Gpr86, P2Y13, SP174	Surface receptor	NM_028808	-1.3	-0.8	-1.4	0.3	-1.0	-1.7		2.7	1.4	-0.2	0.3			0.1	0.5	0.0	-0.2	
P2Y14	P2ry14 Gpr105 P2Y14	GPR	NM_133200	0.0	-0.3	0.4	0.5	-1.0	-0.7	-1.2	0.2	0.3	-0.3	0.4	0.5	-0.3	-0.2	-0.2	0.0	0.6	0.3
p47phox	neutrophil cytosolic factor 1 (Ncf1), NOXO2, Ncf-1, p47phox	Macrophage related	NM_010876		-0.9		0.0		-0.6	-0.2	1.4	6.4						2.2			4.3
PCSK5	proprotein convertase subtilisin/kexin type 5, PC5	BMPs	XM_129214			-0.4	-1.9	1.6	-0.9			1.9	1.3	-2.3	0.7			-0.7	-4.2	-1.2	0.2
PCSK6	proprotein convertase subtilisin/kexin type 6, SPC4	BMPs	XM_355911			0.8	0.1		-1.3			0.3	-0.2					-0.9	-0.8		1.9
PCSK7	proprotein convertase subtilisin/kexin type 7, PC7	BMPs	NM_008794		0.4	-5.8	1.8			-0.5	1.0	6.6	-3.1	-0.1		-4.2	1.6	6.7	-1.6	-1.7	
PF4	CXCL4, platelet factor 4 (Pf4)	Chemokine	NM_019932	-0.9	-1.7	-0.5	-2.4	0.1	-0.6	0.6	0.3	-0.2	2.6	1.4	2.0	0.8	0.3	0.4	2.3	1.1	1.9
PGF	placental growth factor (Pgf)	Cytokine	NM_008827		-0.7			2.0			2.8			-8.2							
PGK1	phosphoglycerate kinase 1 (PGK1)	House keeping	NM_008828	1.1	0.1	0.2	-0.4	-0.3	-1.1	0.0	-0.3	0.2	0.3	-0.1	0.6	-0.4	-0.5	0.1	0.4	0.5	0.7
PILR-a	paired immunoglobin-like type2 receptor alpha, PILRA	Surface receptor	NM_153510	0.4	-0.3	0.4	0.7	-0.7	-1.4	0.3	0.7	0.4	0.0	0.4	0.6	0.0	-0.1	0.3	0.0	0.4	0.5
PIM1	proviral integration site 1 (Pim1)	Signalling	NM_008842	0.5	1.4		0.5				0.8	0.3	0.0	-1.7	0.1	-0.2	-1.8	0.6	-0.1	-0.7	1.0
PIR-A1	paired-Ig-like receptor A1 (Pira1)	Surface receptor	NM_011087		-0.6			-1.9	-0.6		2.0	-0.9	-2.2	2.1	-2.2		-1.3	-1.3	-0.2	0.9	-0.4
PIR-A2	paired-Ig-like receptor A2 (Pira2)	Surface receptor	NM_011089	-0.7	-0.4	0.2	0.5	-0.4	-0.3	0.8	0.2	-0.3	-0.1	0.4	1.0	0.7	0.7	-0.3	0.0	0.0	0.5
PIR-B	leukocyte immunoglobulin-like receptor, subfamily B, member 1, CD85, ILT2, LIR1, MIR7, CD85J, LIR-1	Surface receptor	NM_011095	1.3	-0.3		2.3	-1.0	-2.1		1.5	0.1	-1.4	0.1	1.5		2.7	0.6	-1.5	-0.1	0.8
PIR-B	paired immunoglobulin-like receptor B (PirB)	Surface receptor	AF148880	2.3	-0.8		1.1		0.1	2.7	2.2	0.9	-0.7			3.1	0.0	1.3	-1.4		-3.3
PLAUR	plasminogen activator, urokinase receptor (Plaur)	Surface receptor	NM_011113	0.3	-0.1	1.0	2.0	0.2	0.9		0.0	0.0	-1.8	0.0	-0.9	0.2	-0.5	-0.5	-2.1	-0.7	-1.1

PLD2	phospholipase D2, PLD2	Phospholipase	NM_008876		-3.1						4.4	1.0	-5.5	0.3				-1.3			
PLD3	phospholipase D family, member 3, PLD3	Phospholipase	NM_011116	-0.7	-0.2	0.0	0.1	0.3	-0.3	0.4	0.0	-0.7	-0.2	-1.2	0.6	-0.4	0.6	-0.5	0.2	0.8	0.6
PLD4	phospholipase D family, member 4, PLD4	Phospholipase	NM_178911	-2.0	-0.7	-1.4	0.0	-4.1	-2.0		0.5	2.9		2.3			-0.8	3.4	-0.2	2.1	0.7
PPARa	peroxisome proliferator-activated receptor alpha	PPAR	NM_011144		-1.7	0.7	-0.4	0.0	-2.0		1.8		1.6	-0.3	1.4		0.8	-1.6	-0.1		1.2
PPARb/d	peroxisome proliferator-activated receptor delta	PPAR	NM_011145	0.6	0.7	0.4			-0.2	-0.4	-0.1	0.0			-0.4	-1.0	0.5	-1.9	0.7		-0.4
PPARg	peroxisome proliferator-activated receptor gamma	PPAR	NM_001127330	-0.7	2.3		2.0	0.4	2.4	4.3	0.7		-0.4	0.8	-1.5	3.6		0.3	-0.7		
PPIA	peptidylprolyl isomerase A (cyclophilin A) (PPIA)	House keeping	NM_008907	0.1	-0.2	0.1	0.9	1.5	0.5	0.7	-0.6	-0.1	-0.6	-0.7	0.9	-0.2	0.2	-0.4	-0.7	0.0	0.6
PTGES(2)	prostaglandin E synthase 2 (Ptges2)	Cytokine	NM_133783	-0.7	-1.0	-0.3	-2.2	0.3	-0.1	0.6	1.0	0.3	2.7	-0.5	0.4	0.2	1.2	0.6	2.8	-0.7	-0.3
PTX3	pentraxin related gene (Ptx3), TSG-14	Chemokine receptor	NM_008987		-2.8		-1.2	-5.9	-0.1		4.2	1.5		4.0	1.1				1.4		0.4
PU.1	proviral integration oncogene spi1	Signalling	NM_011355		-1.5	-1.4	-1.4	-1.3	-0.8	0.7	0.8	-4.3	0.2	-0.1	0.5		-0.5	1.0	1.5	-0.1	0.3
RANK	TNF receptor superfamily member 11a (Tnfrsf11a)	Cytokine	NM_009399		-2.0		0.6		-1.5		4.9		0.4		2.0	2.4	3.6				1.0
RANKL	ODF, OPG, OPGL, RANKL, Ly109l, Trance, tumor necrosis factor (ligand) superfamily, member 11	Surface receptor	NM_011613	-1.0	-0.2	-0.7	-0.5	-0.6	-0.4	0.8	0.2	0.0	1.6	-0.3	0.8	0.9	1.2	-0.2	1.9	0.1	-0.2
RANTES	CCL5	Chemokine	NM_013653	-1.0	0.6		-0.1		-0.6		0.1		-0.3		0.8		-1.7		0.6		0.7
RARa	retinoic acid receptor, alpha (Rara)	Signalling	NM_009024		-2.3		2.0	1.8	1.0		2.7		0.5	-3.9	-0.8		-4.5		2.8	-3.7	-1.4
RelA	v-rel reticuloendotheliosis viral oncogene homolog A	Signalling	NM_009045	-0.9	-0.2	0.3	-1.9			-2.5	1.1	-1.8	0.7				0.3	1.2	-1.6		
RelB	reticuloendotheliosis viral (v-rel) oncogene related B	Signalling	NM_009046	-0.2	0.4	-0.4	-2.2	-0.8	-0.5	0.5	0.5	0.9	2.6	0.0	0.9	0.6	0.5	1.3	2.6	-0.4	0.5
Resistin	resistin (Retn)	Macrophage related	NM_022984	-1.5	-0.2		1.7			0.8	1.9					5.0	-3.0	-0.1			
RGMA	Repulsive Guidance Molecule A	BMPs	NM_177740	0.4	0.4	-0.4	0.0	0.2	-0.3	0.0	0.0	-0.2	0.2	-0.2	-0.3	0.1	0.7	0.1	0.5	-0.1	-0.2
RGMB	Repulsive Guidance Molecule B, Dragon	BMPs	NM_178615		0.7	0.6		1.8	-0.7		1.6	-1.3	0.6	-2.7	0.8		1.0	-0.8			0.3
RGMC	(Hfe2) Repulsive Guidance Molecule C	BMPs	NM_027126	5.0	0.1			1.8	0.1	4.3	1.9		2.4	-3.4	0.1	3.0		0.7	2.6		-0.7
RIG-I	DEAD (Asp-Glu-Ala-Asp) box polypeptide 58 (Ddx58)	TLR related	NM_172689	0.3	-2.2	1.7	1.1	-0.6	1.4	-1.0	2.0			2.5			1.4	1.0	-1.0	2.7	1.8
RPL11	ribosomal protein L11 (RPL11)	House keeping	NM_025919	0.0	0.0	-0.2	-0.6	0.5	0.0	0.5	-0.6	-0.1	0.7	-0.1	0.8	-0.2	-0.2	0.1	0.6	0.1	0.6
RPL13A	ribosomal protein L13a (RPL13A)	House keeping	NM_009438	-0.6	0.0	-0.4	-0.5	0.7	-0.7	0.7	-0.4	-0.1	1.1	-0.9	0.6	0.4	0.2	0.8	1.0	-0.9	0.9
RPL19	ribosomal protein L19 (RPL19)	House keeping	NM_009078	0.1	0.2	0.1	-0.6	1.1	-0.3	-0.3	-1.0	-0.7	0.8	-0.6	0.2	-0.2	-0.2	0.1	0.8	-0.8	0.7
RPL32	ribosomal protein L32 (RPL32)	House keeping	NM_172086	0.2	-0.5	0.8	1.1	0.4	-0.1	0.1	-0.2	0.5	-1.2	0.3	0.3	-0.6	0.3	0.1	-0.7	-0.9	0.8
RPS18	ribosomal protein S18 (RPS18)	House keeping	NM_011296	0.3	-0.4	0.3	1.4	0.1	-0.9	0.0	-0.8	0.1	-1.6	0.2	0.3	-0.1	-0.1	-0.2	-1.1	-0.6	0.8
RPS27A	ribosomal protein S27a (RPS27A)	House keeping	NM_024277	0.2	-0.5	0.4	0.5	0.6	0.1	0.1	-0.6	-0.1	-0.2	0.3	0.9	-0.5	0.2	-0.1	-0.4	-0.4	1.0
RSK1	ribosomal protein S6 kinase polypeptide 1 (Rps6ka1)	Signalling	NM_009097	-3.7	-0.6	-4.6	2.5	2.6	-1.7	2.2	2.2	-8.7		-3.6				0.8	3.1		2.1

RSK2	ribosomal proteinS6k polypeptide3 (Rps6ka3) MPK-9	Signalling	NM_148945			-3.5		-1.7	-3.2				-2.5	-3.1	-1.2			-0.1			1.0
RSK3	Rps6ka2 Rsk3 p90rsk pp90rsk	Signalling	NM_011299		-0.7		0.6	3.6		1.8	2.5	-0.9	1.5	-3.0		-3.0	-1.1	1.3	-0.1		
Runx-1	Runx1, CBFA2	BMPs	NM_001111021	0.7	-0.3	0.2	-0.2	-1.1	-1.5	-1.0	0.0	0.6	0.4	-0.2	1.2	-0.5	0.2	0.5	0.7	-0.3	0.9
RXRg	retinoid X receptor gamma (Rxrg)	Signalling	NM_009107	-1.6	-0.3	-0.5	-2.2	-0.7	-0.7	1.3	0.8	-0.5	2.9	-0.2	0.7	0.8	0.9	0.6	3.1	-0.4	0.0
SCARF2	scavenger receptor class F, member 2 (Scarf2)	Macrophage related	NM_153790		-0.6			1.1	0.3		2.4		1.9	-2.1	-0.2					-0.3	-0.3
SDF1a/b	CXCL12	Chemokine	NM_021704	-0.3	-0.1		0.5	-1.8	-0.6		0.4	0.9	0.3	2.0	0.7		0.0	-0.5	0.7	0.0	1.0
SDHA	succinate dehydrogenase complex, subunit A, flavoprotein (Fp) (SDHA)	House keeping	NM_023281	0.7	0.3	-0.5	-0.6	-1.8	-1.0		-0.1	0.4	0.4	1.4	0.5	-0.1	-0.6	0.8	0.5	1.4	0.3
Siglec-1	sialic acid binding Ig-like lectin1, sialoadhesin CD169	Lectin	NM_011426		-1.9	0.0		1.8	-0.6		3.2	0.3	1.4	-2.0	1.1				0.9	-3.0	0.1
Siglec-5	sialic acid binding Ig-like lectin 5, siglec-F, mSiglec-F	Lectin	NM_145581		0.3		-3.1				1.3		-0.7				-0.4		-0.7		
siglec-e	Cd170, Siglec5, Siglec9, Siglecl1, mSiglec-E	Lectin	NM_031181	0.3	0.0		1.2	1.1			1.3			-2.7			-1.0	1.7	-2.2		
Siglec-g	sialic acid binding Ig-like lectinG, Siglec10,mSiglec-G	Lectin	NM_172900		-0.8			0.2	0.0		2.8			-0.4	-0.1				0.9	-0.6	-0.5
Siglec-H	sialic acid binding Ig-like lectin H (Siglech)	Lectin	NM_178706	0.4	-1.2		0.7			0.6	2.5	1.8	-0.3		-0.8		0.0	0.5	-0.7		-1.2
SIGNR1	CD209b, SIGNR1, mSIGNR1	Macrophage related	NM_026972	-3.1	-1.3	-4.5	1.4	-0.3	-4.0		2.3			-3.0	5.1			0.3			2.5
SIRPa	signal-regulatory protein alpha (SIRPA)	Surface receptor	NM_007547		0.6	-3.5		0.5	-0.6		2.7	0.5			0.5			1.2	3.3	-1.7	0.4
SLC	CCL21	Chemokine	NM_011124	-0.4	-0.6	1.2	0.4	0.0	-2.5		0.7	0.2	-0.1	-0.3	2.4	-1.4	0.0	-0.5	0.0	-0.6	2.1
SMAD1	MAD homolog 1	BMPs	NM_008539	-0.2	-1.3	1.5	1.2	-3.3			0.9	-0.4		0.6		-0.6	0.4	-0.1	-0.5	-0.2	
SMAD4	MAD homolog 4 (Drosophila) (Smad4)	Signalling	NM_008540	-3.5	-2.1		3.2				2.4						1.6				2.5
SMAD5	MAD homolog 5	BMPs	NM_008541	-0.1	0.9	-3.4	0.2	-1.7	-2.3	0.7	0.0	1.8	-0.4	-0.5		-1.0	-0.7	3.3	0.3	0.5	0.2
SMAD6	MAD homolog 6 (Drosophila) (Smad6)	Signalling	NM_008542	0.1	-0.1	-0.1	-0.1		-2.2	0.0	0.7	0.7	-0.4		1.7		0.1	1.0	-0.3		
SMAD7	MAD (mothers against decapentaplegic, Drosophila) homolog 7	BMPs	NM_001042660		-1.4						2.2	5.0	-1.1					6.3	3.5		
SNX10	sorting nexin 10, SNX10	Other (nexin)	NM_028035	1.6	-0.2	1.0	2.4	-1.1	-0.8		0.5	-0.3	-2.5	0.9	0.3	-1.0	-2.9	0.5	-2.5	0.6	0.5
SOCS1	suppressor of cytokine signaling 1 (Socs1)	Signalling	NM_009896	0.6	0.7	0.1	-0.7	-1.0	-1.3	-0.4	-0.3	0.2	0.8	-0.3	1.2	-0.7	0.2	0.5	0.9	-0.3	0.8
SOCS2	suppressor of cytokine signaling 2 (Socs2)	Signalling	NM_007706	0.3	0.9	4.3	1.7	-0.1	-1.7	-3.1	0.6	0.0	-1.2	-1.7	0.5		-0.9	0.3	-0.8	-1.8	
SOCS3	suppressor of cytokine signaling 3 (Socs3)	Signalling	NM_007707	-0.8	0.6	-1.0	-2.2	-0.4	-0.6	0.7	0.2	-0.2	2.6	-1.0	0.9	0.4	0.5	1.3	2.8	-0.9	0.5
SOD2	superoxide dismutase 2, mitochondrial (Sod2)	Macrophage related	NM_013671	0.3	0.0	0.1	-0.7	-1.4	-1.7	0.2	-0.4	0.2	0.2	0.9	1.6	-0.4	-0.1	0.7	0.5	0.5	1.3
SOSTDC1	sclerostin domain containing1,Ectodin,USAG-1,DCR5	BMPs	NM_025312		-0.8	-0.6	-1.9	1.6	1.0		1.6	-0.1	3.1	-1.4	0.4			-0.6	0.1	-4.1	0.3
Sox-4	SRY-box containing gene 4 (Sox4)	BMPs	NM_009238	1.5	-0.9	2.6	0.7				1.3		-4.2				-0.2	0.6	-1.4		0.6
SP1	trans-acting transcription factor 1 (Sp1)	Signalling	NM_013672	0.4	-2.0	-0.4	0.2			0.7	0.7	0.4	-1.3			-1.7	-0.3	1.2	2.5		
SR1	macrophage scavenger receptor 1, SR-A,CD204, phSR1, phSR2, SCARA1	Macrophage related	NM_031195	-1.1	-0.6		-0.3	-0.3	-0.4		0.9		0.9	0.7	0.3	0.2	-0.6		0.5	0.1	0.2
ST3Gal1	ST3 beta-galactoside alpha-2,3-sialyltransferase 1 (St3gal1)	Sialyltransferase	NM_009177	0.2	-0.4	0.3	-1.7	0.4	-0.6	-0.1	0.1	-0.6	2.3	-0.7	1.2	-0.1	0.3	0.3	2.0	-0.5	0.8
ST3Gal2	ST3 beta-galactoside alpha-2,3-sialyltransferase 2 (St3gal2)	Sialyltransferase	NM_009179	-0.5	-5.6				-4.4	5.5	6.5							0.9			2.6

ST3Gal3	**ST3 beta-galactoside alpha-2,3-sialyltransferase 3 (St3gal3)**	**Sialyltransferase**	**NM_009176**			-0.4	-0.9		-1.1						-1.2			-2.8			0.5
ST3Gal4	**ST3 beta-galactoside alpha-2,3-sialyltransferase 4 (St3gal4)**	**Sialyltransferase**	**NM_009178**	-2.6	-1.5		1.8	-2.5	-1.3	1.1	1.4	0.6	-0.5	1.5	0.4	-0.5	1.1	0.7	-0.5	2.3	0.2
ST3Gal5	**ST3 beta-galactoside alpha-2,3-sialyltransferase 5 (St3gal5)**	**Sialyltransferase**	**NM_001035228**	-0.9	-0.7	1.0	-0.1	-1.5	-0.4		1.3	-0.4	0.3	1.1	-1.9	-0.5	-2.0	-0.2	0.2	0.4	-0.3
ST6Gal1	**beta galactoside alpha 2,6 sialyltransferase 1 (St6gal1)**	**Sialyltransferase**	**NM_145933**		0.9		-2.5	2.3	-2.3		0.8			-2.8						-6.4	2.2
ST6Gal2	**beta galactoside alpha 2,6 sialyltransferase 2 (St6gal2)**	**Sialyltransferase**	**NM_172829**	-0.2	-0.7	0.4	0.8	-0.7	-0.9		0.6	-1.8	-1.0	0.2	1.1	1.5	-0.3	0.1	0.7	-0.2	1.1
ST6Galnac1	**ST6 (alpha-N-acetyl-neuraminyl-2,3-beta-galactosyl-1, 3)-N-acetylgalactosaminide alpha-2,6-sialyltransferase1 (St6galnac1)**	**Sialyltransferase**	**NM_011371**	-1.4			-1.8						2.8			4.1			3.6		
ST6Galnac2	**ST6(alpha-N-acetyl-neuraminyl-2,3-beta-galactosyl-1, 3)-N-acetylgalactosaminide alpha-2,6-sialyltransferase 2(St6galnac2)**	**Sialyltransferase**	**NM_009180**		2.5	0.2	-0.6	0.0	-0.2		-0.5		0.4	-2.6	0.5				-1.9	2.2	-0.3
ST6Galnac3	**ST6 (alpha-N-acetyl-neuraminyl-2,3-beta-galactosyl-1, 3)-N-acetylgalactosaminide-2,6-sialyltransferase3**	**Sialyltransferase**	**NM_011372**		2.6	-3.1	-1.7					0.4	0.9				-1.6	-0.1	-2.5		
ST6Galnac4	**ST6(alphaNacetyl-neuraminyl2,3betagalactosyl1)-N-acetylgalactosaminide alpha-2,6-sialyltransferase 4**	**Sialyltransferase**	**NM_011373**		-2.7						1.7							-1.0	1.7		
ST6Galnac5	**ST6(alpha-Nacetyl-neuraminy2,3-beta-galactosyl-1,3)-Nacetylgalactosaminidealph-2,6sialyltransferase5**	**Sialyltransferase**	**NM_012028**		-3.5	1.2	-1.4	-0.3	-1.7		1.5		0.5	-1.8	-2.9		0.9	-2.2		-2.2	1.1
ST6Galnac6	**ST6(alpha-N-acetyl-neuraminyl2,3beta-galactosyl1,3)-N-acetylgalactosaminide alpha-2,6-sialyltransferase6**	**Sialyltransferase**	**NM_001025311**	-0.7	-0.4			-2.2	-2.4		0.8			0.7		1.6		0.5	-0.5	-0.1	2.9
ST8Sia1	**ST8 alpha-N-acetyl-neuraminide alpha-2,8-sialyltransferase 1 (St8sia1)**	**Sialyltransferase**	**NM_011374**	0.4		-4.5	-1.3	2.5	-0.9	3.3			2.4	-3.2	0.9	1.9		1.8	2.6	-3.0	0.5
ST8Sia2	**ST8 alpha-N-acetyl-neuraminide alpha-2,8-sialyltransferase 2 (St8sia2)**	**Sialyltransferase**	**NM_009181**		1.4		0.0		-1.2		1.0		0.3		0.6				0.6		0.9
ST8Sia3	**ST8 alpha-N-acetyl-neuraminidealpha-2,8-sialyltransferase 3 (St8sia3)**	**Sialyltransferase**	**NM_009182**	-0.8	-0.4	-0.7	-0.3	-1.0	-1.0	0.7	0.2	0.0	1.4	-0.6	1.5	0.8	1.2	-0.1	1.7	-0.2	0.6
ST8Sia4	**ST8 alpha-N-acetyl-neuraminide alpha-2,8-sialyltransferase 4 (St8sia4)**	**Sialyltransferase**	**NM_009183**		0.3		2.2				1.4	-4.7					-0.7	2.0			
ST8Sia5	**ST8 alpha-N-acetyl-neuraminide alpha-2,8-sialyltransferase 5 (St8sia5)**	**Sialyltransferase**	**NM_153124**		-0.5			0.4			1.2							1.2	2.1	-1.5	
ST8Sia6	**ST8 alpha-N-acetyl-neuraminide alpha-2,8-sialyltransferase 6 (St8sia6)**	**Sialyltransferase**	**NM_145838**			-2.8		4.4	2.8			2.8	2.2	-3.5	-0.4	1.6		0.2	1.4		-0.5
STAT1	**signal transducer and activator of transcription 1**	**Signalling**	**NM_009283**				1.1	0.0			2.7			-4.6					5.4		
STAT2	**signal transducer and activator of transcription 2**	**Signalling**	**NM_019963**		-0.2		-2.0				2.0			-0.9	3.8	4.7	-1.1			-2.9	0.7
STAT3	**signal transducer and activator of transcription 3**	**Signalling**	**NM_213659**	-1.4	0.6	0	1.3	0.2	-6.6	-0.9	2.0	6.3	3.1	-0.6	5.3	3.5		7.4	2.5		6.8
STAT4	**signal transducer and activator of transcription 4**	**Signalling**	**NM_011487**	-1.7	-4.7	-5.0		4.2			6.2	-1.9		-4.0				0.2			
STAT5A	**signal transducer and activator of transcription 5a**	**Signalling**	**NM_011488**	0.4	-1.6		0.4	1.2	-0.6	-0.3	2.9		0.4	-1.7	2.2	-0.4	-0.3		0.8	-2.5	3.5
STAT5B	**signal transducer and activator of transcription 5b**	**Signalling**	**NM_011489**		0.5		1.6	-0.2	-2.1		0.6		0.7	-2.2	0.5	6.7	-0.4		0.6	-5.7	-0.1

STAT5B(2)	signal transducer and activator of transcription 5B2	Signalling	NM_001113563		0.2	-0.6					2.9	0.7			0.4			-0.1	-1.2	-2.5	-0.1
STAT6	signal transducer and activator of transcription 6	Signalling	NM_009284	-0.2	0.2		1.2			1.1	1.4	0.0	-1.4				-0.2	1.2			
Syk	spleen tyrosine kinase (Syk)	Signalling	NM_011518	-2.7	0.6	-1.3	0.5	0.3	-0.7		2.2	-2.5	-1.7	-1.3	0.0	3.4		0.4		-4.3	-0.2
TARC	CCL17	Chemokine	NM_011332		-1.8	-0.6	-0.5			7.8	2.8	3.3		-0.9		3.9	-1.0	2.2	2.3	0.2	
TBP1	TATA box binding protein 1 (TBP1)	House keeping	NM_011603	-1.1	1.0						1.3	-3.7	-1.9					-2.8	-1.6		-0.2
TECK	CCL25	Chemokine	NM_009138		-1.9		-1.7	-2.2	-0.5		3.3		-0.4	1.2			2.5				
TFRC	transferrin receptor (p90, CD71) (TFRC)	House keeping	NM_011638	2.4	-0.8	-1.6	0.1	1.9	-1.7	3.2	2.3	0.8	1.1	-2.8	-0.4	1.0		0.7	-4.4	-2.8	1.1
TGFb1	transforming growth factor, beta 1 (TGFB1)	Cytokine	NM_011577	-0.2	-0.3	2.9	1.4	-7.0	-5.0		1.0	-5.2	-1.1	3.1	-0.4	0.4	-1.0	0.3	-0.8	2.6	
TGFb2	transforming growth factor, beta 2 (TGFB2)	Cytokine	NM_009367	0.4	0.9	-1.5	0.6	1.3	0.8	0.2	0.6	0.3	-0.9	-0.9	1.3	0.0	-0.9	0.9	-0.4	1.2	0.3
TGFb3	transforming growth factor, beta 3 (TGFB3)	Cytokine	NM_009368	-1.5	0.7	0.6	1.7	0.4	0.0	1.0	1.0	-0.1	-0.2	-0.3	1.0	-0.1	0.7	-0.1	0.3	0.4	0.4
TGFbR1	transforming growth factor, beta receptor I (TGFBR1)	Cytokine receptor	NM_009370		0.3	-1.9		-0.5	3.0		2.0	3.3		0.3	-2.6	3.3	1.6	1.1	-4.1	2.0	-2.9
TGFbR2	transforming growth factor, beta receptor II (TGFBR2)	Cytokine receptor	NM_009371	-0.8	0.6	0.5	-0.3	-0.6	-1.1	0.1	0.8	-0.7	-0.7	0.2	0.3		-0.4	0.1	-0.1	0.2	0.6
TGFbR3	transforming growth factor, beta receptor III (TGFBR3)	Cytokine receptor	NM_011578			0.9	0.0	0.3	-0.6			0.2	1.7	0.0	0.4				2.7	2.2	0.1
TICAM2	toll-like receptor adaptor molecule 2 (Ticam2) TRAM	TLR related	NM_173394			-3.3		1.2				3.1	0.5	-0.5				3.3		-1.6	
TIMP1	tissue inhibitor of metalloproteinase 1 (Timp1)	MMP/TIMP	NM_001044384	1.0	0.4	0.3	0.3	-3.0	-0.6	-0.9	-0.3	-0.3	-0.6	2.6	0.7	0.4	-1.3	0.6	-0.9	0.7	1.4
TIMP2	tissue inhibitor of metalloproteinase 2 (Timp2)	MMP/TIMP	NM_011594	0.2	-0.7	1.3	-1.7	0.4	0.4	-0.9	0.7	0.2	2.5	1.9	0.7	0.0	0.4	-1.3	2.4	-0.1	0.5
TIMP3	tissue inhibitor of metalloproteinase 3 (Timp3)	MMP/TIMP	NM_011595		-0.2	1.1	0.8	2.9	2.6		1.8		-1.2	0.6	0.1		-1.0	0.1	2.4	1.3	-1.3
TIMP4	tissue inhibitor of metalloproteinase 4 (Timp4)	MMP/TIMP	NM_080639	5.2	-1.9		-1.0	-2.6			3.8		-0.1	0.6		-0.9	-1.0		1.0		
TIRAP	toll-interleukin 1 receptor (TIR) domain-containing adaptor protein (Tirap), Mal, wyatt, Tlr4ap	TLR related	NM_054096	-1.8	-1.2		4.8	-3.1	-1.0		1.5	0.7	-1.0	2.5	0.0	-0.2	-0.5	1.6	-0.8	0.7	1.6
TLR1	TLR1	TLR related	NM_030682	-1.0	-0.3	0.2	-2.0	1.2	0.9	0.6	0.8	-0.2	2.6	-0.8	0.5	0.4	1.0	-1.2	2.4	-0.4	0.1
TLR11	tlr11	TLR related	NM_205819	1.0	-0.7	0.9			4.9		3.0	1.1	0.0		-4.4		-0.4	2.8	1.1		-3.5
TLR12	tlr12	TLR related	NM_205823	-0.3	-0.6	2.2	1.8		-1.2		0.9	0.2	0.3		0.9	0.3	-0.9	0.8	-1.1		0.2
TLR13	tlr13	TLR related	NM_205820	-0.6	-0.7	1.5	5.3	-0.2	-1.1		1.0	-0.2	-1.1	-1.0	0.3	-3.1	-3.2	-0.5	-1.3	-0.9	-0.7
TLR2	toll-like receptor 2	TLR related	NM_011905		-1.2	-2.5	-0.7				3.2	0.9		3.0	-1.0			1.2	0.7		-2.6
TLR3	TLR3	TLR related	NM_126166	-0.3	0.4		3.3	-3.7	-1.6		1.3	1.2	-1.1	3.3	1.0		-0.3	2.0	-2.6	3.2	-0.5
TLR4	Toll-like receptor 4	TLR related	NM_021297	-0.2	-1.8	0.2	-0.3	0.1	-0.8		1.1	0.0	0.9	-0.2	0.3	1.1	-0.1	0.0	1.1	-0.2	0.1
TLR5	TLR5	TLR related	NM_016928	0.3	-2.1	0.6	0.5	-0.4	-1.0		1.1	0.1	-0.8	-0.2	0.3	0.4	0.0	-0.9	-0.3	-0.5	0.6
TLR6	TLR6	TLR related	NM_011604	-0.5	-1.5	-0.8	1.3	-4.5	-4.4	-0.8	1.5	1.0	0.5	0.9	0.7	0.5	0.0	1.3	0.4	0.8	0.3
TLR7	toll-like receptor 7	TLR related	NM_133211		-0.6	0.9	1.0		1.7		2.8	2.1					-1.7	-2.4	0.2		-3.7
TLR8	TLR8	TLR related	NM_133212	0.1	-2.2	0.3	0.2	-1.2	-0.4	-1.4	0.5	0.4	-0.3	0.7	0.1	-0.3	0.1	-0.3	-0.2	1.1	0.0
TLR9	TLR9	TLR related	NM_031178	0.4	0.1	-0.4	-1.0	0.0	-0.7	-0.1	-0.3	-0.2	0.7	-1.7	0.8	-0.5	0.6	-0.4	1.3	-1.8	0.5
TNF	tumor necrosis factor (TNF superfamily, member 2)	Cytokine	NM_013693	0.2	0.0	-0.8	-1.6	-1.9	-0.6	-1.6	-0.2	-0.3	1.1	0.2	1.1	-0.3	0.2	0.7	1.1	0.3	0.7
TNFR1	tumor necrosis factor receptor superfamily, member 1A, TNFR1	Cytokine receptor	NM_011609	0.1	0.8	-0.6	-0.4	0.1	-0.3	0.4	-0.2	-0.1	0.5	-0.4	1.1	0.0	0.2	1.1	0.9	-0.7	0.5

TNFR2p75	tumor necrosis factor receptor superfamily, member 1b, p75,TNFR2, CD120b	Cytokine receptor	NM_011610	-0.1	-0.1	-0.4	-1.1	0.5	-0.1	0.5	0.1	0.3	0.7	-0.1	0.5	0.6	0.4	0.7	1.6	-0.9	0.3
TNFRSF14	TNF receptor superfamily, member 14 (herpesvirus entry mediator), HVEM, ATAR, TR2, LIGHTR, HVEA	Cytokine receptor	NM_178931		0.1		-0.2			1.3	1.6			1.3			-0.6	1.8		0.0	
tnfsf10	tumor necrosis factor superfamily, member 10, TL2, APO2L, CD253, TRAIL	Surface receptor	NM_009425	-3.4	-1.1	-0.1		0.2		4.3	3.6		0.3	-1.2		3.4		-0.4	-2.8	-0.1	
TOLLIP	toll interacting protein (Tollip)	TLR related	NM_023764	-2.7	-0.3		4.7			5.0	2.6	-3.5	-2.1	4.2	-0.5	3.4	0.2	0.4	-2.2	5.3	0.2
TRADD	TNFRSF1A-associated via death domain (Tradd)	Apoptosis	NM_001033161		-0.2		3.4		-3.3	1.3	2.2		-3.3		1.2		-0.7		-2.1		0.4
TRIF	TLR adaptor molecule1,PRVTIRB,TICAM-1	TLR related	NM_174989		-0.2	0.4		0.7	-0.3	5.3	3.4	1.4	0.1	-0.6	0.3	4.5	0.6	0.8	-0.9	-0.7	-0.8
TRIM14	tripartite motif-containing 14 (Trim14)	TRIM Family	NM_029077	-3.4	1.0		3.4	-2.4	2.3	5.0	-0.8			3.1		5.3		0.8	1.4	1.4	-3.2
TRIM20	Mediterranean fever (Mefv) pyrin TRIM20	TRIM Family	NM_019453		-1.7	2.2			0.8		4.9	0.0	-0.1		-1.1		1.6	0.0	-1.5		
TRIM21	tripartite motif-containing 21 (Trim21)	TRIM Family	NM_009277	2.3		0.9	0.5			-0.5		0.8	-0.6	0.4		-0.9		0.2	-0.4	-0.8	-0.4
TRIM25	tripartite motif-containing 25 (Trim25)	TRIM Family	NM_009546	-0.6	0.1	-0.8	-1.5	0.6	0.0	1.2	-0.3	-1.0	1.0	-0.7	0.5	-0.1	0.1	0.8	1.1	-0.2	0.2
TRIM27	tripartite motif-containing 27 (Trim27)	TRIM Family	NM_009054	0.1	-0.5	0.0	1.5	0.4	-0.5	0.6	0.0	0.2	-1.4	-0.7	0.3	-0.5	0.5	-0.2	-1.5	0.1	0.1
TRIM3	tripartite motif-containing 3 (Trim3)	TRIM Family	NM_018880	-2.0	-0.3		0.1	0.4	0.7	0.7	1.4		-0.1	0.6	0.2	1.6	0.0		0.0	0.1	0.6
TRIM30	tripartite motif-containing 30 (Trim30)	TRIM Family	NM_009099	0.1	-0.2	-0.1	-1.3	1.0	-0.1	-1.2	0.5	-1.0	1.6	-0.3	0.2	0.4	0.9	0.7	1.4	-0.2	0.0
TRIM34	tripartite motif-containing 34 (Trim34)	TRIM Family	NM_030684	0.1	-0.4		2.0	-1.2	0.4		1.6			1.9			-1.0		-0.4	0.7	
TRIM35	tripartite motif-containing 35 (Trim35)	TRIM Family	NM_029979	0.3	0.2	-0.4	-1.1	-0.7	-1.1	0.2	-0.6	-0.1	0.6	0.6	1.3	-0.5	-0.2	0.9	1.0	0.1	1.1
TRIM6	tripartite motif-containing 6 (Trim6)	TRIM Family	NM_001013616	-0.6	0.0	-0.9	-0.6	0.0	-1.2		0.0	-0.9	0.6	-1.7	0.7	-2.1	0.0	1.0	0.6	0.0	0.1
TRIM8	tripartite motif protein 8 (Trim8)	TRIM Family	NM_053100	2.4	-0.7						2.6	1.3	-3.3	-0.4		3.0				2.5	
TUBB3	tubulin, beta 3 (TUBB3)	House keeping	NM_023279	0.1	-0.2	0.1	1.4	2.0	0.7	-1.3	-0.1	0.8	-1.5	0.1	0.8	-0.4	-0.4	-0.1	-0.8	0.1	0.3
TUBB4	tubulin, beta 4 (TUBB4)	House keeping	NM_009451				-1.8	-2.5						0.7		4.8				0.2	
TWSG1	Twisted Gastrulation, tsg	BMPs	NM_023053	0.8	-0.3	-0.1	-0.8	0.0	-0.4	-0.3	-0.6	0.1	0.7	-0.4	1.1	-0.2	0.2	0.4	0.8	-0.6	0.6
TYK2	tyrosine kinase 2 (Tyk2)	Signalling	NM_018793	-1.1	0.3	-1.6	1.7	1.8	0.3	-1.5	2.0		-1.3	-2.2		4.1	0.2	0.0	-2.7		0.8
UBC	ubiquitin C (UBC)s	House keeping	XM_001471699	0.6	0.1	-0.3	-0.5	-1.2	-1.0	0.0	-0.4	-0.3	0.3	-0.6	1.1	-0.6	0.6	-0.5	0.8	-0.7	0.7
VDR	vitamin D receptor, VDR	Surface receptor	NM_009504	0.4	-0.1	0.7	1.9	1.2	1.0	-5.2	1.4	-1.2	-1.4	-0.9	0.6		0.4	-0.5	-1.5	-0.2	-0.1
VEGFa	vascular endothelial growth factor A (Vegfa)	Cytokine	NM_001025250		-5.3		0.2	0.6	-0.6		8.2		2.4	-0.8	0.6				2.4		-0.2
VEGFb	vascular endothelial growth factor B (Vegfb)	Cytokine	NM_011697	0.4	1.4			-2.9	-3.2	2.1	0.6		0.5	0.4	0.1	1.2	-4.9		-0.1	1.3	-0.3
VEGFc	vascular endothelial growth factor C (Vegfc)	Cytokine	NM_009506	-0.1	0.0	0.2	0.7	-0.2	-0.1		0.4	0.3	-0.2	0.5	1.4		-0.1	-0.2	-0.4	0.4	1.2
Wnt5a	wingless-related MMTV integration site 5A (Wnt5a)	Signalling	NM_009524		-1.3			-3.1	-1.6		1.7	-7.1	-4.1	1.3		4.1	-1.6	-2.2		-1.6	0.5
Wnt7b	wingless-type MMTV integration site, member 7B	Signalling	NM_009528	0.3	-0.5	0.7	1.3	-1.6	-0.4		1.3	0.3	0.0	1.3	-0.7		2.0	-0.1	0.4	1.7	-1.7
YM1	chitinase 3-like 3 (Chi3l3) Ym1 ECF-L eosinophil chemotactic factor-L	Macrophage related	NM_009892	-1.0	0.0	-1.2	-1.3	0.0	-1.3	1.0	0.0	-0.7	1.3	-1.6	0.8	0.0	0.0	1.3	1.3	0.0	0.2